A GRIDLESS, VARIABLE PERVEANCE PIERCE ELECTRON GUN

By Bruce David Foulis

submitted in fulfilment of the
academic requirements for the degree of
Doctor of Philosophy in the Department of
Electronic Engineering at the
University of Natal

1994

This thesis covers the design and development of a modulated Pierce electron gun used in the construction of experimental travelling wave tube (TWT) amplifiers. The gun incorporated an open aperture switching electrode, positioned mid-way between anode and cathode, to pulse the beam. This method of modulation did not have the same adverse effects on electron trajectories as in the case of a conventional mesh grid, but rather the electrode could be used to alter the focus conditions within the gun and subsequently improve certain beam characteristics. Ion focusing effects could also be eliminated with the electrode, allowing dual mode operation of the guns without the complications normally associated with such a practice.

The switching electrode was simulated to ascertain its effect on electron trajectories within the gun, using finite element analysis as well as an electron optics design program. A test gun was constructed in a glass envelope in order to investigate the performance of the new design. The glass gun allowed a beam analysis to be performed, as well as thermal measurements to be made. Results from this gun compared favourably with earlier simulations. The results of two metal/ceramic construction TWTs are presented, showing the beneficial effects of the switching electrode on the performance of the tubes as a whole, and the electrode's potential to compensate for constructional anomalies.

The joining of metals to ceramic using active brazing techniques is also an important aspect tackled by the thesis, with several innovative ideas being implemented in the construction of the devices. A simple yet reliable electrical feed-through was developed for those guns having a ceramic envelope.

Extensive work was also performed on the manufacture of impregnated tungsten cathodes for use in the electron guns. Several test diodes, including a water-cooled demountable test vehicle, were constructed to test the performance of the cathodes. An analysis was performed on the patchy behaviour of some of the initial cathodes to improve the preparation methods used in the laboratory. The emission results obtained from the cathodes are documented, as is the successful incorporation of several of them into the new modulated gun design.

The work outlined in this document was performed at the Department of Electronic Engineering's Materials Science Laboratory at the University of Natal, under the supervision of Professor H.L. Nattrass, and forms a small part of the ongoing research into the development of the technological capability of manufacturing travelling wave tubes in South Africa.

There were many people involved in the research, each covering widely overlapping areas of interest, and each subscribing to the overall objectives of the project. However, it must be stated that the final content of this thesis, unless specifically indicated to the contrary in the text, is the author's own work, and has not been submitted in part, or in whole to any other University for degree purposes.

This thesis documents a small fraction of the work carried out by the author and his colleagues during the years spent on the project. Much of the time was consumed by the seemingly impossible task of surmounting the many obstacles which presented themselves around every corner. None of this work would have been possible without the input and encouragement of the following people, to whom the author would like to extend his gratitude and thanks:

Professor H.L. Nattrass, for being an undefinable source of encouragement and motivation throughout the project, and for allowing me the opportunity to pursue other interests.

Nick Vassilopoulos, for endless hours of constructive brainstorming, and many more engaged in idle chatter!

Chris Reynolds, for a wealth of theoretical input on travelling wave tube operation.

Clyde Johnson, for his patience and resolve whilst machining components of impeccable quality and workmanship.

Clive Booth, for making my stay in the Materials Science Laboratory a pleasant and rewarding one.

Mr W. Drijfhout and his team at Mikomtek, CSIR, for their technical and financial assistance throughout the project.

The members of staff of the Department of Electronic Engineering.

The Department of Electronic Engineering and the FRD for financial assistance during my university studies.

TWT	Travelling Wave Tube
PPM	Periodic Permanent Magnet
RF	Radio Frequency
DC	Direct Current
OFHC	Oxygen Free High Conductivity
CW	Continuous Wave
SWS	Slow Wave Structure
TEM	Transverse Electro-Magnetic

ϵ_o	permittivity of free space = 8.854×10^{-12} F.m^{-1}
m	electron mass = 9.1×10^{-31} kg
e	electron charge = 1.6×10^{-19} C
h	Planck's constant = 6.626×10^{-34} J.s^{-1}
k	Boltzmann's constant = 1.381×10^{-23} J.K^{-1}
A_0	Richardson-Dushman constant = 1.20×10^{6} A.m^{-2}.deg^{-2}

V_{ao}	applied anode voltage
x	distance from cathode surface
V(x)	potential at distance x
u(x)	electron velocity at distance x
ρ	volume charge density
J	current density
d	anode to cathode spacing
k'	linear electrode scaling factor
B_z	axial magnetic flux density
β	ratio of switching electrode to anode potentials
a	electron beam outer radius
I_0	electron gun beam current
V_0	electron gun applied voltage
η	electron charge to mass ratio
μP	gun micro-perveance
μ_c	beam cut-off amplification factor
Θ	gun cone half angle
G	travelling wave tube gain

N	number of wavelengths in SWS
T	cathode temperature
ϕ	cathode work function
E	electric field at cathode surface
J_0	Richardson-Dushman current density
R_s	series resistance of oxide layer
α	figure of merit for cathode emission density profile
r	cathode radius
p_0	diode perveance per unit area
i	normalised cathode current
v	normalised anode voltage

CHAPTER 1.

INTRODUCTION

The input power to a travelling wave tube (TWT) is in the form of a high velocity beam of electrons, originating from an electron gun. The energy is imparted to the electrons via a high voltage anode which accelerates the electrons emitted thermionically from a cathode. It is this beam of electrons which interacts with the RF signal within the tube and results in amplification of the signal. Consequently, the performance of the TWT is largely dependent on the nature of the electron flow emerging from the electron gun. While the basic principles of electron gun operation have not changed, the application of modern materials and design mediums has resulted in considerable improvements in tube performance.

The original gun design for the TWT project at the University of Natal was performed and documented by D.M. Smith [1], and was based on the design philosophy of J.R. Pierce [2]. Although the gun produced very functional results, there were a number of drawbacks inherent in the construction and assembly of the device. The sandwich type construction of the metal/ceramic tube made accurate jigging of the electrodes and the axial alignment of the gun and tube axes difficult, resulting in the position and diameter of the emerging beam's waist and the current density distribution of the electrons being far from ideal. The ability of the magnetic focusing field to confine the beam to predetermined dimensions was thus impaired, with less than 80 per cent of the gun's electron beam finally reaching the collector. Finally, an effective means of pulsing the beam so that the average beam power could be reduced during adjustment and optimisation of the magnetic focusing stack was not available with the existing design.

In the light of these problems, and following extensive discussions with members of the TWT research group, the author decided to introduce a switching electrode to the gun design. Although multi-electrode guns have been developed for such purposes

as the empirical design of gun focusing systems by Frost *et al* [3], and the reduction in the effect of the anode aperture in high perveance guns by authors such as Shimada [4], Becker [5] and Kirstein *et al* [6], no reference was found in the literature to the implementation of such an electrode to switch the electron beam, alter the focus conditions during different modes of operation of the tube, and generally enhance the performance of a working electron device. The result was a considerable improvement in the electron beam characteristics, while an effective yet simple means of beam modulation was obtained (It must be noted that the term "modulation" as used in this context refers to switching the beam either on or off). The extra degree of freedom offered by the switching electrode allowed the perveance of the gun to be varied for a fixed electron gun geometry. The time-consuming and expensive task of PPM magnet stack "tweaking" could also be eliminated by applying a feedback control to the switching electrode potentiometer, which would automatically minimise current interception by the RF helix by altering the gun focusing as opposed to the stack focusing. This also proved effective in eliminating the effects of ion focusing during long-pulse or CW operation of the tubes, a problem which generally restricts the use of fixed focus guns to single mode operation.

A new approach was also taken to the construction of the gun module itself. Ceramic rods were used to support the electrodes of the gun, in place of the more conventionally used glass supports, increasing the resistance of the device to mechanical shock and allowing for greater assembling accuracy. The "sandwich" type construction of the gun envelope also restricted the number of electrical connects that could be brought out of the tube, and so special attention had to be paid to designing reliable metal feed-throughs in the ceramic wall of the envelope. The difficulties associated with brazing thick-walled ceramic shells to metallic cups for TWT applications are outlined by Yeh & Yeh [7]. Ironically, to keep the component construction as simplistic as possible, the author opted for the infinitely more vexing task of producing a reliable joint between the thick-walled ceramic envelope and *solid* metal pins.

Chapter 2 begins by briefly outlining the principles of space-charge-limited electron flow between electrodes, the problems generally associated with experimental guns,

and different means of modulating the electron beam. The switching electrode is then introduced in Chapter 3, along with the results of various simulations performed on this and other gun designs.

Chapter 4 documents the results of the first test gun constructed to verify the principle of the switching electrode, as well as the results of the travelling wave tube demonstrators that incorporated such guns in their construction.

During the course of the project, a switch was made from using oxide-coated cathodes to the more robust and reliable impregnated cathodes. This move also enabled various intricate cathode shapes to be machined from the porous tungsten substrate, allowing greater flexibility during the development of the tubes. Chapter 5 outlines the theory behind impregnated tungsten cathode preparation and operation, while Chapter 6 analyses the results of such cathodes manufactured in the Materials Science Laboratory by the author, using an unusually simple procedure.

REFERENCES

[1] D.M. Smith, "The Theoretical and Practical Analysis of Low Perveance Pierce Electron Guns", University of Natal M.Sc.Eng. thesis, 1990.

[2] J.R. Pierce, "Theory and Design of Electron Beams", New York: Van Nostrand, 1955.

[3] Frost, Purl and Johnson, *Proceedings of the IRE*, vol. 50, p 1800, August 1962.

[4] T. Shimada, "Experiments on High-Perveance Electron Guns with a Subfocusing Electrode", *IEEE Transactions on Electron Devices*, pp. 663-664, July 1969.

[5] R. Becker, "Two Electron Guns with Adjustable Beam Compression and Perveance", *Nuclear Instruments and Methods*, vol. 187, pp. 255-258, 1981.

[6] P.T. Kirstein, G.S. Kino and W.E. Waters, "Space-Charge Flow", New York, McGraw-Hill Book Company, 1967, pp. 412-415.

[7] H-Y. Yeh and H-G. Yeh, "Failure Analysis of Ceramic Feedthroughs Used in Travelling Wave Tubes", *IEEE Transactions on Electron Devices*, vol. ED-34, No. 8, pp. 1862-1867, August 1987.

CHAPTER 2.

ELECTRON GUNS

The two-electrode vacuum tube, or diode, is the simplest form of electron device and as such makes an excellent starting point for analysing electron flow between electrodes. The diode consists of a thermionic cathode and a beam terminating anode, which when positive with respect to the cathode, allows electron flow from cathode to anode.

If an aperture is made in the anode allowing electrons to pass through, a crude electron gun is obtained. By using suitable beam forming electrodes in the interelectrode space, greater current densities are obtainable by converging the beam through the anode aperture, resulting in a more useful electron source.

This chapter is not intended to delve into the theory of electron behaviour, but merely to acquaint the reader with the concept of space-charge-limited electron flow between electrodes, and the practical aspects of Pierce electron gun design.

2.1 SPACE CHARGE FLOW BETWEEN ELECTRODES

2.1.1 The Planar Diode

Consider two plane electrodes separated by a distance which is small compared to the linear dimensions of the electrodes themselves. We can thus safely ignore the effect of fringing at the edges of the electrodes, and can assume the fields in the interelectrode space to be normal to the electrodes. A qualitative picture of the potential distribution and electric fields in the interelectrode space is shown in figure 2.1 for different values of cathode emission current.

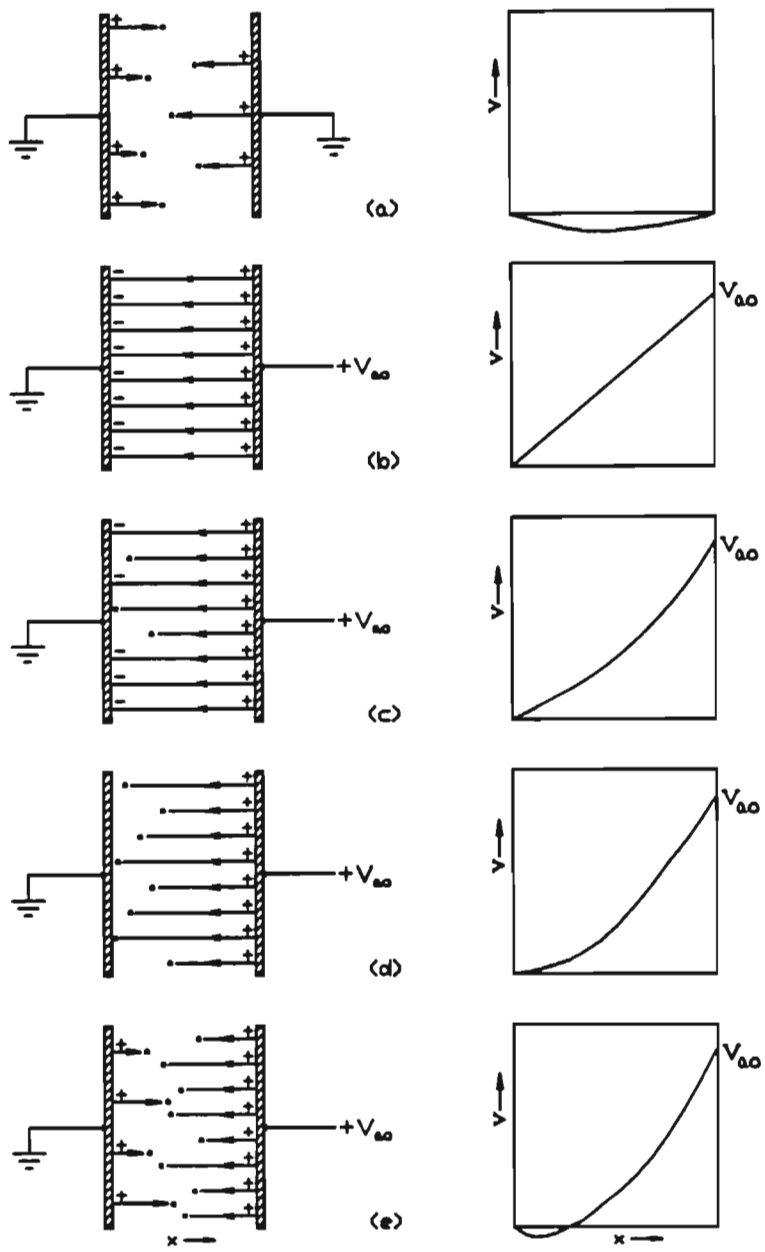

Figure 2.1 Field Lines and Potential Distribution in a Plane Diode [1]

In figure 2.1(a) the anode is held at the same potential as the cathode while electrons are emitted from the cathode. The presence of the electrons results in a reduction of the potential between the electrodes, reaching a minimum somewhere between the two plates. The electrons being emitted from the cathode have varying initial velocities due to thermal energy supplied to them. Those electrons with sufficient energy to pass through the potential minimum do so and eventually reach the anode, while those having smaller initial velocities will return to the cathode. As the number of electrons to the left of the potential minimum is larger than that to the right due

to some electrons returning to the cathode, the electron density at points of the same potential will be larger to the left of the minimum than to the right. Consequently, the position of the potential minimum is displaced to the left of the mid-point between the electrodes.

If a potential V_{ao} is applied to the anode with no cathode emission occurring, the electric field lines originating on the anode terminate on the cathode, and the potential varies linearly between the two plates as shown in figure 2.1(b). For the same applied field but with some small cathode emission, the emitted electrons experience a field due to the applied voltage and are drawn to the anode as shown in figure 2.1(c). All the emitted electrons reach the anode, and the emission is said to be *temperature limited*, since the magnitude of the emission current is dependent on the temperature of the cathode and shows little variation with changes in applied anode voltage.

As the electron emission increases, so the potential profile from cathode to anode is depressed further, until the electric field intensity at the cathode is zero, as illustrated in figure 2.1(d). All the electric field lines originating from the anode are terminated on electrons. If the cathode temperature is raised further, a potential minimum forms in front of the cathode, causing some of the electrons to return to the cathode (figure 2.1(e)). Electron emission would thus decrease, and the electric field at the cathode surface would return to zero. This equilibrium serves to limit the cathode current to a specific value for a given applied anode voltage, and the current is said to be *space-charge-limited*.

During space-charge-limited operation, a change in cathode temperature merely alters the potential at the minimum and has little effect on the overall emission current [2]. Raising the anode potential increases the number of electrons emitted from the cathode, until a point is reached where the potential minimum disappears and temperature-limited emission predominates.

As all the electrons that pass the potential minimum eventually reach the anode, the plane of the minimum is often called the virtual cathode, and is taken into account when determining the current-voltage relationship for a planar diode. However, as the potential minimum is usually small in comparison to the anode voltage, its magnitude

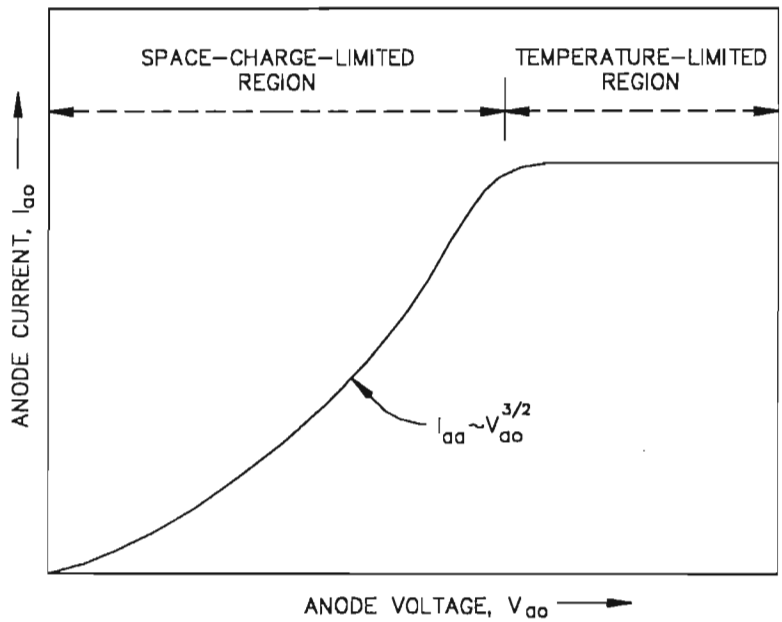

Figure 2.2 Idealised I-V Plot for Planar Diode (after [1])

may be ignored for the purposes of our simplified discussion. Similarly the distance from the cathode to the potential minimum is a small fraction of the cathode-anode spacing, and thus will not be considered at this moment.

If *V(x)* is the potential at a point *x* metres from the cathode, and *u(x)* is the electron velocity at that point, then we obtain three boundary conditions at $x = 0$:

$$V(0) = 0$$

$$u(0) = 0$$

$$dV/dx = 0$$

There are three equations which relate the parameters of interest:

Poisson's Equation

$$\frac{d^2V}{dx^2} = -\frac{\rho}{\varepsilon_0} \tag{2.1}$$

the energy equation

$$\tfrac{1}{2}mu^2 = eV \tag{2.2}$$

and the current density relationship

$$J = -\rho u \tag{2.3}$$

where ρ is the volume charge density.

Integrating the above equations, and using the boundary conditions to eliminate the constants of integration, an analytical solution for the current-voltage relationship for a plane diode may be found [3] as:

$$J = \tfrac{4}{9}\varepsilon_0\sqrt{2(e/m)}\frac{V^{\frac{3}{2}}}{x^2} \tag{2.4}$$

Substituting values for the constant terms, taking $V = V(x)$ as the anode potential, and $d = x$ as the cathode to anode spacing gives:

$$J = 2.33\times10^{-6}.\frac{V^{\frac{3}{2}}}{d^2} \quad A.m^{-2} \tag{2.5}$$

Thus the emission from a cathode under space-charge-limited conditions varies approximately as the 3/2 power of applied anode voltage divided by the square of the anode-cathode distance. This relationship is known as the Child-Langmuir Law.

Although (2.4) has been derived for the simple case of a planar diode, it can also be shown that the space-charge-limited flow in cylindrical and spherical diodes is also proportional to the 3/2 power of applied anode potential [4]. Furthermore, if two similar diodes differ in their linear dimensions by a factor k', then the same cathode current will flow in each diode if the same anode voltage is applied to both. Of particular interest to tube engineers is the case of arbitrary electrode shape, as this would enable a beam of electrons to be extracted from the diode.

2.1.2 Diodes of Arbitrary Electrode Shape

In the three diode geometries mentioned thus far, namely planar, cylindrical and spherical diodes, the electron trajectories have all been parallel to the electric field lines. If the field lines were not straight, the electrons would tend to cross over the lines due to their inertia, as shown in figure 2.3 for a diode consisting of a parabolic-shaped cathode and planar anode.

If the applied anode potential of the diode is varied, the electron trajectories are unaffected so long as the geometry is unchanged. If the anode potential is scaled by a factor k', Poisson's Equation leads to the solution that the potential and space charge in the interelectrode region will be $V = k'.V_1$ and $\rho = k'.\rho_1$ respectively where the subscript 1 denotes the values before scaling [6]. Thus the potential at any point in a space-charge-limited diode of arbitrary shaped electrodes is proportional to the applied anode voltage, and consequently the electron trajectories will not be affected by changes in anode voltage.

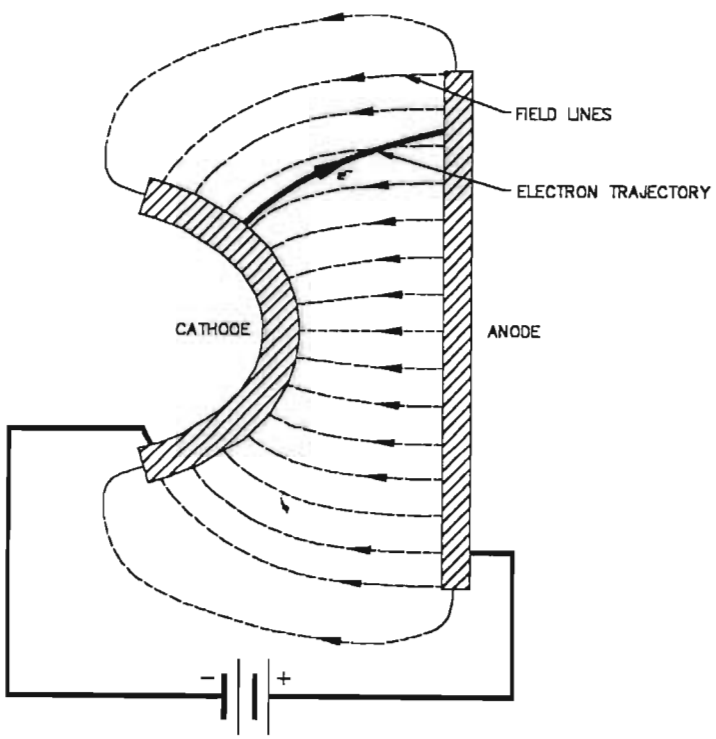

Figure 2.3 A Diode of Arbitrary Shaped Electrodes (after [5])

Now, from the energy equation:

$$\frac{1}{2}mu^2 = eV \tag{2.6}$$

it can be seen that the velocity u of an electron at any point is proportional to the square root of the potential at that point, and hence by the above argument is proportional to the square root of the applied anode voltage. The charge density ρ is directly proportional to the potential at any point as given by Poisson's Equation:

$$\nabla^2 V = -\frac{\rho}{\varepsilon_0} \tag{2.7}$$

Since the Laplacian operator is linear, the charge density must also be proportional to applied anode potential. Finally, the current density under space-charge conditions is:

$$J = -\rho u \tag{2.8}$$

Hence, the current emission in a space-charged-limited diode of arbitrary electrode shape is proportional to the 3/2 power of applied anode potential.

2.2 THE PIERCE ELECTRON GUN

2.2.1 Pierce Electrodes

Often in microwave tubes the electron beam current density required for interaction with the microwave signal if far greater than the current density that the cathode can safely deliver. This high current density is necessary to increase the efficiency and bandwidth of the tubes. To reduce the stress on a cathode and thus prolong cathode life, it was necessary to make convergent electron guns. If segments of a cylindrical or spherical diode are used, the necessary convergence can be obtained. Since cylindrical symmetry of the beam is often required, we shall consider the case of the spherical diode segments.

The electron flow in a spherical diode is rectilinear in nature, with all electrons travelling in straight lines. If we consider the practical case of two segments of the spheres making up the cathode and anode as shown in figure 2.4(a), things are somewhat different. The negative space charge within the electron beam causes divergence of the beam as the electrons repel one another. The equipotential lines

between the two electrodes are distorted and are no longer spherical. To confine the electron flow, focus electrodes are required which, when tipped in towards the electron beam, return the equipotentials to the shape they would be if no electrons were present, ie. spherical in this case.

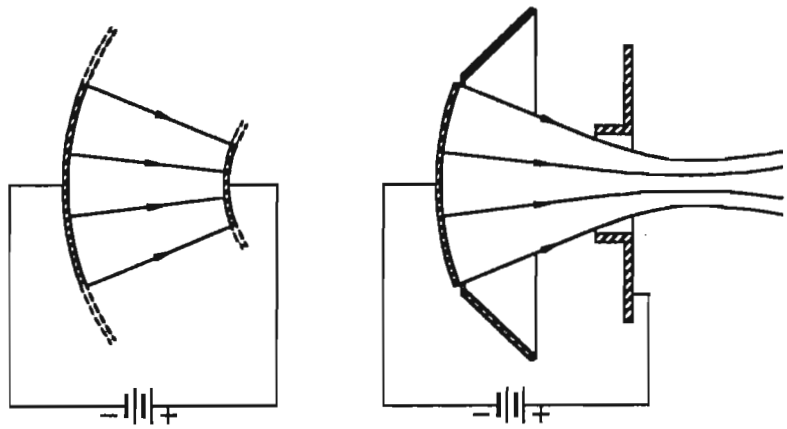

Figure 2.4 (a) Convergent Electron Flow and (b) The Beam Forming Electrode [7]

Because of the pioneering research on and elegant documentation of convergent electron guns done by J.R. Pierce [8], the beam forming electrodes have acquired the name of Pierce electrodes, and convergent electron guns of this nature, Pierce guns. Consider the shape of the electrode close to the cathode where the low velocity of the electrons results in the most deflection by transverse forces. If we look at a very small section of the cathode edge as shown in figure 2.5, we can approximate the cathode as being planar and the problem becomes two-dimensional.

In this small region near the cathode the potential varies, as in the case of a planar diode, as:

$$V = Ax^{\frac{4}{3}} \tag{2.9}$$

where A is a constant and x is the distance from the cathode.

It can be shown [9] that if $V=f(x)$ is the potential on the x-axis, and that if the potential is symmetrical about the x-axis of a Cartesian coordinate system, then the potential throughout the x-y plane is given by:

$$V = Re\, f(x+jy) = \frac{1}{2}[f(x+jy)+f(x-jy)] \tag{2.10}$$

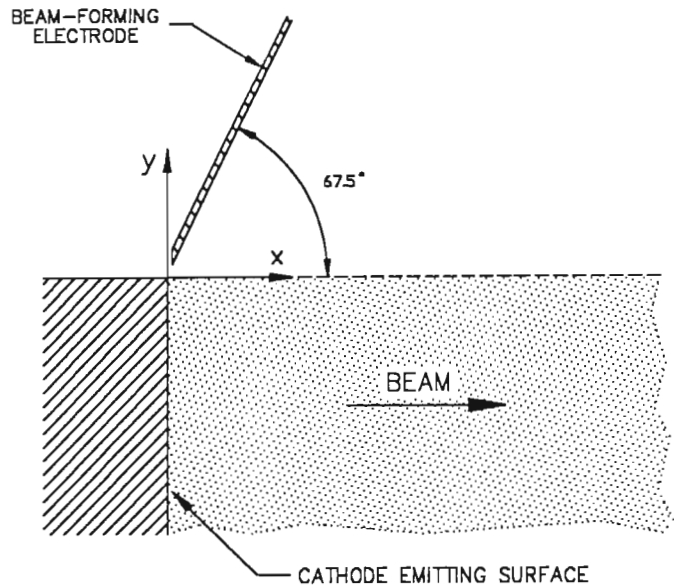

Figure 2.5 The Beam Edge Near the Cathode (after [1])

The fact that the potential is symmetrical about the x-axis implies that $dV/dy = 0$ at $y = 0$. Furthermore, we require (2.9) to be satisfied at $y = 0$. A function of potential in the charge-free region which satisfies both these requirements and yet has the form of (2.10) is:

$$V = Re\ A(x+jy)^{\frac{4}{3}} = \frac{A}{2}[(x+jy)^{\frac{4}{3}} + (x-jy)^{\frac{4}{3}}] \qquad (2.11)$$

Any electrode which has a shape and potential as defined by (2.11) would satisfy all boundary conditions and would consequently result in no transverse force on the electrons at the edge of the beam. A convenient potential to choose for the electrode would be the cathode potential as no biasing would be required. The solution to this particular case is obtained by setting $V = 0$ in equation (2.11), giving:

$$y = (1+\sqrt{2})x \qquad (2.12)$$

Equation (2.12) is that of a straight line making an angle of 67½ degrees with the x-axis. As the above derivation is a good approximation to the potential very close to the cathode, the beam forming electrode close to the beam edge will thus have an angle of 67½ degrees with the beam edge. The shape of the electrode further away from the beam should also be such that the potential along the edge of the beam is the same as that which it would have been if the electron flow was

rectilinear between concentric spheres. This shaping is often achieved by using an electrolytic tank to plot potential contours.

2.2.2 Anode Aperture

In order to utilise the electron beam formed by the spherical diode, an aperture has to be cut in the anode to allow the electrons to exit. The result is a distortion of the equipotential lines within the electron gun and the introduction of an axial component of electric field. The off-axis electrons therefore experience a force away from the axis, and the beam diverges. Furthermore, the distortion of the equipotential lines means that uniform electron emission across the cathode surface is no longer possible.

If electron emission is space-charge-limited then the ratio of beam current to the 3/2 power of beam voltage is known as the *perveance* of the gun, and is a measure of the amount of beam current a gun can produce for a fixed anode voltage. High perveance guns involve high convergence of the beam, and as a result are more severely affected by the defocusing effect of the anode aperture, as illustrated in figure 2.6.

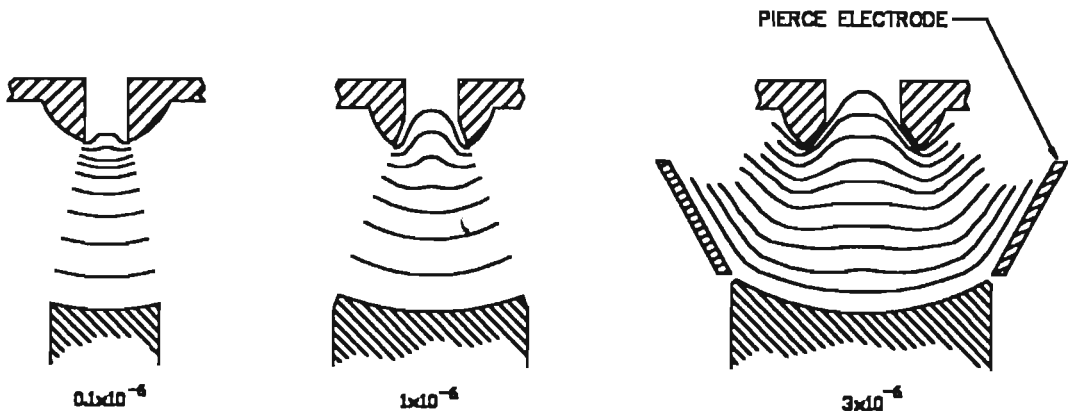

Figure 2.6 Effect of Anode Aperture on Equipotential Profiles for Various Perveance Values [10]

Attempts to minimise this defocusing of the beam in high perveance guns by using an additional electrode were made by Shimada and Nishimaki [11]. By placing a sub-focusing electrode in close proximity to the entrance of the anode aperture, the effect of the equipotential bending could be reduced, resulting in a reduced beam minimum diameter and improved cathode emission uniformity. As the electron guns employed in the TWT amplifiers under development at the University of Natal were to be low perveance guns, this form of compensation was not seen by the project as either necessary or potentially effective.

The absence of any beam forming electrodes outside the electron gun allows the space charge of the beam to cause further divergence of the electrons. The result is that the beam, which was initially converging as it passed through the anode aperture, reaches a minimum diameter and then starts to diverge again. It is at this minimum diameter that the beam is usually captured by the magnetic focusing system of the travelling wave tube, and therefore the quality of the electron flow at this point is of great importance. There are many factors which can affect the beam quality, especially those related to experimental guns, and it would perhaps be pertinent at this point to examine some of them in greater detail.

2.3 EXPERIMENTAL GUNS AND ASSOCIATED PROBLEMS

In order to allow the beam to interact with the microwave signal applied to the travelling wave tube and produce some signal gain, it must be contained over a certain distance after it has left the confines of the gun electrodes. To achieve this, several magnetic focusing techniques can be used. The most popular technique is that of periodic permanent magnets (PPM), and was the method employed at the University of Natal. The principles of magnetic focusing are eloquently documented by a member of the Materials Science Research Group, Mr A.W. Stokes [12]. Periodic magnetic focusing can best be described as a series of equi-spaced magnetic lenses such that the diverging effect of the electrons under space-charge repulsive forces between the lenses is reversed as the electrons pass through the lens. The beam thus exits the lens converging at the same rate as it was diverging before entering the lens, only to experience space-charge repulsion once more, and the process is repeated. The mean diameter of the beam is thus kept constant with a limited

periodic radial ripple superimposed.

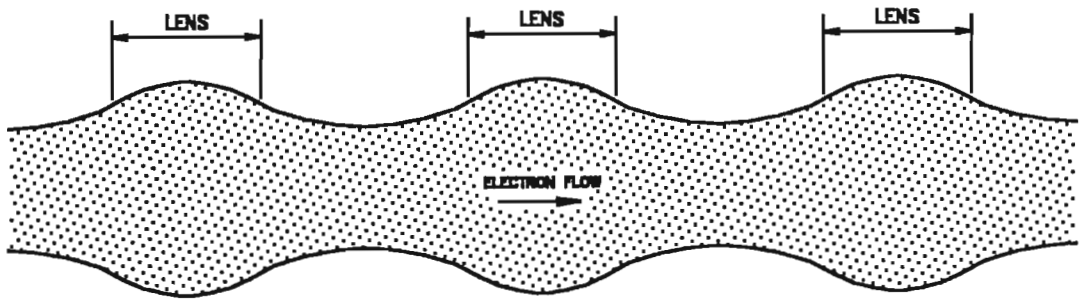

Figure 2.7 The Focusing Action of Periodic Lenses [13]

If effective focusing is to be achieved, the beam entering the magnetic focusing stack must demonstrate certain qualities, several of which are discussed in the following section.

2.3.1 The Nature of the Beam

The paraxial-ray equation [14] describes the motion of an electron in an axially symmetric magnetic field. Its solution is complicated, and may be obtained if the initial radial velocity of the electrons entering the magnetic field is assumed to be zero. This implies that all the electrons within the beam have only an axial component of velocity and therefore travel parallel to the beam axis at the beam minimum. This condition of parallel trajectories is known as laminar electron flow, and is essential if severe beam ripple, or scalloping, is to be avoided. Incorrect focusing conditions with the electron gun itself are a primary cause of non-laminar flow, as the electrons are either under- or over-focused as they exit the anode aperture.

As the electrons enter the focusing stack, they experience a radial component of magnetic field due to the magnetic flux leaving the first pole piece. Thus component is proportional to the radius of the electron trajectory, and hence the entire electron beam is set into rotation as a rigid body. The tangential component of the now rotating electrons, crosses the axial magnetic field in the centre of the magnetic lens, resulting in a radial force inwards on the electrons. If the outward force on the electrons due to the radial electric field of the beam is exactly balanced by the inward force of the axial magnetic field, Brillouin flow is said to occur. The value of magnetic field (RMS value in the case of a periodic field) thus required for Brillouin flow is

dependent on the beam diameter at the point of entry to the magnet stack. The diameter of the beam at this point is determined by the gun design, and must be known accurately. Furthermore, the axial position of the beam minimum must also be predictable, as it is at this point that the beam is captured by the magnet stack and focused down the centre of the RF helix. Pierce [8] derives a further constraint that the beam minimum must occur at a distance of 0.14 times the pole piece radius in front of the first pole piece. Again, if the focusing conditions of the electron gun are not correct, there will be an uncertainty in the axial position of the beam minimum.

The magnetic flux density required for Brillouin flow is given by the following relationship:

$$B_z^2 = \frac{\sqrt{2} I_0}{\pi \varepsilon_0 \eta^{\frac{3}{2}} V_0^{\frac{1}{2}} a^2} = \frac{0.69 \times 10^{-6} I_0}{V_0^{\frac{1}{2}} a^2} \qquad (2.13)$$

where a is the beam outer radius and η is the electron charge to mass ratio. Since (2.13) is independent of electron radial position, it is only valid for uniform current density across the beam diameter. Thus the electron beam, on exiting the anode aperture, should in practice be as nearly uniform in cross-sectional current density as possible. Poor gun design can result in a beam having a concentration of electrons at its centre, or even beams of hollow cross-section.

To obtain Brillouin flow, the axis of the electron beam must coincide with that of the magnetic stack, else perturbations in the focused beam will result. Similar problems will occur if the two axes are tilted with respect to one another, and the electrons are launched at an angle to the magnetic axis.

2.3.2 Ion Focusing

If the kinetic energy of electrons travelling down the tube is larger than the ionisation energy of the residual gas molecules within the tube, then any collisions between the electrons and gas molecules will result in the generation of heavy positive ions which move "slowly" towards regions of lower potential. If the ions should pass through the anode aperture, they will be accelerated rapidly towards the cathode. Not only

will this result in damage to the cathode surface from bombardment by the ions, but the positive charge of the ions throughout the tube reduces the negative space-charge within the beam. As the mutual repulsion between electrons is now reduced, the beam becomes over-focused and the laminar properties destroyed.

The ionisation efficiency, S_e, is defined as the number of ion pairs (one electron and one positive ion) produced by one incident electron per centimetre of travel at 1 torr and 0°C [15]. A simple model [16] for the ion current in an electron beam can be written as:

$$I_i = pI_bS_el \qquad (2.14)$$

where I_i = ion current, p = tube pressure, I_b = beam current, and l = length of beam.

Von Engel [15] gives the ionisation efficiency of N_2 at 4.5 kV as approximately 1 ion pair/cm.mm Hg. For a beam current of 80 milliamperes and a tube pressure of 10^{-6} torr, an ion current in the region of 2 microamperes can therefore be expected. Although this flow of ions represents only a small fraction of the total beam current, the total *number* of ions present can be very large, and the effects on the over-focusing of the beam can be quite significant. Beck and Smith [16] monitored the drift tube electron currents in a 25 kW klystron at various residual gas pressures, and found a great reduction in interception currents due to the neutralisation of space-charge at high operating pressures. This was as a result of the beam constricting under the reduced space charge.

The most significant consequence of ion focusing is the effects of ion build-up with time. The ion current typically takes several hundred microseconds to form at normal tube pressures, and hence the *average* ion current differs for different anode voltage pulse widths. Furthermore, the build-up of ions during the first part of a long pulse causes changing focusing conditions during this period. For very short pulse widths ($<20\mu s$) the effects of ion focusing can be neglected, whilst for long pulse widths ($>400\mu s$) the effects can be quite severe. The difficulty arises when guns are required to be dual mode in nature, as the focusing conditions under CW or pulsed operation are therefore different. Very often two completely separate electron guns

with different focusing arrangements are incorporated into a single vacuum tube to account for the two modes of operation. As this is a costly process, it would be advantageous to be able to adjust for these different conditions by some other means.

2.3.3 The Effect of Tolerances

Amboss [17] provides an analytical solution to the perturbations in conical flow Pierce guns as a result of tolerances in gun construction. The results allow one to calculate the effect a change in dimension or position of an electrode will have on the current density or geometry of an electron beam. Of more importance to us is a feel for what practical effects errors in construction of an experimental gun will have on the beam leaving the anode aperture.

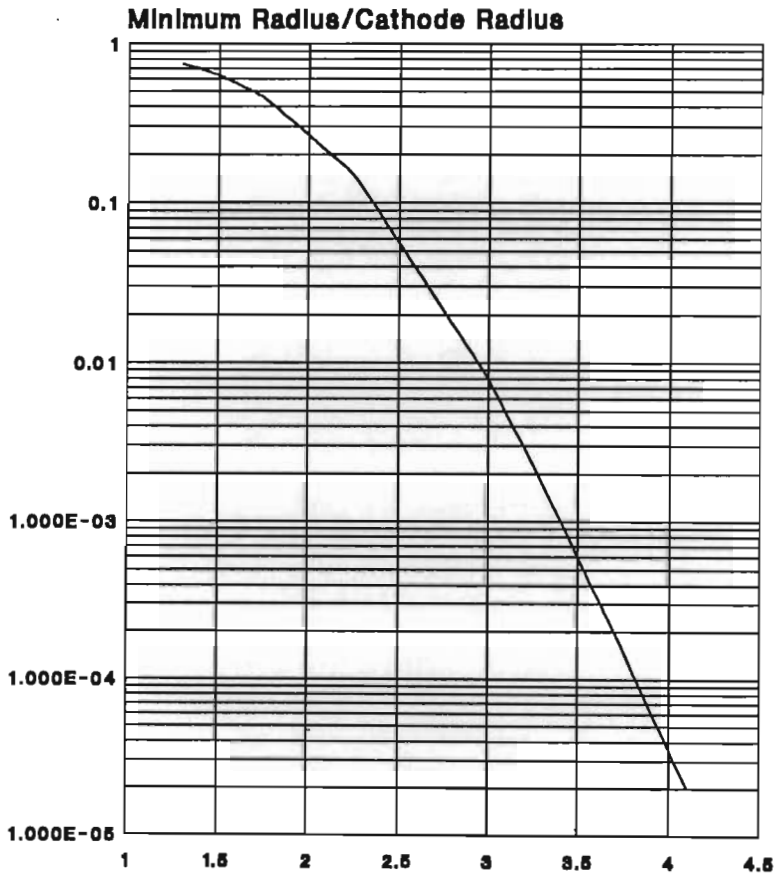

Figure 2.8 Pierce Gun Design Curve

Looking at the Pierce gun design curve in figure 2.8, we can see that if the ratio of cathode radius to anode radius is increased from say 2.5 to 2.6, a mere 4 per cent,

then the reduction in the normalised minimum beam radius is almost 40 per cent. This tolerance figure seems high, yet it is not entirely difficult to obtain errors of this sort of magnitude in a gun which is functioning over a wide range of operating conditions, as experimental guns generally do. If a cathode supporting sleeve manufactured from molybdenum, and having a length of 20 millimetres, is heated to 1100°C, the increase in length of the tube is 0.12 millimetres. This represents a change in anode-cathode spacing of over 2 per cent for a gun having a 5 millimetres spacing at room temperature. Lampel *et al* [18] found that an axial displacement of the cathode with respect to the focus electrode in an experimental gun by a mere 1.2 per cent resulted in a factor of two variation in the perveance of the gun.

An analysis was conducted on the existing Pierce electron gun using the Pierce Gun Design program [19] to determine the effect of errors in the gun construction. The first source of possible beam disturbance is a change in the cathode radius of curvature. The cathode emitting surface is machined from a porous tungsten plug, making extremely accurate dimensioning difficult. If a spherical radius of 11 millimetres is obtained as opposed to the design figure of 13 millimetres, the anode beam radius was calculated to reduce by 10 per cent, from 1.11 millimetres to 0.99 millimetres. If the error is of this magnitude at the anode aperture, then the effect further away at the beam minimum is sure to be far larger!

Figure 2.9 shows the effect of displacing the cathode and focus electrode transversely by a small amount. Not only does it cause the trajectories of the electrons exiting the anode aperture to be displaced, but resulted in the above analysis in a decrease in the current density by approximately 5 per cent for a transverse displacement of 0.5 millimetres.

An increase in current density of 5 per cent was observed for a reduction in anode-cathode spacing of only 0.1 millimetres, while the beam radius at the anode aperture increased by 0.01 millimetres for the same reduction in spacing. Furthermore, by tilting the focus electrode 5 degrees with respect to the gun axis, the beam current was reduced by 10 per cent while an axial electron was displaced by 0.38 millimetre at the anode plane.

The above calculations serve to illustrate the drastic effect that tolerances can have

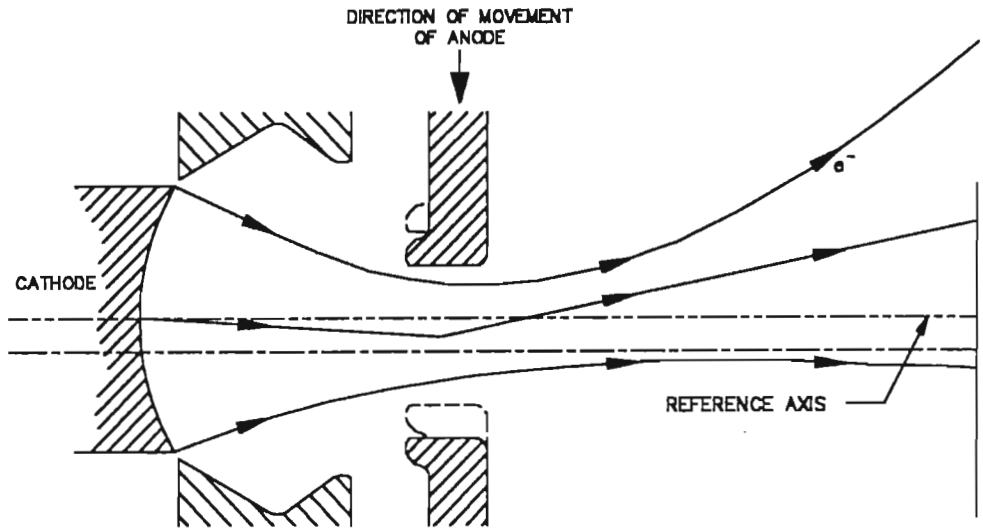

Figure 2.9 Effect of Transverse Displacement of Anode [17]

on the quality of the beam entering the magnetic focusing stack. Experimental guns especially are prone to exhibiting constructional errors once assembled. Attempts to correct for these errors by the biasing of the focus electrode result in tremendous defocusing of the beam, and only compound the existing perturbations.

2.3.4 Existing Gun Designs

The project on which the author was working was to demonstrate the technological capability of manufacturing travelling wave tube amplifiers. The tubes were to have a helix slow wave structure, PPM focusing, and were to be of a metal/ceramic construction. The gun required for the tubes had the following specifications:

Beam voltage:	*4.5 kV*
Beam current:	*80 mA*
Beam minimum diameter:	*1.5 mm*
Minimum gun perveance:	*0.25 μP*

The initial design was carried out by Mr D.M. Smith [3] and was based on the Pierce Gun Synthesis Program written by Vaughan [20]. An assembly diagram of the final construction is shown in figure 2.10. The cathode used was a nickel based oxide-coated cathode, heated indirectly by an anti-phase wound heater. The cathode

spherical radius was 13.1 millimetres, while its cylindrical radius was 2.35 millimetres. The Pierce focus electrode was made of 0.1 millimetre thick ferry sheet, and was designed to operate at cathode potential. The anode, with a spherical radius of 6.21 millimetres, was made from Oxygen Free High Conductivity (OFHC) copper and had an aperture radius of 1.34 millimetres.

The heater, cathode, focus electrode and anode were all supported on separate kovar disks and insulated from one another by ceramic spacers. The ceramic spacers were brazed to the kovar using active brazing techniques, and formed the vacuum envelope for the tube. This method of construction posed several problems to the operation of the tube.

Because the electrodes were all supported by the ceramic spacers making up the vacuum envelope, the interelectrode spacing was determined solely by the dimensions of the ceramic and braze material after the braze was performed. The difficulty of cutting ceramic to accurate dimensions combined with the unpredictable compression properties of the CH4 filler material led to irregularities in the electrode spacing, the adverse effects of which have been examined earlier in this chapter.

The focus electrode was supported on a separate kovar disk to the cathode, even though it was designed to operate at the same potential. This was so that the potential of the focus electrode could be modified to compensate for any displacement of the electrode from the cathode potential position. As the cathode support tube was heated, thermal expansion resulted in the focus electrode being displaced axially with respect to the cathode emitting surface, and a negative bias was necessary to restore the shape of the gun's equipotential contours. It was found that this negative biasing had detrimental effects on the electron beam and was thus undesirable.

Although the tube was to be operated under CW conditions, it is useful and sometimes essential to pulse an experimental tube while the magnet focusing stack is adjusted. The PPM magnet stack of a TWT generally needs to be fine tuned in the presence of an electron beam by shunting adjacent magnets until no helix interception is obtained. If the full beam power had to be intercepted by the helix during this process, irreparable damage could be caused and the tube would be lost.

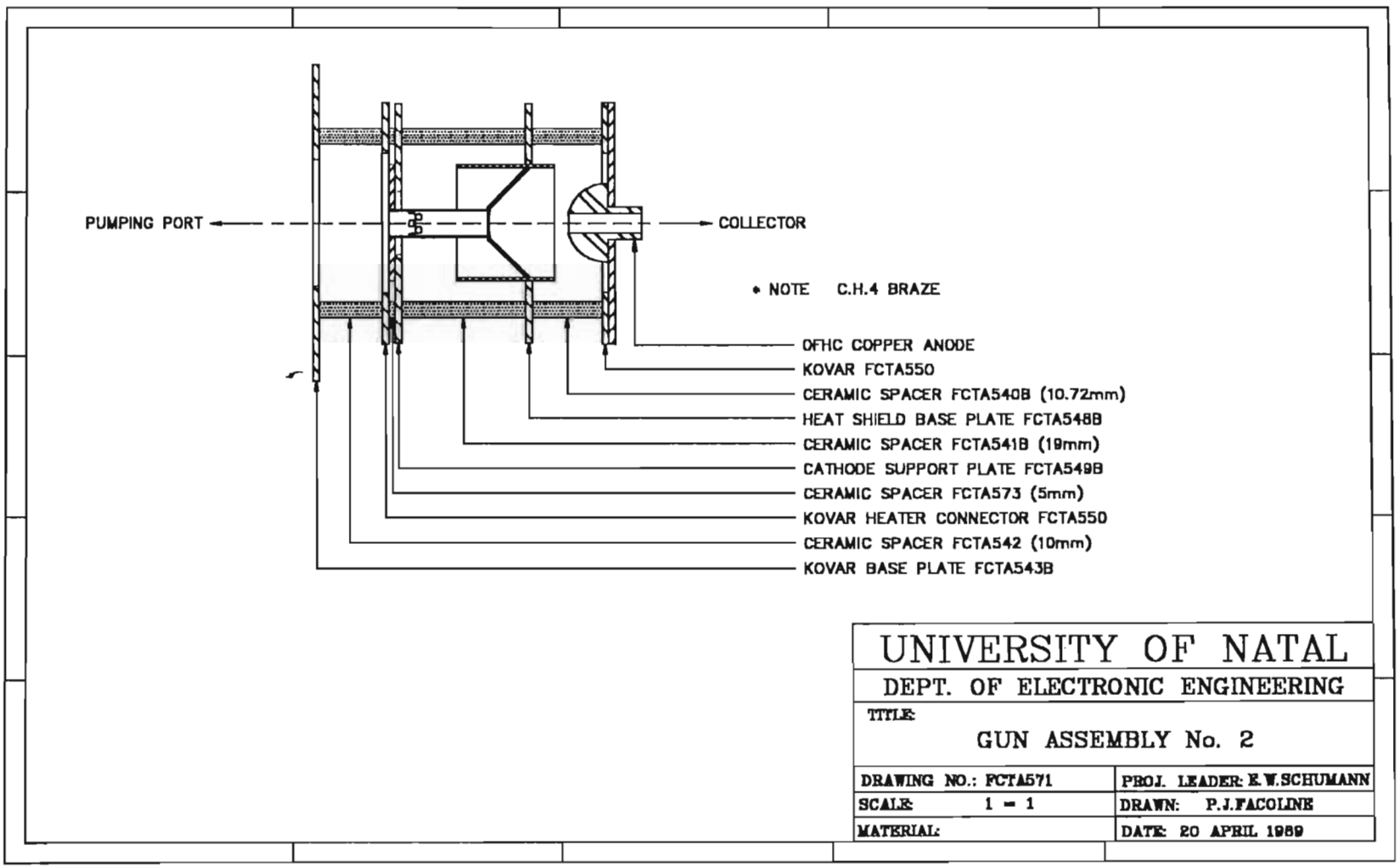

Figure 2.10 The Original Pierce Gun Assembly

For this reason, pulsing of the tube is necessary to reduce the overall power in the beam. By placing a sufficiently high negative bias on the focus electrode of a Pierce gun (-900 V with respect to the cathode in our case), the beam can be "pinched off" and modulated in this manner. However, this is a cumbersome method and requires a large negative power supply and modulator. A useful addition to the gun, therefore, would be a grid of some sorts, so that the tube could be easily operated under CW or pulsed conditions.

Several problems with the existing gun design have been outlined above. The solution to these problems along with some general improvements made by the author are addressed in Chapter 4 of this thesis. Before we can introduce the switching electrode which was responsible for many of the improvements, we need to take a closer look at different means of gun modulation, and the relative merits of each.

2.4 MODULATED ELECTRON GUNS

2.4.1 GRIDS

A fine mesh or grid is often placed in close proximity to the cathode so that a very small control voltage applied to the grid will switch the beam current on and off. Consequently, a low powered modulator is all that is required to pulse the tube.

A simple grid placed in the path of the beam intercepts as much as 15 per cent of the cathode current, resulting in power loss and excessive heating of the grid. Furthermore, grid-controlled tubes have been found to be unstable due to secondary emission from the grid structure. The interception can be reduced by placing a shadow grid between the cathode and the control grid, which shields the control grid from electrons leaving the cathode. The shadow grid is operated very near the cathode potential to reduce heating, and is sometimes bonded to the cathode itself. The latter case facilitates the alignment of the two grids which is essential for efficient operation of the control grid. Figure 2.11 shows several shadow grid structures.

The use of a grid, however, has detrimental effects on the electron trajectories within

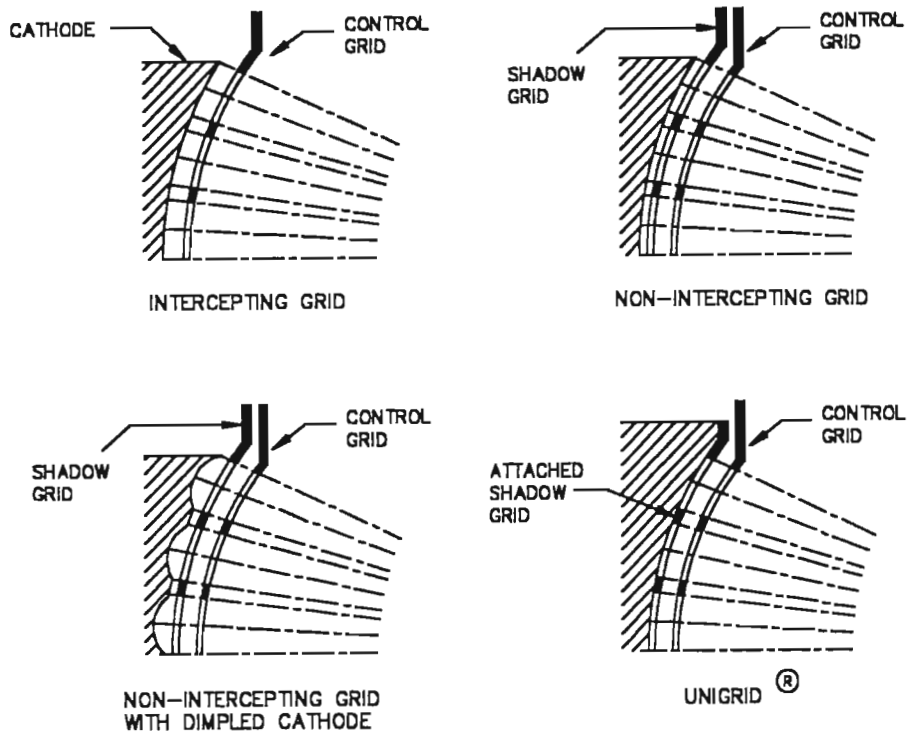

Figure 2.11 Grid Structures used for Current Control [13]

the electron gun, and the resultant beam is thus far from laminar on exiting the anode aperture. An increase in helix interception is a common result when using a grid, and the efficiency of the tube is thereby reduced.

2.4.2 Control Focus Electrodes

As mentioned previously in this chapter, the beam may be cut-off by applying a negative bias to the focus electrode of a Pierce electron gun. A disadvantage of this method is that the negative potential required for cut-off is very large. This potential may be reduced if an additional electrode is located in the centre of the cathode as shown in figure 2.12.

This method is not useful, however, for intermediate control of beam current due to the severe defocusing it causes to the electron beam. Becker [21] reports that biasing the focus electrode slightly with respect to the cathode allows the electrode to be used as a Wehnelt electrode, which has the advantage of permitting adjustment of

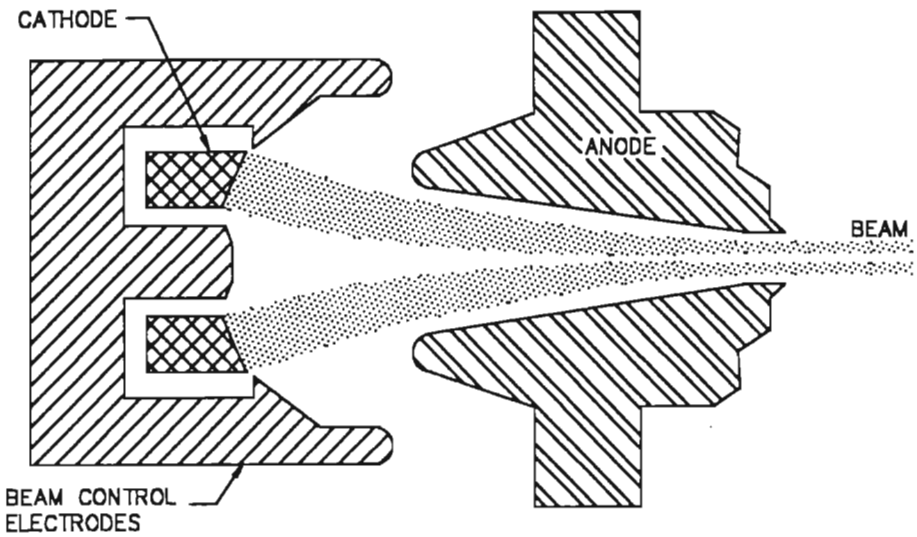

Figure 2.12 Control Focus Electrode Gun [13]

the beam compression-perveance relation at the expense of some deterioration of beam quality.

2.4.3 Modulating Anodes

If the anode of a Pierce gun is insulated from the tube, and a second accelerating anode is placed between the first anode and the drift tube, then the beam may be modulated by varying the potential of the first anode (see figure 2.13). Although this provides good focusing at intermediate voltages, the voltage range over which the modulating anode must be varied is very large. Furthermore, the configuration is only useful in confined flow guns where the presence of a magnetic field within the gun prevents the beam from spreading under space-charge forces once it has left the modulating anode.

The cut-off amplification factor μ_c is defined as the ratio of beam voltage to the negative beam control electrode voltage needed for cut-off. The intercepting and shadow grid configurations both have high values for μ_c, but the laminar nature of the beam is severely affected. The modulating anode exhibits good beam focusing at low voltages but has a low value for μ_c, while the control focus electrode is poor in both regards.

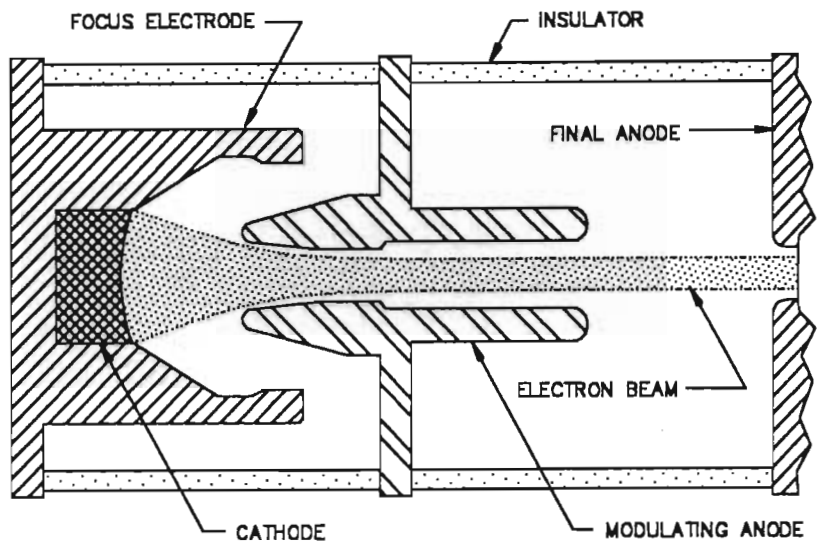

Figure 2.13 Modulating Anode Gun [13]

SUMMARY

Space-charge emission between electrodes was investigated, and the equations governing such flow. The electron current was found to be proportional to the 3/2 power of applied anode voltage for diodes of any electrode shape, provided that the current was limited by the negative space-charge of the electrons. By making an aperture in the anode, a beam of electrons can be obtained, but beam forming electrodes are required to prevent the beam from diverging due to the radial electric field of the beam itself. Practical electron guns were found to be far from ideal, with constructional tolerances having a large influence on the quality of the electron beam. Shortfalls of the existing design being used were outlined. Finally, a look was taken at different methods of modulating an electron beam, and some of the advantages and disadvantages of each. It now remains to develop a means of compensating for perturbations in the electron beam, and of switching the gun simply, effectively, and with the minimum effect on the electron trajectories.

REFERENCES

[1] J.W. Gerwartowski and H.A. Watson, "Principles of Electron Tubes", New York: Van Nostrand, 1965.

[2] I. Langmuir and K.T Compton, "Electrical Discharges in Gases, Part II", *Review of Modern Physics*, vol. 13, pp. 191-256, 1931.

[3] D.M Smith, "The Theoretical and Practical Analysis of Low Perveance Pierce Electron Guns", University of Natal M.Sc.Eng. thesis, 1990, pp. 20-23.

[4] reference [3], pp. 26-34.

[5] reference [1], p. 120.

[6] reference [1], p. 121.

[7] reference [1], p. 137.

[8] J.R. Pierce, "Theory and Design of Electron Beams", New York: Van Nostrand, 1954.

[9] reference [8], pp. 175-177.

[10] A.S. Gilmour, "Microwave Tubes", Dedham: Artech House, 1986.

[11] T. Shimada and M. Nishimaki, "A Method of Reducing the Effects of Anode Aperture in High-Perveance Convergent Electron Guns", *IEEE Transactions on Electron Devices*, vol. ED-15, no. 11, pp.907-914, November 1968.

[12] A.W. Stokes, "Magnetic Focusing of Electron Beams for Linear Beam Tubes", University of Natal M.Sc.Eng. thesis, 1990.

[13] reference [1], p. 103.

[14] reference [10], p. 28.

[15] A. von Engel, "Ionised Gases", Clarendon Press, Oxford, 1955, pp.46-58.

[16] A.H.W. Beck and J.K Smith, "Residual Gas Effects in a 25kW Ceramic Envelope Klystron", *4th International Symposium on Residual Gases in Electron Tubes*, pp. 255-263, 1971.

[17] K. Amboss, "The Effect of Tolerances in Conical Flow Pierce Guns", *IEEE Transactions on Electron Devices*, vol. 13, pp. 313-321, 1965.

[18] M.C. Lampel, R.E. Rand, D.Y. Wang and W.B. Herrmannsfeldt, "Sensitivity of Perveance to Cathode Placement in a Low Perveance Electron Gun", *IEEE Transactions on Nuclear Science*, vol. NS-32, no. 5, pp.1776-1778, October 1985.

[19] reference [3], pp. 132-135.

[20] J.R.M. Vaughan, "Synthesis of the Pierce Gun", *IEEE Transactions on Electron Devices*, vol. 15, pp. 37-41, January 1981.

[21] R. Becker, "Two Electron Guns with Adjustable Beam Compression and Perveance", *Nuclear Instruments and Methods*, vol.187, pp.255-258, 1981.

CHAPTER 3.

A SWITCHING ELECTRODE

One of the principal objectives of this design was to improve the characteristics of the electron beam emerging from the anode aperture for various gun operating conditions. It was hoped to increase the laminarity of the electron flow at the beam minimum and thus reduce the radial component of electron velocity at this point, a condition necessary for Brillouin flow. A further condition, and one which the design hoped to achieve, is the attainment of a uniform current density across the diameter of the beam. Although this is an ideal situation difficult to obtain in practice, the cross-sectional beam profile of previous guns showed a considerably high current density towards the centre of the beam, and undue anode interception of beam-edge electrons.

The electron beam is injected into the magnetic field of the PPM stack at the point of minimum beam diameter, and as such the axial position and diameter of this point must be known accurately. An analysis performed by Mr D. Smith [1] showed that the actual position of the beam minimum in a practical Pierce gun differed somewhat from the design figure, as did the beam diameter. If some sort of electron lens could be incorporated into a gun design, the diameter and axial position of the beam minimum could be varied within limits to suit the magnet stack entrant conditions. The different focusing requirements of CW or pulsed operation could therefore also be accommodated. Furthermore, constructional errors could be compensated for to produce a tube that meets its specifications more closely.

Finally, modulation of the tube in a manner that was simple and inexpensive in terms of manufacturing processes was required. Mesh grids in close proximity to the cathode, although providing excellent cut-off amplification factors, are costly to implement by virtue of their complexity. Furthermore, the perturbing effects they have on the electron trajectories would not assist in making the improvements suggested above.

One possible means of modulation would be to introduce a modulating anode. However, as the gun in question does not operate under confined-flow conditions, the electrons would diverge under space-charge repulsion on exiting the first anode. If the single Pierce anode is pulsed, the full gun voltage would have to be switched, requiring an expensive and complex modulator. For this reason, an additional open aperture electrode was introduced between the cathode and anode, which would operate at a much lower voltage than a modulating anode, and which would provide an extra degree of freedom to the beam formation process. A schematic of the switching electrode gun is shown in figure 3.1.

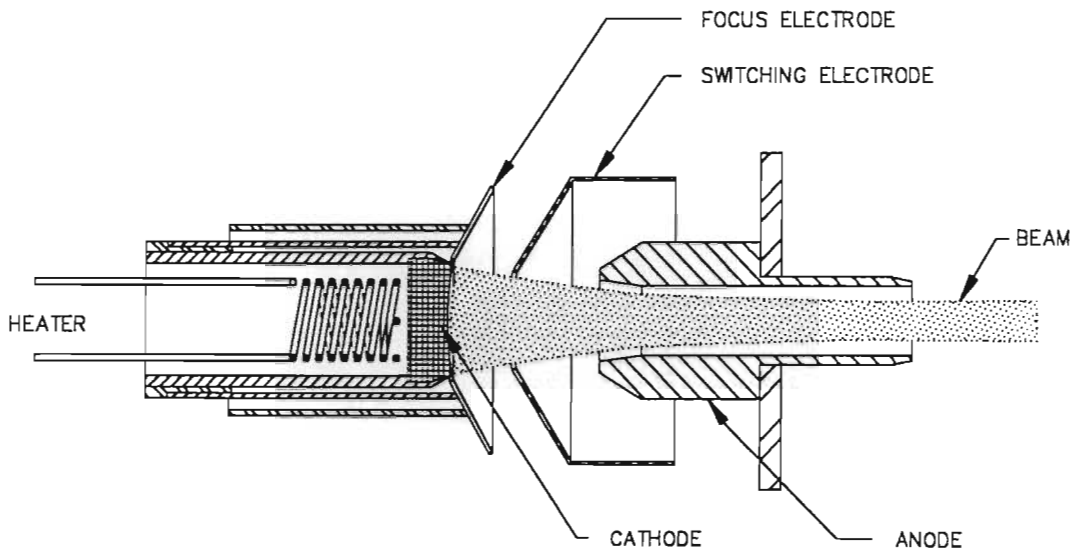

Figure 3.1 Switching Electrode Gun Schematic

The position and shape of the electrode, as well as its bias voltage, were the critical factors to be considered. The further the electrode was from the cathode, the more effective it would be at switching off the beam, while the potential that would have to be switched would also increase. The effect of the electrode position on the laminar nature of the electron beam was the dominant factor as it determined the extent to which the transverse forces on the beam-edge electrons could be reduced.

3.1 TRANSVERSE FORCES ON BEAM EDGE ELECTRONS

The importance of a laminar beam at the beam minimum, ie. all electrons travelling in paths which are parallel to one another, has already been stressed. To achieve this, each electron should only experience a radial component of electric field, and no transverse field. The space-charge repulsion of the beam tends to force the electrons away from the axis of the gun, and needs to be balanced by the external electric field due to the electrode potential.

The potential profile from cathode to anode inside the beam is somewhat depressed due to space-charge effects compared with the profile without space-charge just outside the beam edge. This difference causes bending of the equipotentials in this region, and the result is a deflection of the electron trajectories (see figure 3.2).

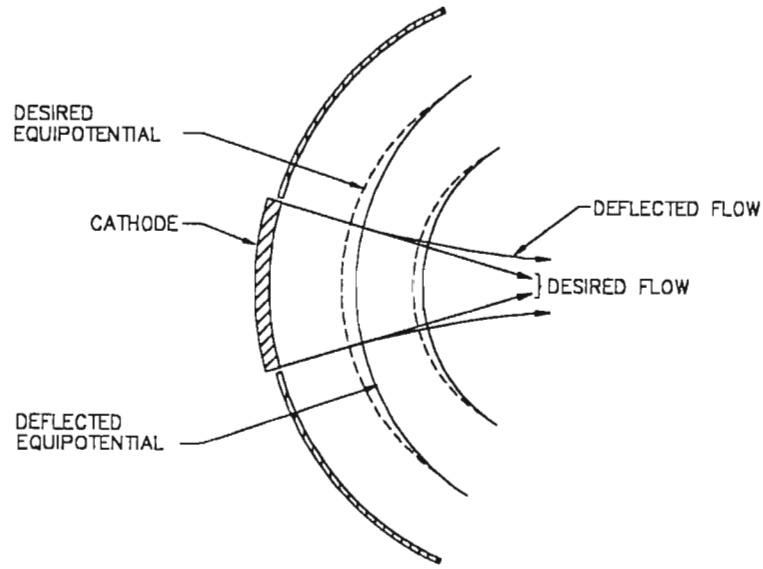

Figure 3.2 Bending of Equipotentials in Spherical Diode (after[2])

Equation (2.5) described the current-voltage relationship for space-charge-limited flow in a planar diode. A similar solution for the case of spherical electrodes was found

by Langmuir & Blodgett [3] in terms of a dimensionless quantity α, as:

$$I = 29.33\times10^{-6}.\frac{V^{\frac{3}{2}}}{(-\alpha)^2} \qquad (3.1)$$

where α is a function of the ratio of the anode to cathode spherical radii. For a gun with a cone half angle of Θ, (3.1) reduces to:

$$I_0 = 14.67\times10^{-6}.\frac{(1-\cos\theta)V^{\frac{3}{2}}}{(-\alpha)^2} \qquad (3.2)$$

Pierce [4] tables $(-\alpha)^2$ versus the ratio of cathode to anode radius. A polynomial curve fitting sequence was applied to the tabled data enabling (3.2) to be plotted for a fixed value of current I_0 and cone half angle Θ. The result is a potential profile from cathode to anode for a spherical diode with space-charge, as shown in figure 3.3.

Finite element analysis was used to generate potential profiles in the anode-cathode region for different positions and potentials of the switching electrode. As it is the profile just outside the beam that one is interested in, space-charge was ignored in the analysis. Figure 3.4 shows how the potential profile outside the beam edge can be depressed until it approximates the profile within the beam, by merely lowering the applied voltage to the switching electrode. As the two profiles are approximately the same, there is no bending of the equipotentials at the beam edge, and the transverse force on an electron is reduced. It was this consideration which determined the ultimate position of the switching electrode.

Having determined the optimum position of the electrode aperture, it remained to determine the effect of the electrode shape on beam properties, as well as the extent to which the electrode could be used to control certain beam characteristics.

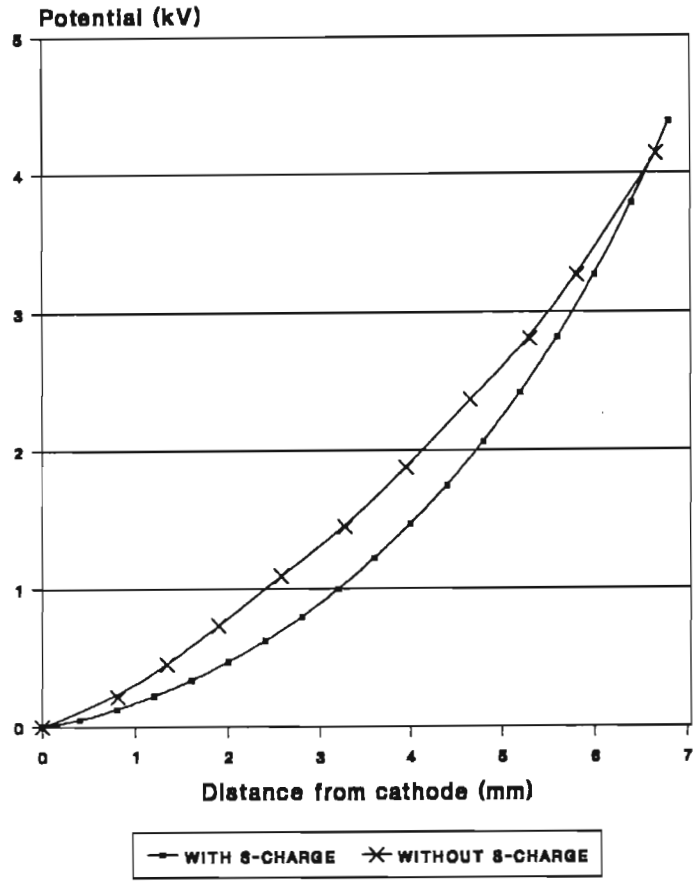

Figure 3.3 Potential Profile from Cathode to Anode with and without Space-Charge

3.2 MODELLING OF THE SWITCHING ELECTRODE

3.2.1 Finite Element Analysis without Space-Charge

As the electric field in the interelectrode space maps applied anode potential linearly, space-charge was initially ignored when analysing the effect of the electrodes on the electric field at the cathode surface. By monitoring the reduction in the near cathode electric field without space-charge, the reduction in beam current with space-charge could be estimated by raising the electric field reduction ratio to the three halves power, in accordance with equation (2.5).

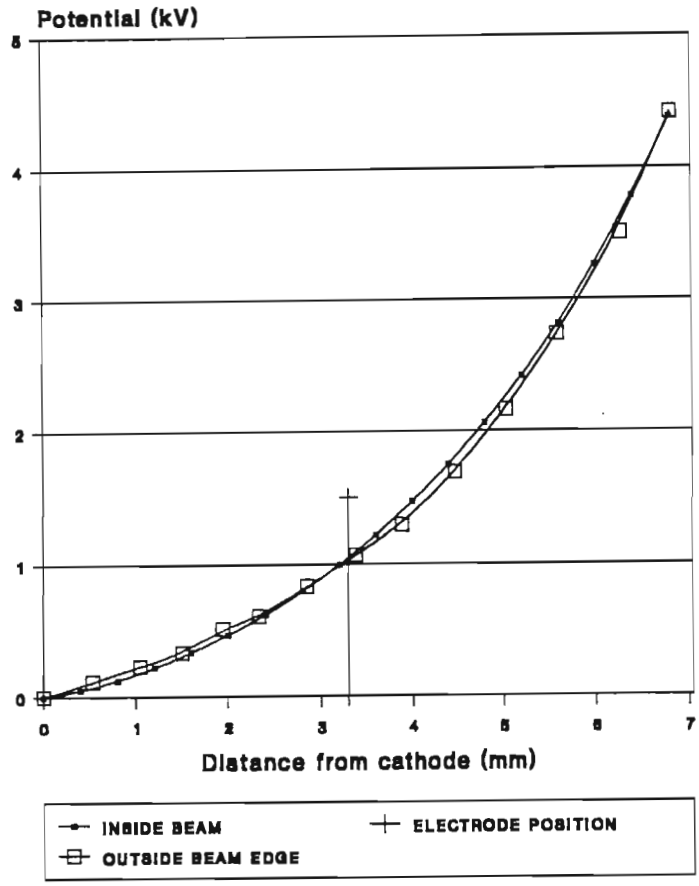

Figure 3.4 Reshaping of Potential Profile in Charge-Free Space Outside Beam

The gain of a travelling wave tube is given by Pierce [5] as:

$$G = -9.54 + 47.3CN \quad db \tag{3.3}$$

where

$$C^3 = (2K)\left(\frac{I_0}{8V_0}\right)$$

and N is the number of wavelengths of the slow wave structure. A design figure of 5 per cent cathode current at cut-off was chosen. Consequently, the defocused current exiting the anode and reaching the collector would be in the order of only a fraction of a per cent, meaning a reduction in the gain of the tube from 30 dB to less than 0 dB, and a reduction in the beam power from 360 Watts to less than 4 Watts.

Using this method of electric field reduction ratio without space-charge, a cathode cut-off current of 4 per cent of normal was calculated for the electrode position and

diameter determined in section 3.1. Furthermore, with the switching electrode in position, the focus electrode was found to be effective only in the near-cathode region, and as a result could be reduced in size, as shown in figure 3.5.

It was also found that the gap between the cathode surface and the edge of the focus electrode caused considerable fringing of the electric field lines in this region. As this would result in the electrons emitted from the cathode edge having transverse velocities, the heat shield and cathode support assembly was redesigned to allow the focus electrode aperture to be made smaller without fear of it coming into contact with the cathode and causing heat loss through conduction.

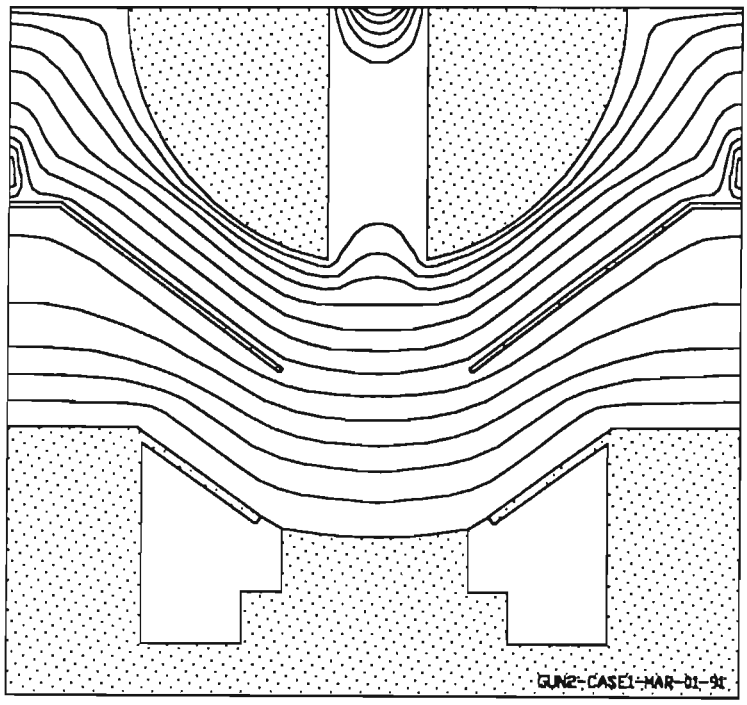

Figure 3.5 Geometry for Finite Element Analysis of Electron Gun Showing Equipotential Contours

3.2.2 An Electron Optics Design Program

Modelling of the switching electrode, taking into account the effects of space-charge, was carried out with the aid of Herrmannsfeldt's [6] electron optics program, *EGUN*. The program solves Laplace's equation for the boundary values specified by the user to find the potential distribution in the interelectrode space. Child's law is then used

to determine the emission current density at the cathode surface, and several electron trajectories are plotted. The space charge distribution obtained from the initial trajectory plots is then used to solve Poisson's equation, giving a new potential distribution, and the iteration process is repeated. The outputs of the program include an electron trajectory plot, a cross-sectional current density profile of the beam minimum, the angles of divergence of all electrons on passing through the minimum, and the various gun current and voltage parameters.

A simulation of Smith's [1] original gun design showed a remarkable correlation with actual results obtained, and lent credibility to the methods used. Furthermore, substantial agreement between simulated and measured data has also been obtained by other authors [7],[8] using *EGUN*, giving this author confidence to continue with the design based on these results. The simulation results for the modulated gun are presented in section 3.3, while the trajectory plot for Smith's gun is shown in figure 3.6.

Using *EGUN* it was found that the switching electrode need not approximate the shape of an equipotential, but could be conical in shape so long as the cone angle was chosen carefully. This meant that the manufacture of the electrode would be much simplified. A final cone half angle of 53.8 degrees was found to give optimum results, corresponding to an electrode angle of 65 degrees with the beam edge. The electron trajectory plot for the modulated gun, showing the position and shape of the switching electrode, is shown in figure 3.7.

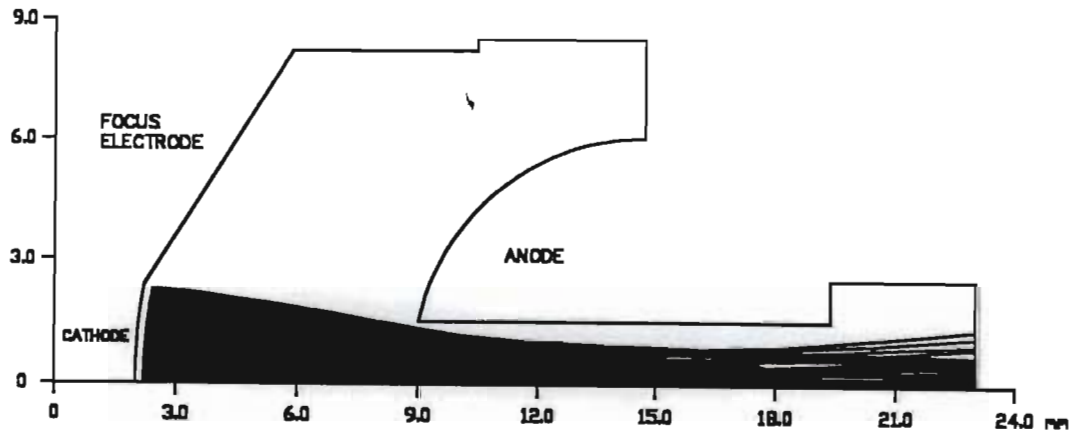

Figure 3.6 Trajectory Plot for Pierce Gun Obtained using *EGUN*

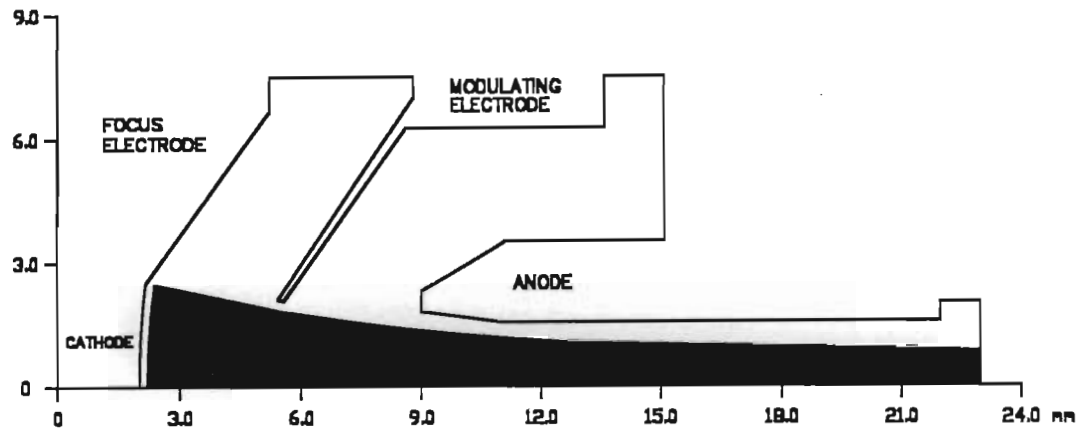

Figure 3.7 Trajectory Plot for Switched Gun

3.3 RESULTS OF SIMULATIONS

3.3.1 Beam Laminarity

The importance of a laminar beam has already been stressed in Chapter 2. The ideal laminar beam would have all electrons travelling parallel to the gun axis at the beam minimum, and their angle of divergence from the axis would thus be zero. For the purpose of simulating a practical gun, all electrons having a divergence angle of less than 30 milliradians (1.7 degrees) shall be considered as laminar in nature.

An analysis of the first Pierce gun used in the project showed that the electrons entering the PPM focusing stack had converging or diverging angles of up to 5 degrees from the stack axis under best case conditions. The introduction of the switching electrode resulted in the maximum deviation from ideal being less than 1 degree (see figure 3.8).

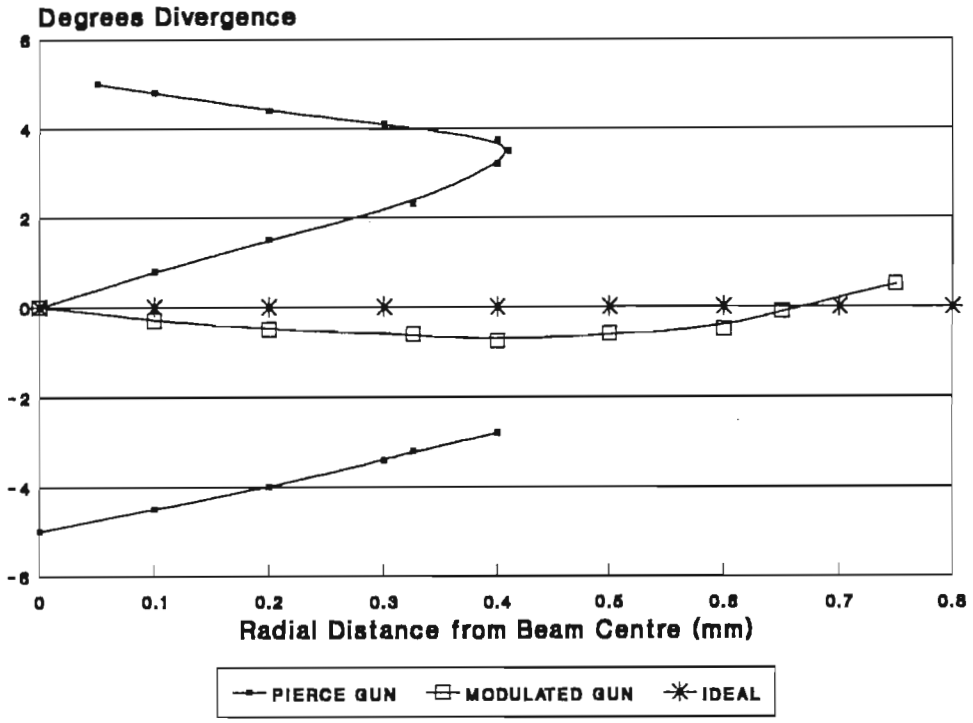

Figure 3.8 Simulated Angle of Divergence of Electrons at Beam Minimum

3.3.2 Position and Diameter of Beam Minimum

By varying the potential of the switching electrode, the axial position of the beam minimum could be moved within bounds. As it is sometimes difficult in an experimental tube to align the beam minimum with the first PPM pole piece, this would be a useful feature. As the potential is varied, there is an effect on the laminarity of the beam, and a trade-off must therefore be reached between the position and laminarity of the beam minimum. Figure 3.9 shows a variation in the minimum position from 18 to 22 millimetres from the cathode surface, and a corresponding increase in the number of electrons having an angle of divergence greater than 30 milliradians from approximately 1 per cent at best to less than 10 per cent at either extreme.

Similarly, the diameter of the beam minimum could be varied from 0.4 millimetres to

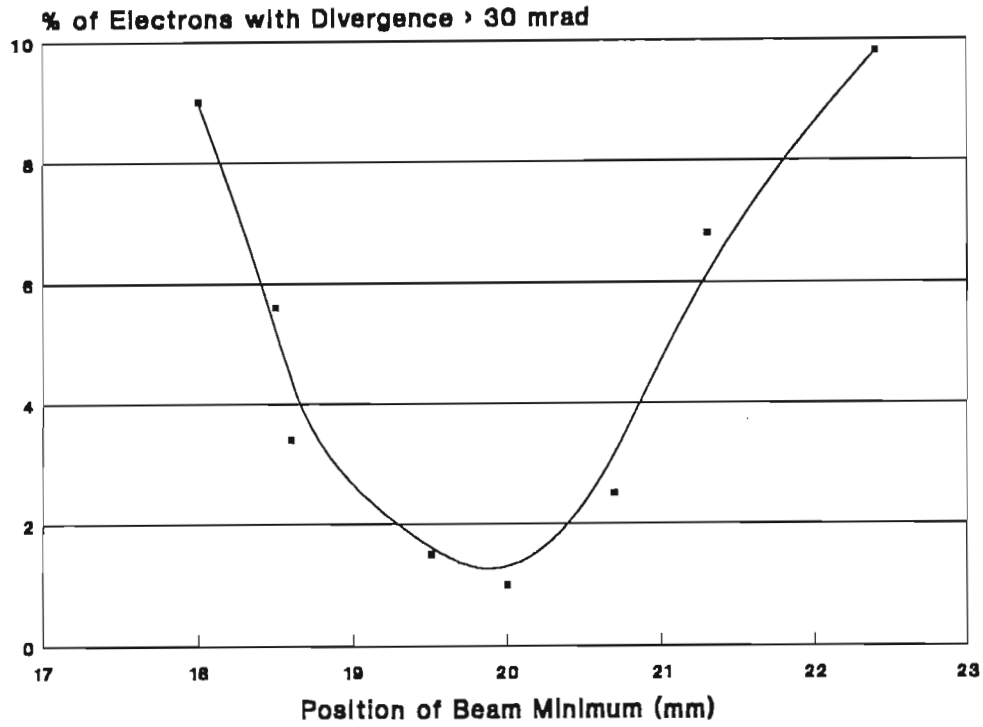

Figure 3.9 Position of Beam Minimum vs Laminarity

1.0 millimetres* for a corresponding variation in the number of non-laminar electrons of less than 10 per cent (see figure 3.10).

3.3.3 Cross-Sectional Current Density Profile

Although a uniform current density profile across the diameter of the beam is desired for Brillouin flow, a real beam profile would show a distinct curved distribution at the beam edge. Even so, a peaked profile displaying a concentration of current density at the centre of the beam should be avoided if the magnetic focusing is to be effective. The simulations showed an improvement in the current density profile at the beam minimum for the case of the modulated gun, as shown in figure 3.11.

*The design figure for beam radius was 0.75 millimetres

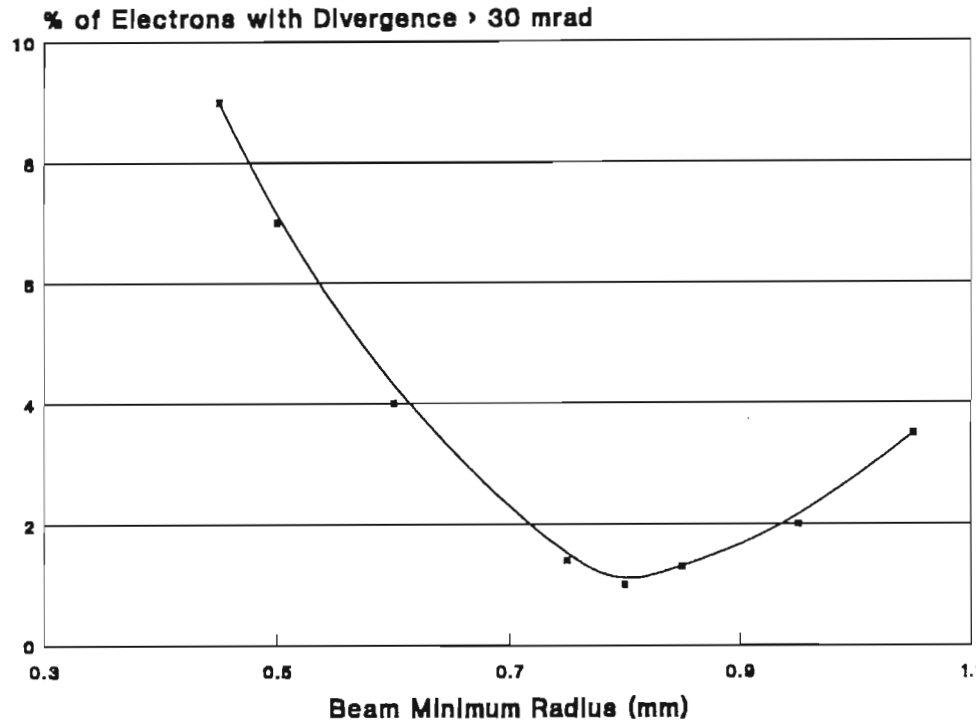

Figure 3.10 Radius of Beam Minimum vs Laminarity

3.3.4 Dynamic Focusing of Electron Beam

It has been shown that the greatest perturbations in the electron beam are caused as a result of shifts in the anode-cathode spacing due to constructional tolerances or due to thermal expansion of gun components. By varying the spacing of the anode and cathode during the simulations, the ability of the switching electrode potential to adjust for this variation could be observed. Although the variation in electrode spacing shown in figure 3.12 is far larger than would be experienced in practice, the curve shows what potential would be needed on the switching electrode to return the axial position of the beam minimum to its original design position.

The lens effect of the switching electrode was also illustrated by the simulations, as shown in figure 3.13. By varying the electrode potential, the beam waist could be enlarged or reduced by the diverging or converging action of the electron lens created by the three gun electrodes. The combined effect of the above two phenomenon is that the characteristics of the gun can be varied to some extent to adjust for non-ideal focusing conditions caused by gun anomalies.

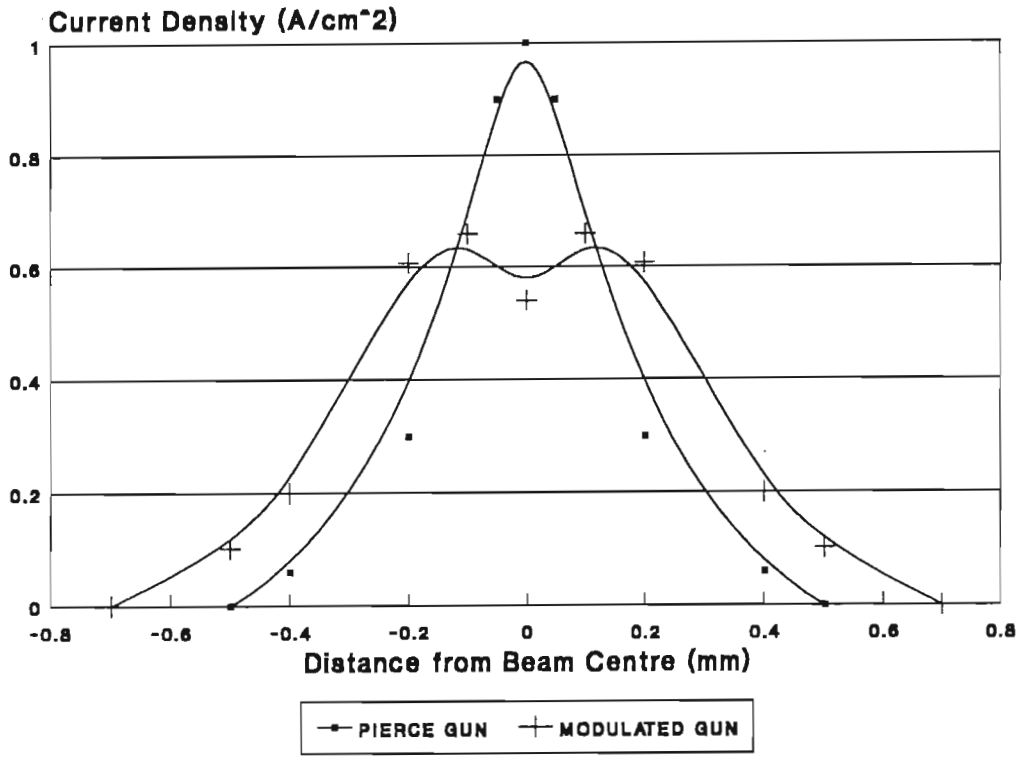

Figure 3.11 Normalised Current Density Profile of Simulated Beams

3.3.5 Variable Perveance

The perveance of a Pierce electron gun is determined by the geometry of the gun, and hence would be reliant on the constructional tolerances of the electrode spacing. To avoid different perveances for each experimental gun developed, it would be useful to be able to adjust the perveance slightly once the geometry was established. For perveance to be variable with switching electrode potential, the ratio between the beam current and the 3/2 power of anode potential must be constant for any one value of switching electrode potential. The effect of different electrode potentials on gun perveance is shown in figure 3.14 by the different slopes of the $I\text{-}V^{3/2}$ plot.

Having established that the perveance is indeed constant over a wide range of anode potentials, the anode potential could then be fixed, keeping the final velocity of the electron beam constant, and the potential of the switching electrode then varied to alter the overall beam current.

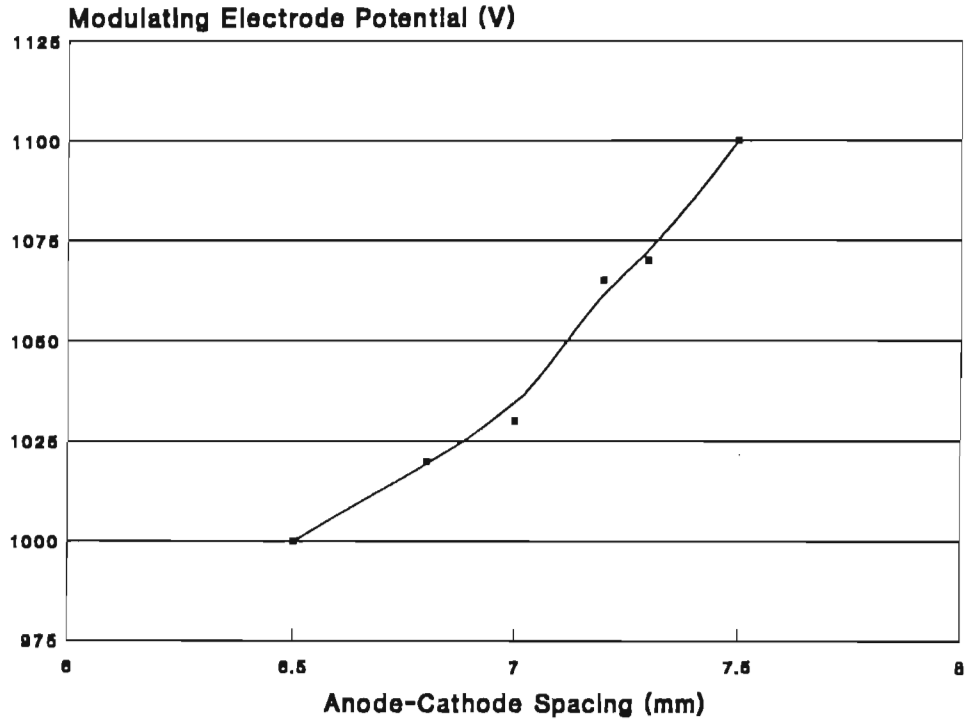

Figure 3.12 Electrode Potential vs Anode-Cathode Spacing for Constant Axial Position of Beam Minimum

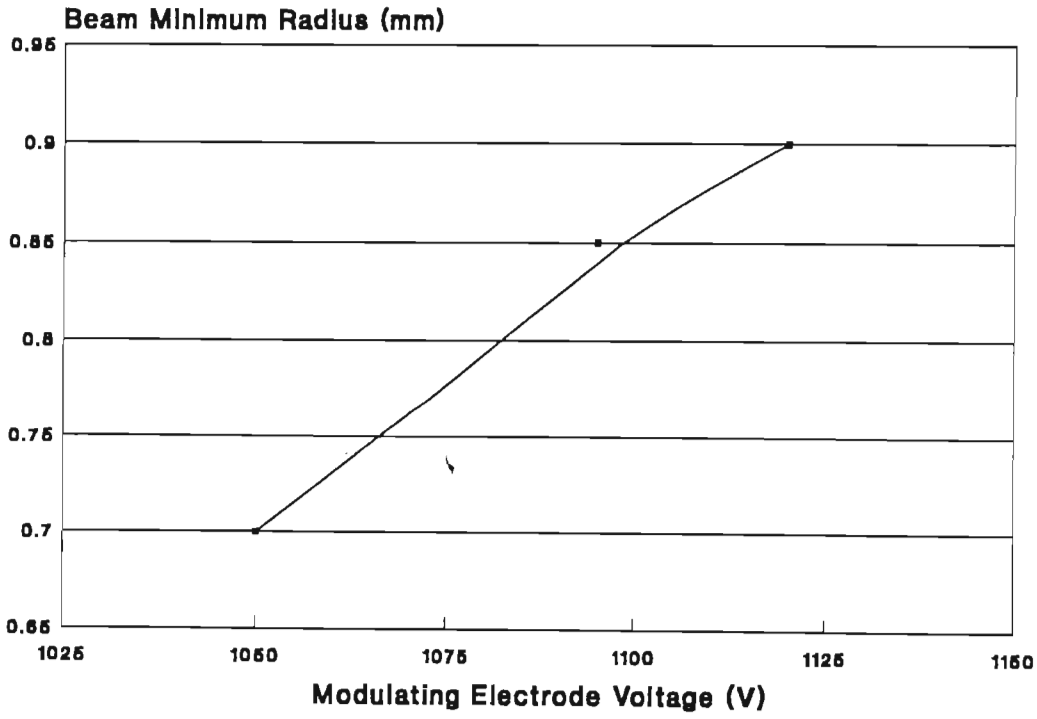

Figure 3.13 Lens Effect of Switching Electrode

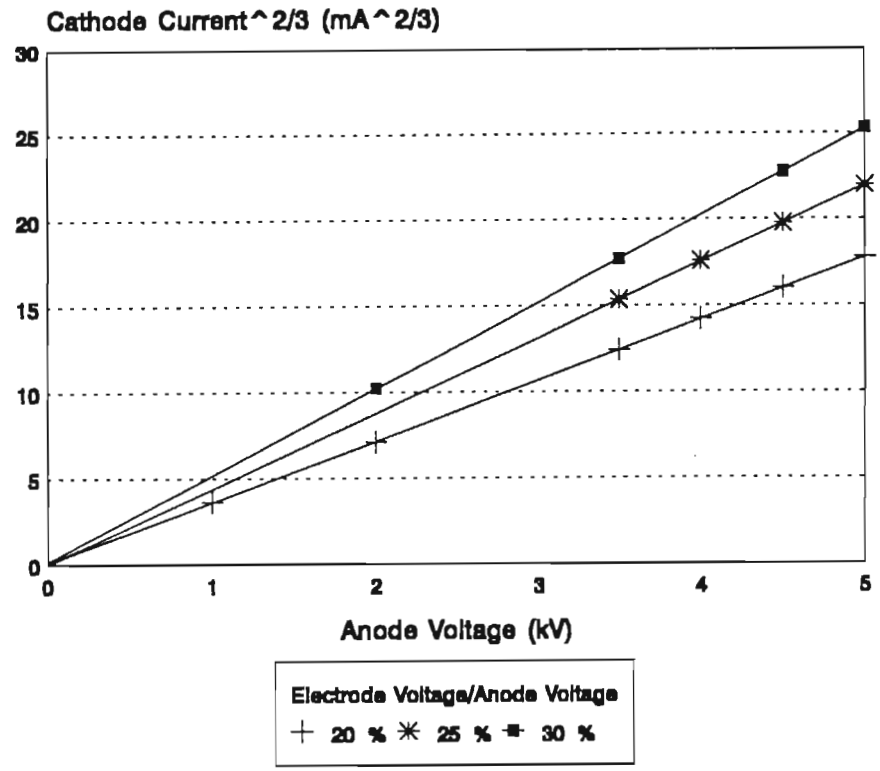

Figure 3.14 Variable Perveance of Electron Gun

3.3.6 Beam Cut-Off

The beam current that would flow under cut-off conditions, ie. switching electrode at same potential as cathode, was already ascertained by using finite element analysis to calculate the change in electric field at the cathode surface, and *EGUN* merely confirmed these findings. However, how the cut-off current was to be collected was accurately observed by means of a trajectory plot for cut-off conditions. As expected, the defocused beam was collected harmlessly by the molybdenum anode, with only a few microamperes passing through the anode aperture.

The *EGUN* simulations also enabled the author to reduce the size and complexity of the anode geometry by ascertaining exactly what aspects of the original Pierce anode were important to the beam formation process. Minor alterations to the design value of anode-cathode spacing and focus electrode dimensions were also made.

SUMMARY

This chapter has seen the introduction of an additional electrode to the Pierce gun, which can be used not only for switching of the electron beam, but also to improve certain beam characteristics, and to compensate for gun anomalies. Although the practical results of the gun have yet to be presented in the following chapter, the initial simulations show very encouraging results indeed. The electron beam has been found to be more laminar in nature at the beam minimum due to the reduction in the transverse forces exerted on the beam edge electrons. The position and diameter of the beam minimum can be varied to suit the magnet stack entrant conditions, while an improvement in the cross-sectional current density profile has also been noted. The perveance of the gun is no longer dependant solely on the electrode geometry, but may be varied during operation by altering the potential of the switching electrode. As the beam is cut-off by merely pulling the potential of the switching electrode down to cathode potential, no power supply is required for the modulator, with the "on" bias being obtained from a resistor divider. The adverse effects of conventional mesh grids has been avoided, as the switching electrode intercepts no beam current at all. As similar simulations performed on the existing gun design showed close correlation with actual results, the author felt confident that the modulated gun would behave as predicted.

REFERENCES

[1] D.M. Smith, "The Theoretical and Practical Analysis of Low Perveance Pierce Electron Guns", University of Natal M.Sc.Eng. thesis, 1990.

[2] A.S. Gilmour, "Microwave Tubes", Dedham: Artech House, 1986, p. 147.

[3] I. Langmuir and K. Blodgett, "Currents Limited by Space-Charge Between Concentric Spheres", *Physics Review*, vol. 24, pp. 49-59, 1924.

[4] J.R. Pierce, "Theory and Design of Electron Beams", New York: Van Nostrand, 1954, p. 183.

[5] J.R. Pierce, "Travelling-Wave Tubes", New York: Van Nostrand, 1950, pp. 16-18.

[6] W.B. Herrmannsfeldt, "EGUN-An Electron Optics and Gun Design Program", Stanford Linear Accelerator Centre, SLAC-331, October 1988.

[7] M.C. Lampel, R.E. Rand, D.Y. Wang and W.B. Herrmannsfeldt, "Sensitivity of Perveance to Cathode Placement in a Low Perveance Electron Gun", *IEEE Transactions on Nuclear Science*, vol. NS-32, no. 5, pp. 1776-1778, October 1985.

[8] Richard True, "The Deformable Relaxation Mesh Technique for Solution of Electron Optics Problems", Electron Tube Division, Litton Industries.

CHAPTER 4.

TEST GUN RESULTS

In order to perform a beam analysis on the test gun, the first modulated gun constructed was done so in a glass envelope. The glass enabled the operator to observe the movement of a beam analyzer plate as it was swung across the path of the beam, as well as to take temperature readings of the cathode surface by means of optical pyrometry. Once the necessary information had been obtained from this gun, the design could be incorporated with confidence into a travelling wave tube of the more robust metal/ceramic construction. As the thermal properties of the heater and cathode support had been characterised, a measurement of heater input power gave an indication of the temperature of the cathode emitting surface. The attributes of the electron beam leaving the gun were uniquely defined by the electrode potentials within the gun itself, again characterised by the results of the glass experimental gun.

As the same gun was to be incorporated into both ceramic and glass envelopes, the design had to be modular in nature, with the electrodes and their supporting structure independent of, but compatible with, the envelope chosen. For this reason, the existing design where the electrode supporting plates were sandwiched between ceramic insulating rings was not acceptable. Instead, the electrodes were to be supported by ceramic rods which formed no part of the gun envelope, resulting in a gun module which could be used in either a glass or metal/ceramic tube, or even moved from one to the other.

Before examining the practical results of the test guns manufactured, it would be informative to look briefly at the construction and assembly of the various gun components.

4.1 COMPONENT FABRICATION

4.1.1 Switching and Focus Electrodes

To facilitate manufacture of the switching and focus electrodes, the switching electrode was designed to have the same cone half-angle as the focus electrode, namely 53.8 degrees. Simulations revealed satisfactory results for this arrangement. The two electrodes were made from ferry, which being non-magnetic did not influence any stray magnetic fields within the gun itself.

A one inch disk was first punched out of a 0.15 millimetre thick ferry sheet before being deep drawn to the approximate electrode shape using a series of dies. A die giving the correct cone angle was manufactured in the department to press the final shape of the electrodes. Each drawn tube was then parted off at the required position and the aperture holes drilled to give two different electrode configurations. Figure 4.1 shows two focus electrodes on the left, two switching electrodes on the right, and the final die in the series in the background.

Figure 4.1 Focus Electrode, Switching Electrode and Final Die

4.1.2 Focus/Heat Shield Assembly

Previously, the cathode and focus electrode were insulated from one another electrically so that a bias potential could be applied to the focus electrode to compensate for errors in their axial alignment. As compensation could now be achieved with the switching electrode, the focus electrode could be operated at the same potential as the cathode, allowing for closer alignment, a smaller focus aperture, and thus reduced fringing of electric fields at the cathode surface.

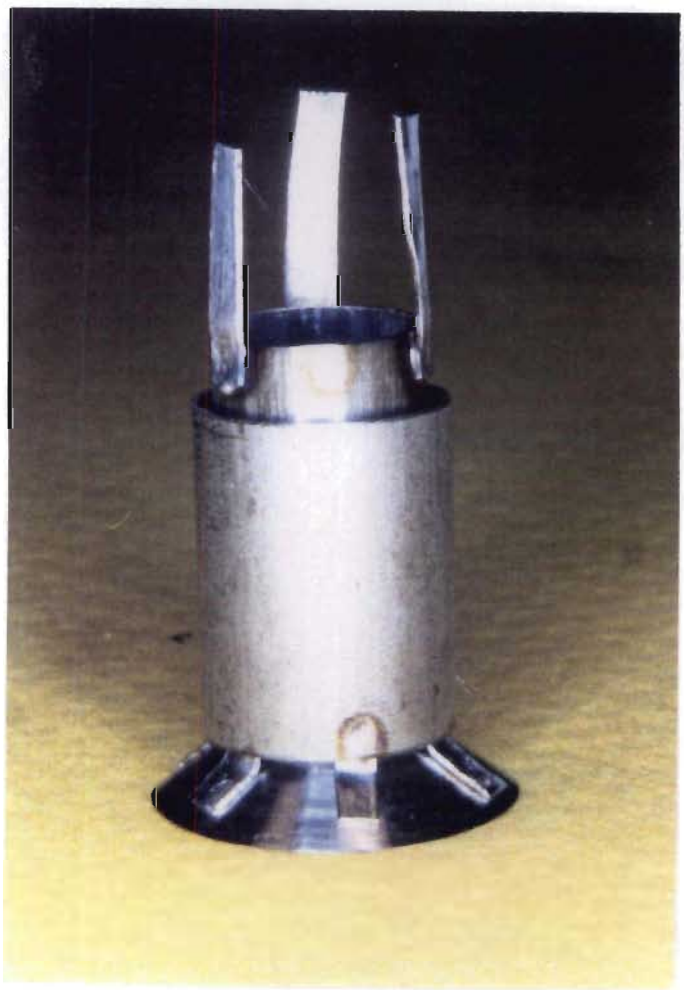

Figure 4.2 Focus Electrode and Heat Shield Assembly

The cathode heat shields, designed to reduce the nett power radiated by the cathode, were both made from 0.25 millimetre thick molybdenum tubing, and were spot welded to the focus electrode using ferry tags. Figure 4.2 shows the two heat shields attached to the focus electrode in this manner. The three ferry tags spot welded to the inner heat shield were used to fix the cathode holder in place.

4.1.3 Cathode Holder

As many tube failures are as a result of cathode poisoning, it is advantageous to design the cathode holder in such a manner that it may be easily removed from a gun and replaced with a healthy cathode in the event of poisoning. Furthermore, most braze materials have a detrimental effect on cathode emission and as such should not be used in the assembly of cathode structures. For this reason, crimping was used to secure the cathode pellet to its supporting structure. The cathodes used were of the tungsten impregnated variety, a topic discussed at some length in Chapter 5. Another advantage of crimping is that it can be performed quickly and cleanly immediately before inserting the cathode into the tube, thus reducing the risk of contamination.

A seat was machined in the inside of a 0.5 millimetre thick molybdenum tube to locate and hold the tungsten cathode pellet. The rim of the seat was filed down to a knife edge so that it could be crimped down onto the edges of the pellet using a suitable crimping tool. The cathode support tube was located inside the heat shields by means of a second molybdenum tube brazed around the base of the support tube. Brazing was achieved using a plasma jet welder with nickel as the filler material. This locating tube was turned down along most of its length to fit the inside of the first heat shield, leaving a 1 millimetre locating lip at its base. Figure 4.3 shows the locating tube, support tube and assembled holder with the cathode pellet in place ready for crimping.

4.1.4 Anode

Because of the high power handling capability of molybdenum, it was chosen as the material of construction for the anode. During cut-off conditions in the gun, the defocused cathode current is collected by the anode, and any thin walled components of the anode drift region would have to be able to handle the high temperatures generated.

Pierce gun design curves [1] give no rules for the shape of an anode so long as some semblance of the equipotential surface at that potential is followed. Consequently,

Figure 4.3 Cathode Holder Components and Assembly

the theoretical shape often assumed is spherical. By using suitable simulations as discussed in Chapter 3, that portion of the anode which was important to the electron beam formation could be determined, and optimised, to produce a simple and functional anode. The resultant anode design is shown in figure 4.4.

The anode is brazed to its kovar support plate using a high melting point (1235 °C) palladium/cobalt alloy, known commercially as Palco.

4.1.5 Electrode Supports

One of the principle drawbacks of using the electrode support plates as electrical connects through the vacuum envelope is the reliance of the electrode spacing on the ceramic envelope spacers. By making the electrode support structure independent of the envelope, greater accuracy can be achieved. A common method of achieving this is to align the electrodes on a central jig and then fuse molten glass rods to the support plates. When the centre jig is removed, the electrodes are fixed in space with respect to one another.

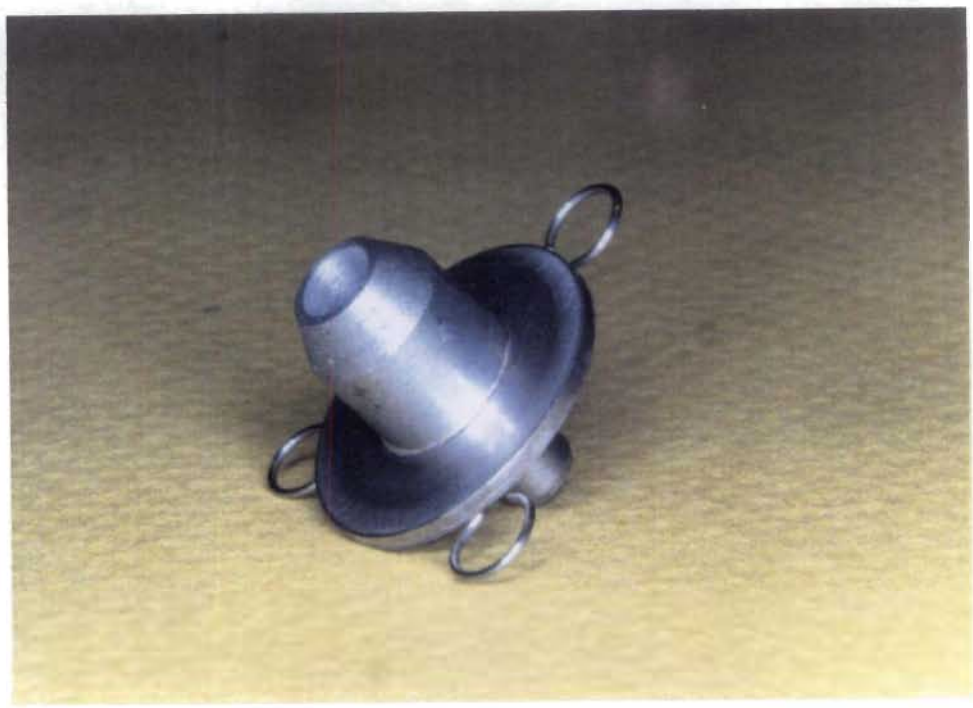

Figure 4.4 The Anode Assembly

Using glass support rods in this manner results in a very fragile structure, prone to cracking due to mechanical or thermal shock. By using ceramic rods for support and insulation, a much more robust system is obtained, provided a reliable joint can be made between the metal electrodes and the ceramic rods. Rings of 0.5 millimetre molybdenum wire, having inside diameters of 3 millimetres, were spot welded to the various electrodes at 120 degree intervals. With the electrodes supported accurately on a stainless steel centre jig, three ceramic rods each having an outside diameter of 3 millimetres were passed through the molybdenum rings. Further rings of active braze material* were placed over the molybdenum rings and the whole structure brazed together in a vacuum furnace.

Figure 4.5 shows two such metal/ceramic joints between molybdenum rings and an alumina rod. Evident from the picture is the excellent flow properties of the braze material on the molybdenum wire, and the neat metal fillets characteristic of a strong joint.

*See Appendix B for material description and brazing profiles.

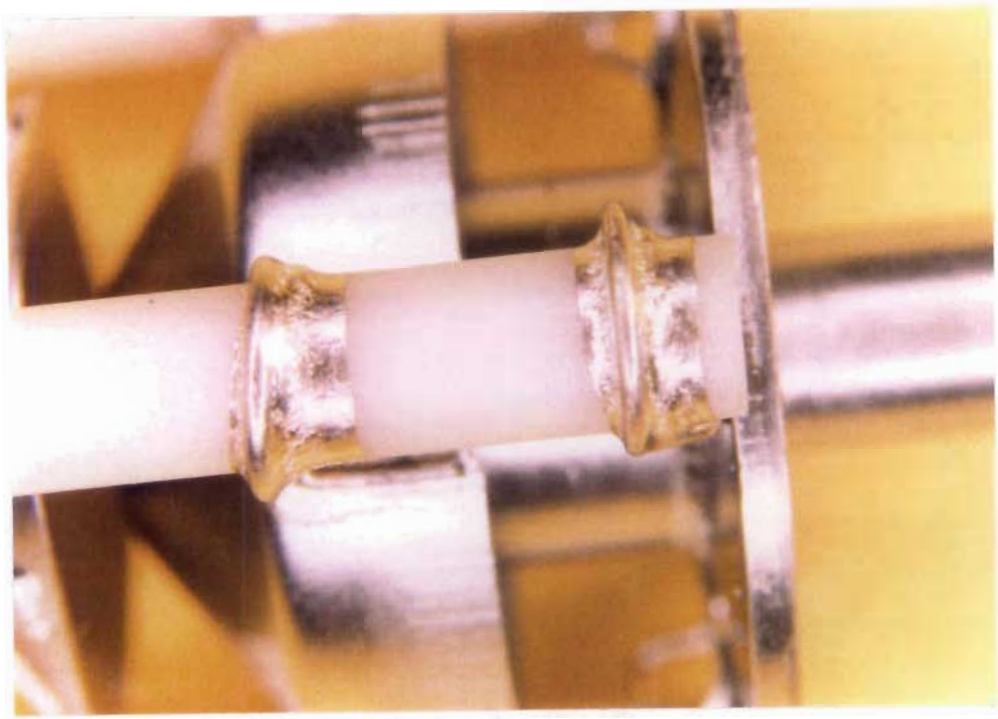

Figure 4.5 Close-up View of two Metal/Ceramic Joints

The final gun module is shown in figure 4.6. The anode plate is spot welded to the base plate of the travelling wave tube, with the vacuum envelope and electrical connects electron beam welded to the tube afterwards. All that then remains is to make the necessary electrode connections and to insert the cathode holder into the first heat shield.

4.1.6 Ceramic Envelope and Electrical Feed-Throughs

The use of metal plates to support the electrodes and to provide an electrical connect through the vacuum envelope poses other problems apart from the jigging of electrodes. The number of connects one can bring out of the tube is limited by the thickness of the ceramic spacers between plates, while the thickness of the spacers is limited by surface tracking between plates. A far more desirable situation would be to have several pins protruding from the ceramic wall, to which the electrodes are connected internally. If the pins are small enough, any number of them may be brought out of the tube, allowing greater degrees of flexibility in tube design. Furthermore, with the correct positioning of the electrodes with respect to one

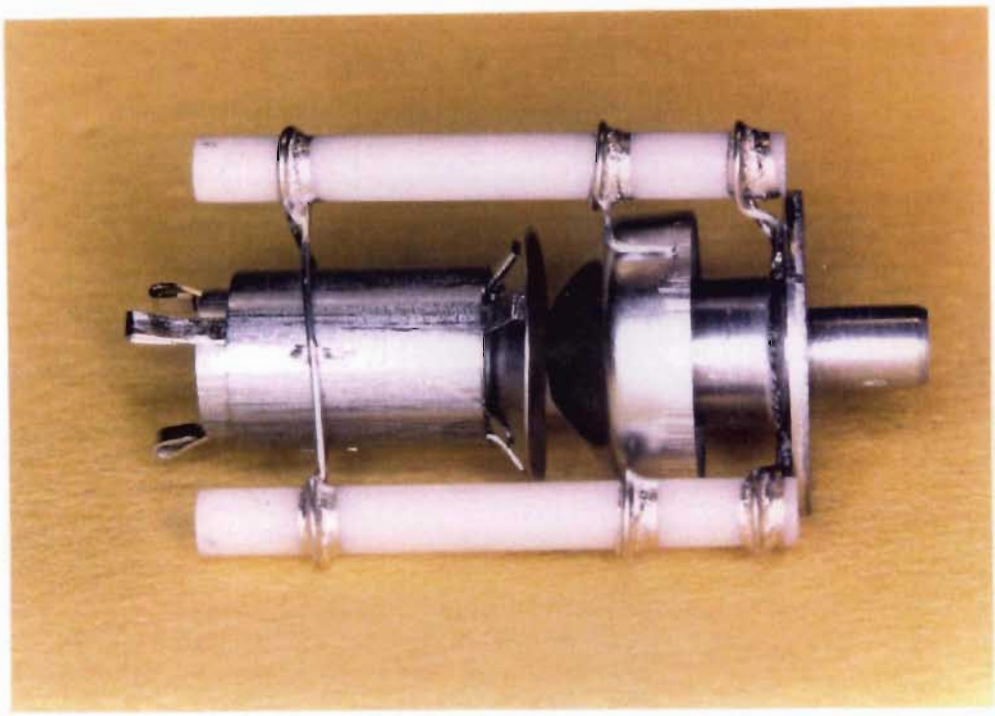

Figure 4.6 Completed Gun Module

another, surface tracking can be eliminated without complex shielding of the insulator.

Kohl [2] outlines the difficulty of making a vacuum tight seal between a metal pin and a ceramic wall. Wherever possible, the metal is made to surround the ceramic so that the latter is in compression in the finished seal. Yeh *et al* [3] found the tensile-compressive strength ratio for alumina to be approximately 1:10, making tensile stresses the dominant cause of joint failure. In the case of pin-type feed-throughs, the greater expansion coefficient of the metal tends to place the metal/ceramic interface in tension, a condition which causes most ceramics to fail. This expansion difference can be alleviated by designing a pin with a thin-walled, flexible interface with the ceramic which will take up any stress in the joint. However, to keep the number of processing steps in the gun manufacture to a minimum, the search for a solid pin joint continued.

The author experimented with kovar, molybdenum and ferry pins, and with different diameters and shapes of the pins. The best flow properties of the braze material were experienced with molybdenum pins, while the only reliable seal occurred when the

joint was designed in such a manner that the thermal stresses between the metal and ceramic were shear in nature. Any tensile stress resulted in the ceramic cracking, while the shear stress was taken up by the ductility of the active braze material. Figure 4.7 shows two such connects.

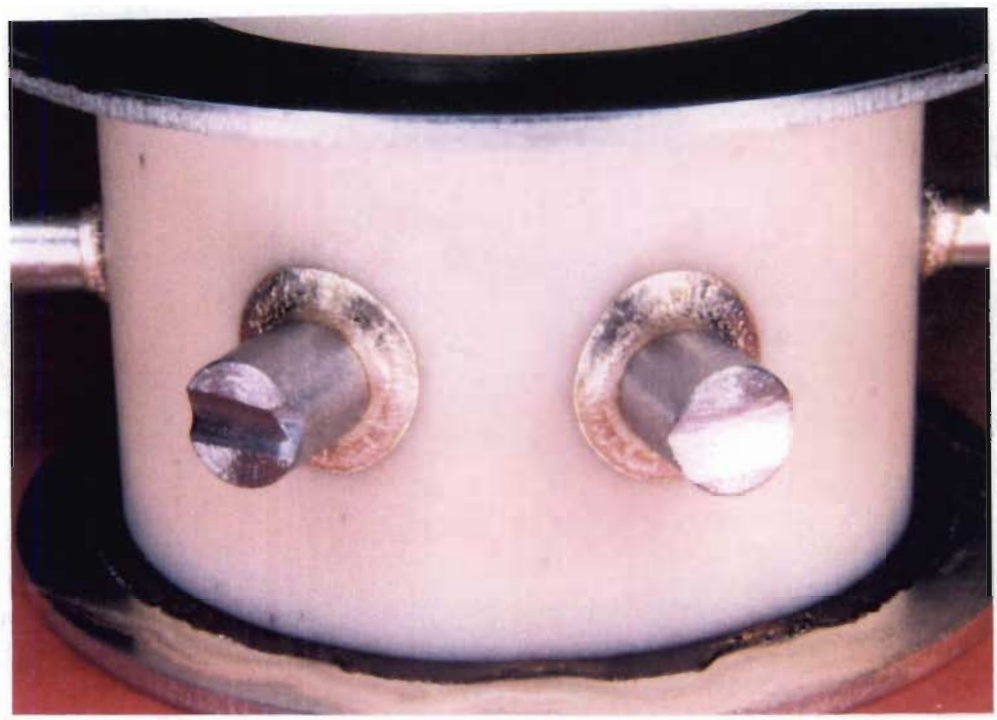

Figure 4.7 Electrical Connects Through Ceramic Envelope

Two kovar disks were brazed to each end of the ceramic envelope in order to electron beam weld the gun to the travelling wave tube and to the pumping port. A completed envelope with four connects brought out is shown in figure 4.8.

Having examined the separate components which are common to all the electron guns, it remains to take a look at the assembly, testing and results of each individual tube.

4.2 RESULTS OF TEST GUN

The gun module used in the first glass modulated gun was somewhat different to that shown in figure 4.6 in that the ceramic support rods were slightly longer to

Figure 4.8 A Completed Vacuum Envelope with Connects

accommodate the mica support disks (See Appendix D for assembly diagram). A sliding glass window was also incorporated into the gun to enable accurate temperature readings to be taken even after the glass envelope had become dirty from barium deposition. Electrical connects were made via an eight pin valve base which was sealed to the glass envelope tube. The energy of the electron beam was dissipated by a graphite collector supported on a single kovar pin. The completed gun module is shown in figure 4.8, just before insertion into the glass envelope. The graphite collector is shown already in position.

The gun was sealed to a pump station consisting of a 30 litres per second ion pump, backed by a separate rotary pump and absorbtion pump. An ion gauge for measuring pressure was located on the medium vacuum side (less than 10^{-3} Torr) while pressure readings for high vacuum were provided by the ion pump power supply. A thermostatically controlled oven was lowered over the tube, which was baked at

Figure 4.9 Completed Gun Module, Collector and Glass Envelope

350 °C for several hours to outgas the gun components.

Cathode temperature readings were obtained using an optical pyrometer**. As a comprehensive set of results on the performance of the cathodes manufactured for the project are documented in Chapter 5, no cathode emission results for the test gun will be presented at this stage.

Although the switching electrode would ultimately be biased using a resistor divider network to eliminate the need for a modulator supply, a 1100 volt variable power supply was used for testing purposes to enable optimisation of the electrode potential. Figure 4.10 shows the gun under test conditions. The blue beam exiting the anode is as a result of ionisation of the residual gas molecules by the beam electrons during the outgassing of the collector.

**See chapter 6 for details on optical pyrometry.

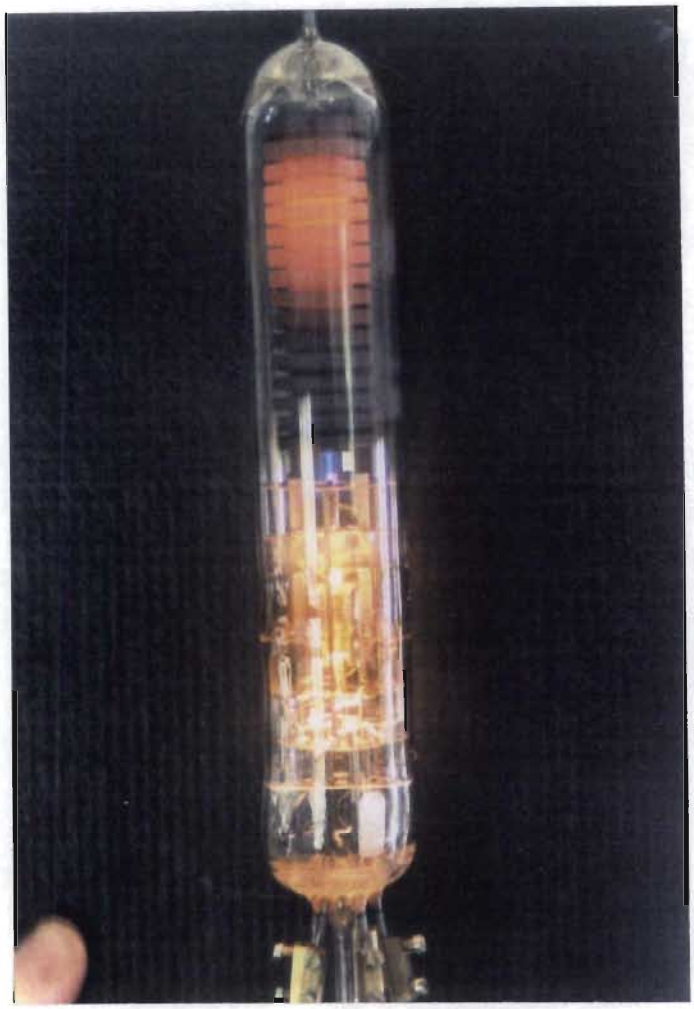

Figure 4.10 Glass Gun Under Test

4.2.1 Beam Modulation

The effectiveness of the switching electrode to switch the electron beam was determined by measuring the currents intercepted by the anode and collector during cut-off conditions, ie. the potential of the switching electrode reduced to that of the cathode. The current of interest is that which passes through the anode aperture, as this must be low enough so as to do no harm to the slow wave structure, and to produce no RF gain from the tube. The cut-off currents for different values of anode voltage are shown in figure 4.11.

At the anode operating voltage of 4.5 kV, less than 4 mA is intercepted by the molybdenum anode, while less than 500 μA passes through the anode to either be dissipated harmlessly by the RF helix, or to be collected by the water cooled collector. Although these currents could have been reduced to zero by moving the

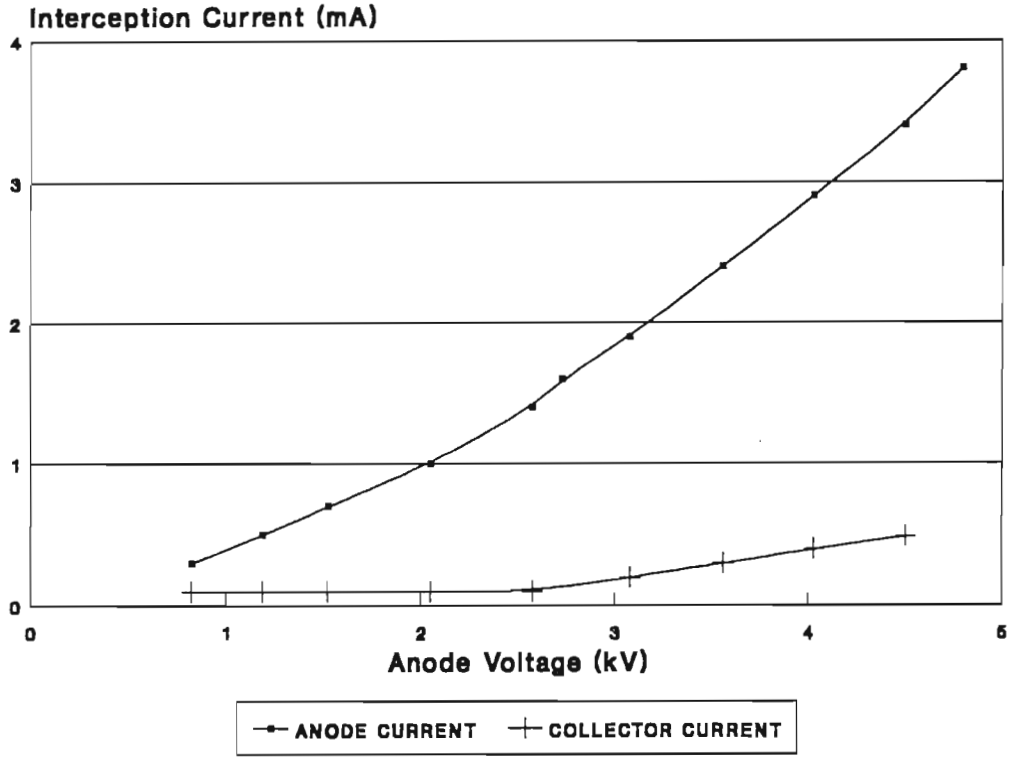

Figure 4.11 Cut-Off Currents vs Anode Voltage

switching electrode further from the cathode, the reduction in current would not justify the increase in switching voltage of the modulator. 500 μA shared between the helix and collector was considered more than acceptable for the purposes of this design.

4.2.2 Optimisation of Switching Electrode Bias Potential

As the anode aperture was of small enough diameter compared to the beam diameter, interception of the electron beam by the anode was considered as an appropriate means of determining the degree to which the beam was focused as it passed through the aperture. By varying the potential of the switching electrode and recording different anode interception currents, the optimal electrode potential could be established for different values of applied anode voltage. The results are shown in figure 4.12.

For low values of anode voltage, the effect of switching electrode potential on anode interception is far greater. This is because the electrons at these lower accelerating

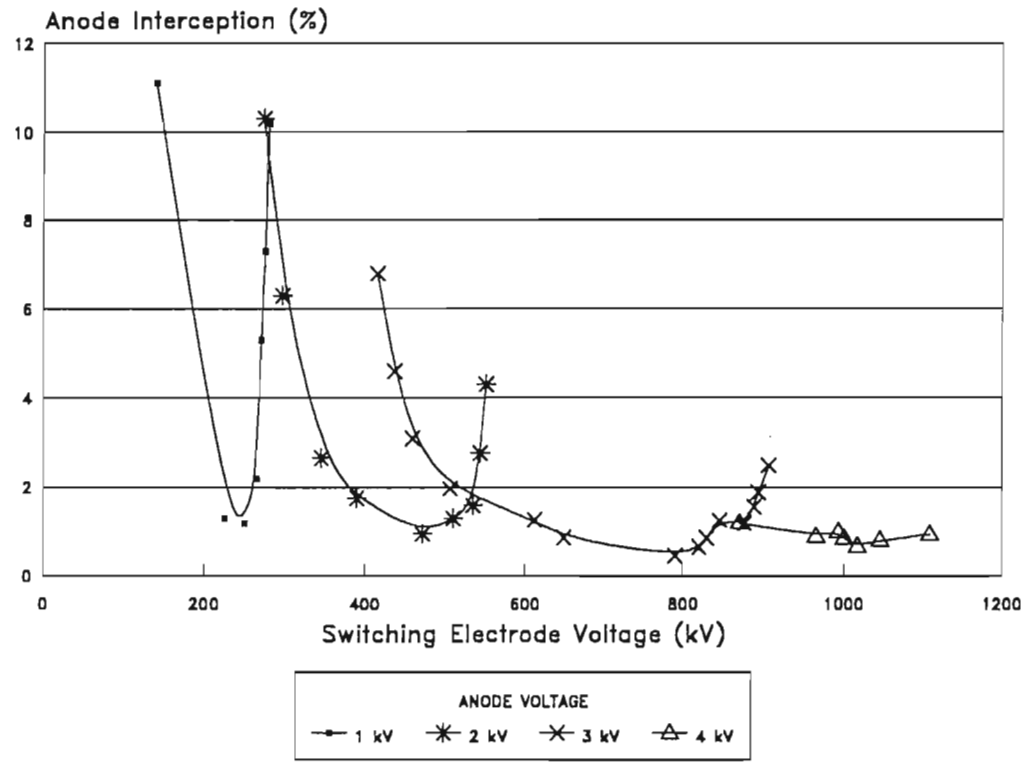

Figure 4.12 Switching Electrode Potential vs Anode Interception

voltages are travelling much slower and are therefore affected more by the diverging and converging effect of the electron lens created by the switching electrode. When the electrons are travelling at velocities closer to that which the gun was designed for, the effect of changing potential on their trajectories is somewhat reduced. Even so, there exists a value of switching electrode potential, for all applied anode voltages, for which the beam is optimally focused and passes through the anode with minimum interception.

4.2.3 Perveance

The perveance of an electron gun is determined by the gun geometry, and as such remains fixed for all values of applied anode voltage. Some small change in perveance is obtainable in gridded guns by altering the potential of the grid, but the effect on the laminar nature of the beam can be disastrous. By varying the potential of the switching electrode, a change in gun perveance of over 50 per cent was obtainable for the glass gun, as shown in figure 4.13. As there is no mesh grid in the path of

the electron beam, the effect on electron trajectories is minimised, a supposition verified by the simulations.

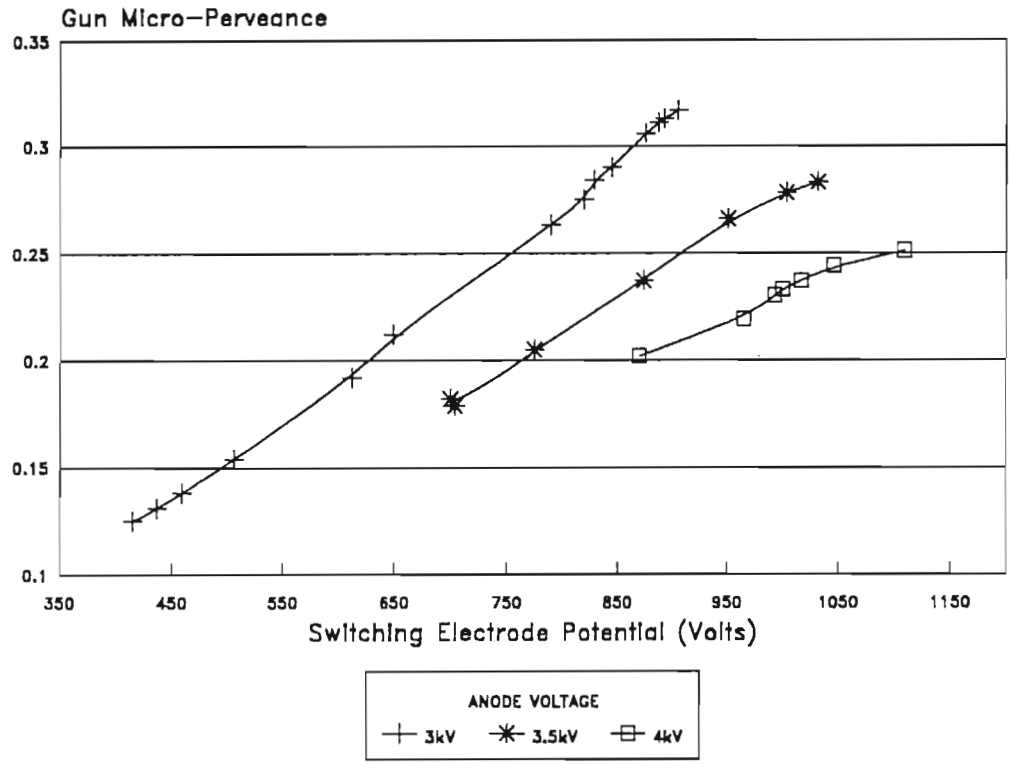

Figure 4.13 Gun Perveance vs Switching Electrode Voltage

4.2.1 Beam Analysis

In order to perform a beam analysis on the gun, it was necessary to remove the gun from the pump station. Once the activation of the cathode was completed and all gun components completely outgassed, the pressure in the tube would remain sufficiently stable. Any residual gas formed in the tube would be removed by the getter ion pumps activated inside the tube after it was pinched off and removed from the pump station.

Once the electron beam had exited the anode aperture, it passed through an analyzer plate located at the desired position of the beam minimum diameter. The analyzer consisted of a 0.25 millimetre molybdenum plate with a 0.3 millimetre diameter aperture punched through it. By rotating the tube in a jig, the analyzer plate was made to swing across the path of the electron beam, allowing only a small portion

of the total current to pass through the aperture. By knowing the dimensions of the aperture, the current density of the beam at that particular position could be calculated, and a current density profile across the beam diameter plotted. Although this method of beam analysis is somewhat crude, time did not allow a more complex method to be employed. Careful interpretation of the results would, however, provide an insight as to the characteristics of the beam profile at the entrance to the magnetic focusing stack.

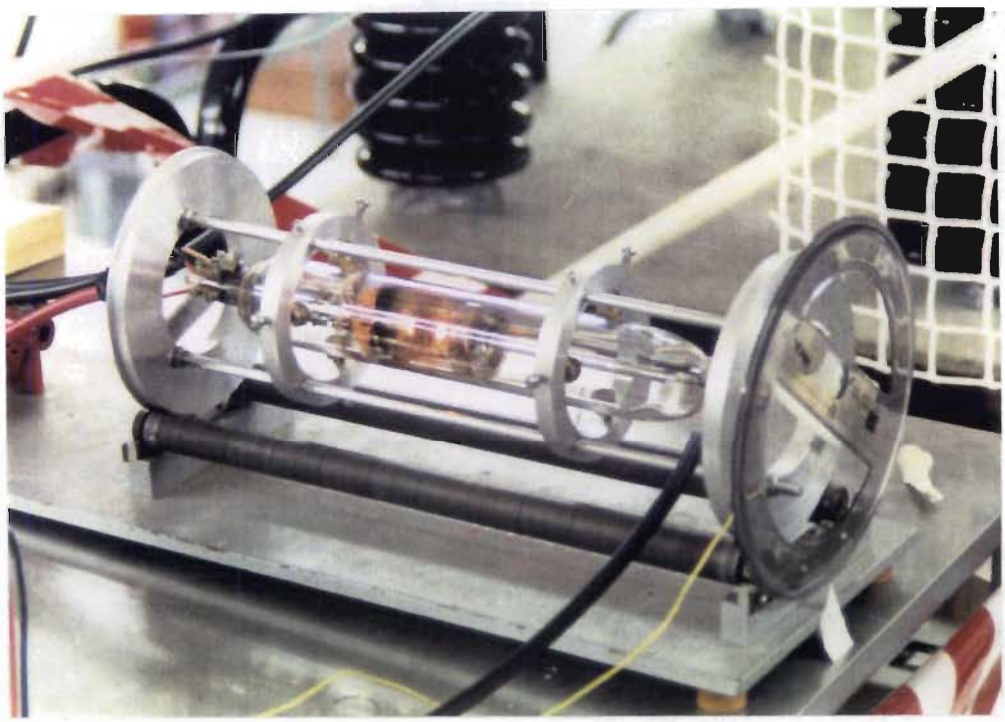

Figure 4.14 Rotating Jig For Beam Analysis on Gun

Unfortunately, an accident which occurred during the pinching off of the tube resulted in the cathode poisoning. Efforts to revive the emission failed, and the cathode current was reduced to 15 per cent of normal emission levels. An analysis at this reduced emission was still performed, as it could be compared with a simulation of similar current conditions using EGUN [4]. Close correlation between simulations and actual measurements had been obtained previously, and thus if similar correlations could be obtained at reduced emission, it was likely that they would hold at full emission as well.

The normalised current density profiles thus obtained are shown in figure 4.15.

Again, the measured data compares well with that predicted by the simulations, even at reduced emission. If these results are extrapolated to full beam current, then the predicted curve of figure 3.11 would be obtained, showing a marked improvement in beam profile from previous designs.

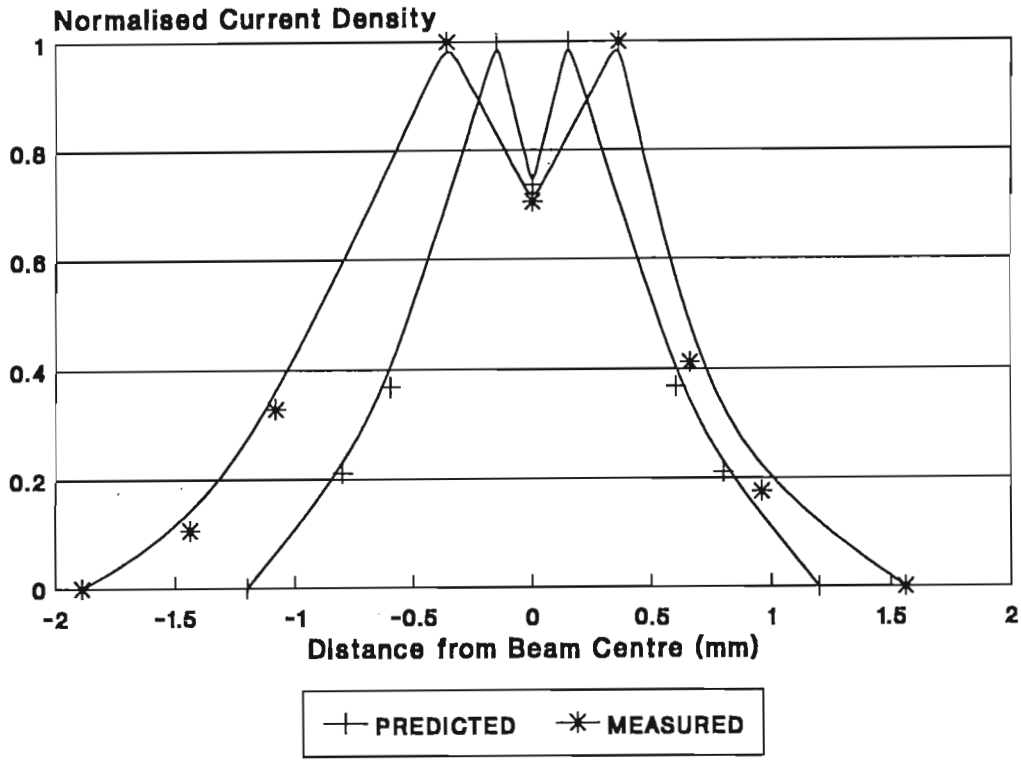

Figure 4.15 Beam Profile of Modulated Gun

SUMMARY

The cut-off currents for the modulated gun were found to be of a low enough level to be harmless to the tube's relatively fragile slow wave structure in the event of electron interception, and low enough to reduce the gain of the system to zero if pulsing of the RF signal is required. The bias potential of the switching electrode was optimised to minimise interception of the beam by tube components. Knowing this optimum potential, a resistor divider may be used to bias the electrode from the applied anode voltage. The perveance of the gun could be varied to compensate for constructional errors, with little influence on the electron trajectories. Although a beam analysis could not be performed at full cathode current, results obtained at low emission compared favourably with simulations of similar conditions, and

extrapolation to a full emission profile could be conducted with confidence.

Having characterised the modulated gun in a glass envelope, some assurance was obtained to incorporate the design into travelling wave tubes of metal/ceramic construction. It was here that the benefits of the new design could really be tested, as for the first time a beam of electrons would be passed down a slow wave structure, confined by a magnetic focusing stack, to interact with and amplify an applied RF signal.

4.3 RESULTS OF TRAVELLING WAVE TUBE DEMONSTRATOR TWT-LP8

The first travelling wave tube to emerge from the project incorporating the new gun design was of metal/ceramic construction (See Appendix D for assembly diagram). The tube was to provide 30 dB of RF gain over a 6 GHz to 8 GHz bandwidth. One of the unique features of the tube was a low profile TEM connect to the helix, whereby, in the event of tube failure, the entire TWT could be removed from the PPM focusing stack without the need to dismantle the stack itself [5]. The significance of this feature in terms of cost efficiency is tremendous, as the major expense in TWT manufacture is the manual adjustment of the magnet stack to produce optimum focusing of the electron beam. The development of the low profile connect was performed by N. Vassilopoulos [6], along with the PPM stack and RF attenuator. Once again, the cathode used in the tube was manufactured in the Materials Science Laboratory.

4.3.1 Perveance

The degree of beam modulation and the optimisation of the switching electrode potential had already been performed on the first test gun which had an identical geometry to the gun used in the TWT. Of interest during the testing of the TWT was the extent to which the perveance could be altered by varying the potential of the switching electrode. In a conventional Pierce gun the beam current can only be varied by altering the anode potential, as the perveance is fixed by the gun geometry. The result of this is a change in beam velocity, and an undesired loss of synchronisation

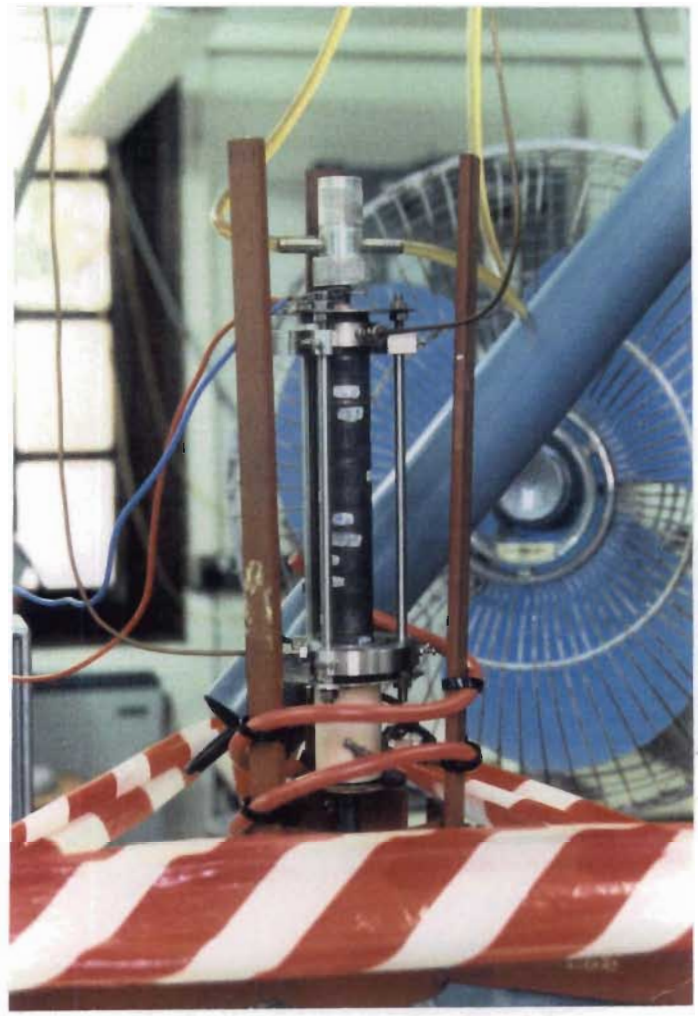

Figure 4.16 TWT on Pump Station

of the beam to the RF signal. A change in the switching electrode potential, however, causes a variation in the beam current without a change in the final beam velocity.

Figure 4.17 shows the variation in perveance obtained from the TWT. Actual beam currents obtained ranged from 50 milliamperes to 90 milliamperes for the same applied anode voltage, with very little disturbance of the beam focusing being observed. This implies that the gain of the tube could be varied merely by altering the potential of the switching electrode, as will be shown in section 4.3.3.

4.3.2 Beam Transmission

In section 2.3.1 the importance of beam quality to the magnetic focusing of the beam was discussed in some length. The theory of magnetic focusing is based on laminar electron flow, and any deviation from this condition can result in severe

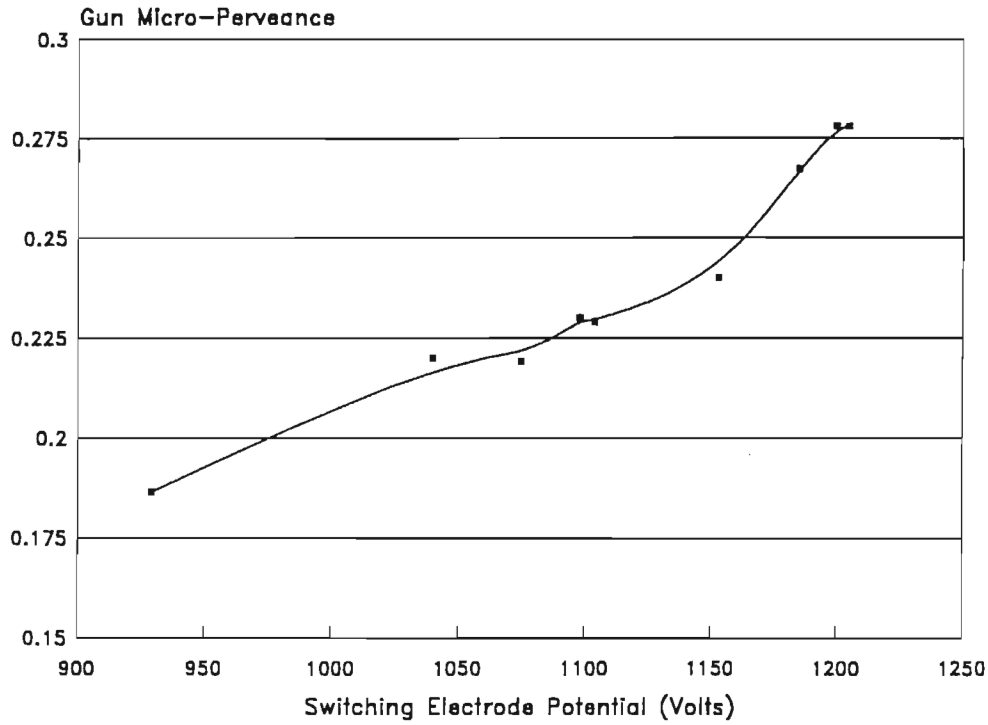

Figure 4.17 TWT Gun Perveance vs Switching Electrode Potential (TWT-LP8)

perturbations in the electron trajectories. Furthermore, Brillouin flow in which the outward force on the electrons due to the radial electric field of the beam is exactly balanced by the inward force of the axial magnetic field, is dependent on the correct positioning and diameter of the beam minimum. As the role of the electron gun in a TWT is to produce a beam of the required nature, a figure of merit for the gun can be determined from the ease of which the magnet stack confines the beam to predetermined dimensions.

A similar PPM stack was used by A.W. Stokes [7] to focus an electron beam produced by a conventional Pierce electron gun. Stray magnetic fields from the magnet stack caused severe defocusing of the electron beam which could not be compensated for, resulting in large anode interception currents, and consequently a cathode to collector transmission in the region of 76.5 per cent [8]. With no extra shielding of the gun, the modulating gun TWT could compensate for the magnetic flux within the interelectrode space to produce transmission figures from cathode to collector of better than 97.7 per cent on average. This means a tremendous reduction in the power dissipated by the anode. Stokes' stack was able to focus

95.6 per cent of the beam from the anode to the collector [9], compared to a figure of 99.4 per cent for the modulated gun TWT with a similar PPM focusing stack, but which had not yet been optimised. These results would imply that the nature of the beam in the latter case was closer to the design figures, as the magnet stack had greater ease in focusing the electrons down the TWT drift tube.

The ease with which the beam transmission can be improved by merely altering the focusing conditions within the gun is a very useful phenomenon indeed. Imperfections in the magnetisation of the PPM stack magnets manifest themselves in transverse components of magnetic field down the drift tube. These components are usually removed by adjusting the orientation of each magnet and by the addition of small magnetic shunts to the outside of the stack. This process is time-consuming and consequently expensive. With the ability of the switching electrode to reduce current interception by the helix, this process can now be eliminated by feeding back the current transmission to the switching electrode potentiometer, thus automatically "tweaking" the gun focusing as opposed to the magnet stack focusing. If a magnet stack with a different field profile is placed over the tube, the feedback loop can again adapt the focusing to suit the new configuration.

4.3.3 Gain Optimisation

A plot of tube gain for various switching electrode voltages and RF frequencies is shown in figure 4.18. There exists an optimum value of switching electrode potential, below which the gain drops as a result of reduced beam current, and above which gain drops due to the defocusing of the electron beam. By merely shifting between several discrete values of switching electrode potential depending on the frequency of operation, the tube gain can be kept at an optimum level across its entire bandwidth.

A frequency sweep was made across the tube bandwidth for a fixed value of gun perveance. A value of perveance was chosen which gave high values of gain for most frequencies. The same sweep was then repeated, but this time the switching electrode potential was adjusted slightly to optimise the gain at that particular frequency. The resultant gain/frequency curves are shown in figure 4.19. An increase

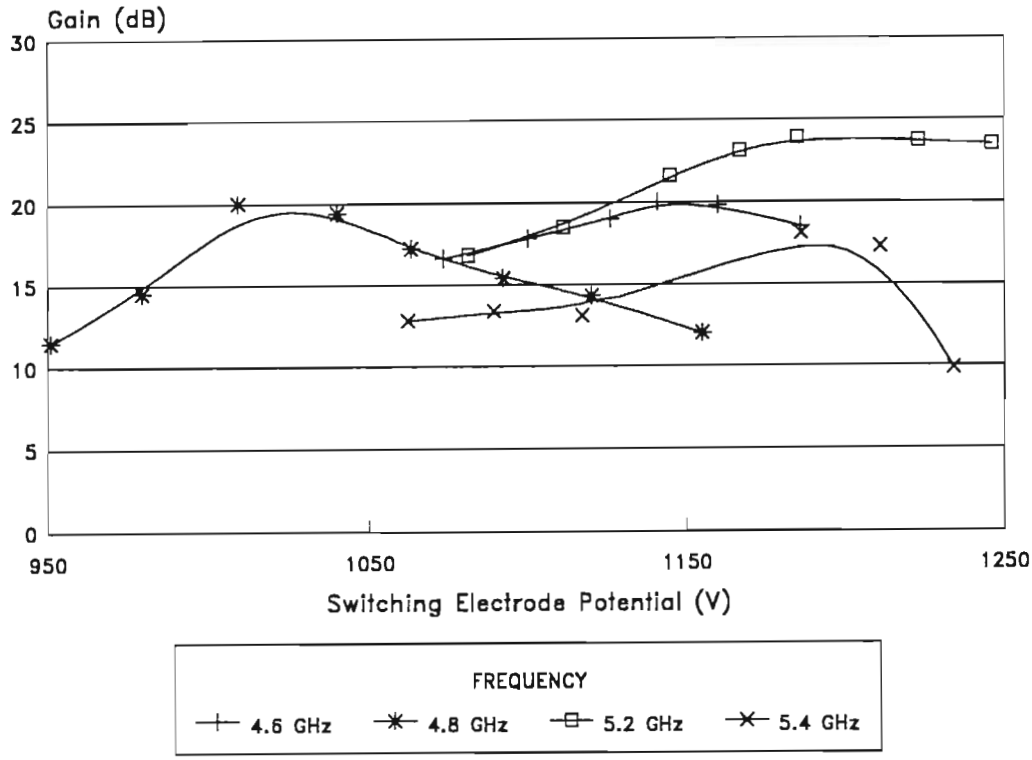

Figure 4.18 TWT-LP8 Gain vs Switching Electrode Potential

in gain of approximately 5 dB was experienced over the bandwidth from 3.8 GHz to 7.5 GHz, a considerable improvement from the fixed perveance case.

4.4 RESULTS OF TRAVELLING WAVE TUBE DEMONSTRATOR TWT-LP10

The gain of TWT-LP8 was somewhat below the design figure of 30 dB, with a gain of only 15 dB being realised. This was because the helix diameter had been chosen oversize to maintain low levels of helix interception during the initial experimental work, and as such the beam fill factor was low. Instabilities due to low internal reflection attenuation also reduced the gain by modulating the beam at frequencies other than the test frequencies. To overcome these problems, the design of the TWT was modified slightly to incorporate a larger attenuator and a narrower helix. With confidence in the abilities of the new modulated gun being strong, it was possible to

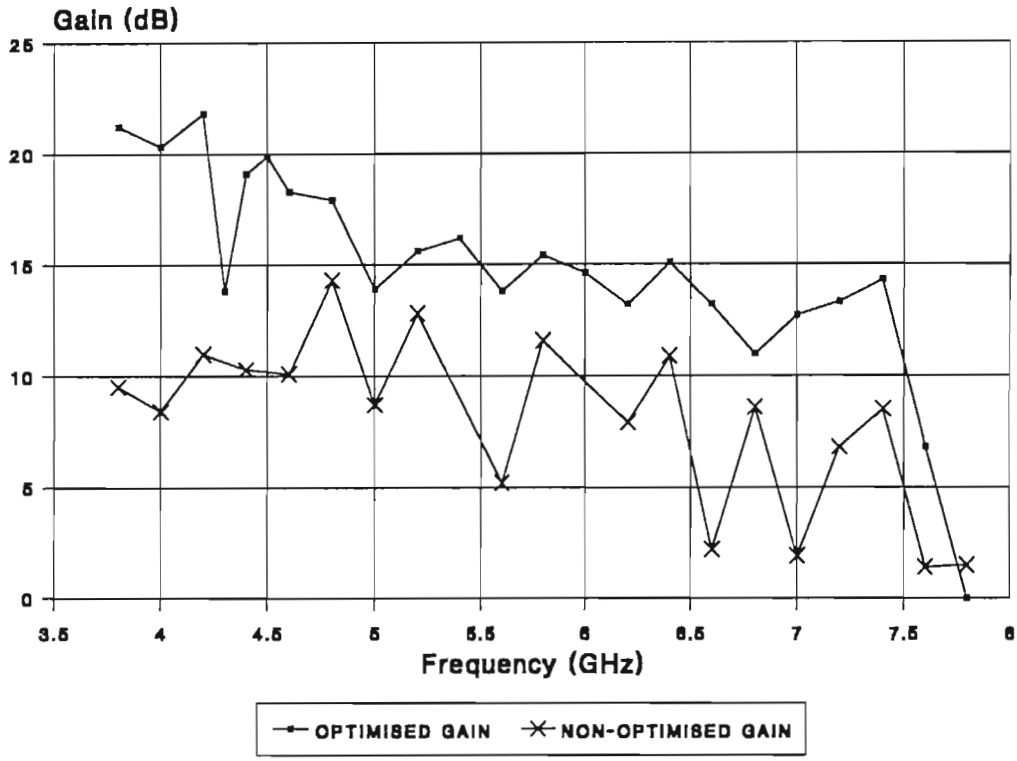

Figure 4.19 Optimised Gain vs Non-Optimised Gain for TWT-LP8

design a tube in which the electron beam filled far more of the helix diameter, resulting in greater interaction between beam and RF signal.

TWT-LP10 had a helix internal diameter of 2 millimetres as opposed to the previous 3 millimetres, with the pitch being reduced proportionally to keep the RF signal in synchronism with the electron beam. The cathode composition and electrode geometries were the same as those used in TWT-LP8. The predicted gain for the new SWS configuration was 45 dB [10].

4.4.1 Perveance

Once again the measured gun results compared very closely with prediction. Figure 4.20 indicates how the perveance of the electron gun could be varied by altering the ratio, β, of switching electrode potential to anode potential as shown by the change in slope of the I-V curves. Because the perveance of the gun remained constant at all anode potentials for any one value of β, the ability of the switching

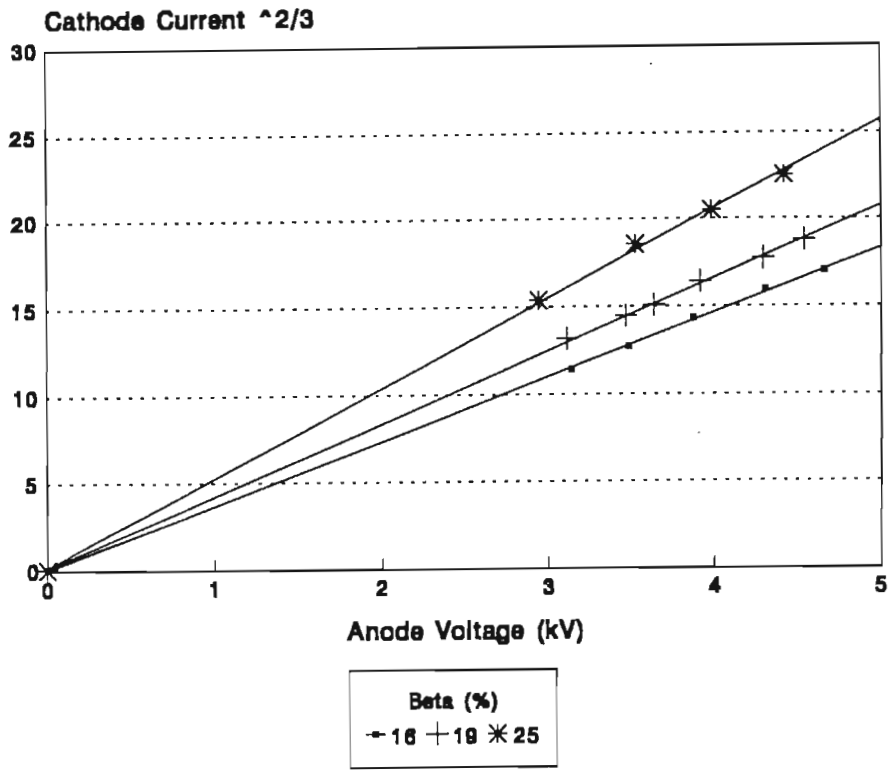

Figure 4.20 Dependence of Perveance on β (TWT-LP10)

electrode potential to determine the gun perveance is well illustrated.

4.4.2 Beam Transmission

The much narrower internal diameter of the RF helix posed more stringent demands on the magnet stack's focusing ability. The magnetic field strength could not be increased from the previous design value as the Alnico-8 magnets were already saturated, and hence an accurate beam minimum diameter and laminar electron flow were essential to ensure minimal perturbations of the beam. The sensitivity of electron interception by the helix to focusing conditions is illustrated in figure 4.21. Low values of anode voltage were chosen to ensure that no oscillations occurred during the measurements which would cause electron bunching and consequently increased interception. For this reason the focusing of the gun was not optimum, and relatively large interception currents were measured during this sensitivity check.

At full anode voltage of 4.5 kV the focusing could be optimised using the switching

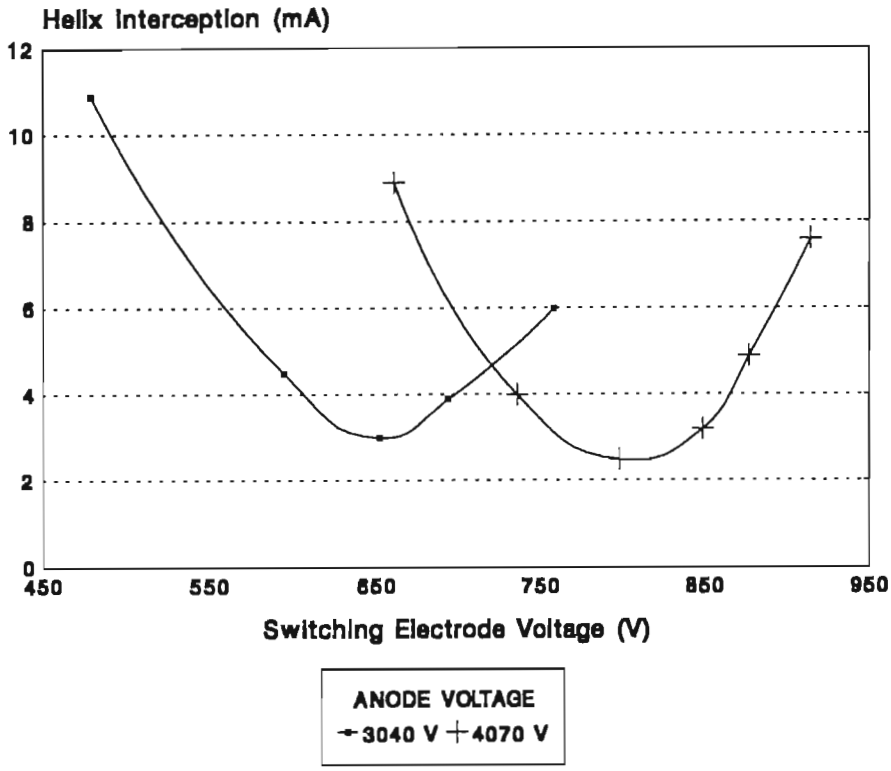

Figure 4.21 Helix Interception vs Switching Electrode Voltage (TWT-LP10)

electrode, to produce transmission figures from cathode to collector in the region of 98.5 per cent for a magnet stack which had not yet been adjusted to reduce transverse fields. These figures were excellent considering that the electron beam diameter had a design value of 1.5 millimetres and the helix inner diameter was now only 2.0 millimetres. The time consuming and expensive task of "tweaking" the magnet stack could now be substituted by the quick and simple one of adjusting the switching electrode potential slightly to compensate for any irregularities in the stack performance. This operation could also be performed under automatic feedback control to continually optimise transmission under different gun operating conditions.

4.4.3 Dual Mode Operation

Due to problems experienced with the switching electrode modulator during the testing of TWT-LP10, pulse widths of less than a few milliseconds were not achievable. This meant that the effect of different pulse widths from CW down to very short pulses could not be observed by this means. As time was short, an

alternative plan was necessary.

The final equilibrium ion current generated in a device is proportional to the residual gas pressure present in the tube. Therefore, by varying the residual gas pressure, the number of ions formed could be controlled and adjusted. The different focusing conditions required for different ion concentrations could thus be related to the effects of ion build-up during a pulse, and to the different requirements for long and short pulse widths.

In order that the high gas pressures did not degrade the emission of the cathode, only "friendly" gases could be permitted to enter the tube. An extremely useful property of palladium is that at temperatures between approximately 300°C and 500°C it is permeable to hydrogen only [11], with hydrogen having no adverse effects on the cathode emission at partial pressures below 10^{-4} torr. In fact, this exclusivity to hydrogen is so pronounced that the hydrogen permeating through the palladium is chemically pure.

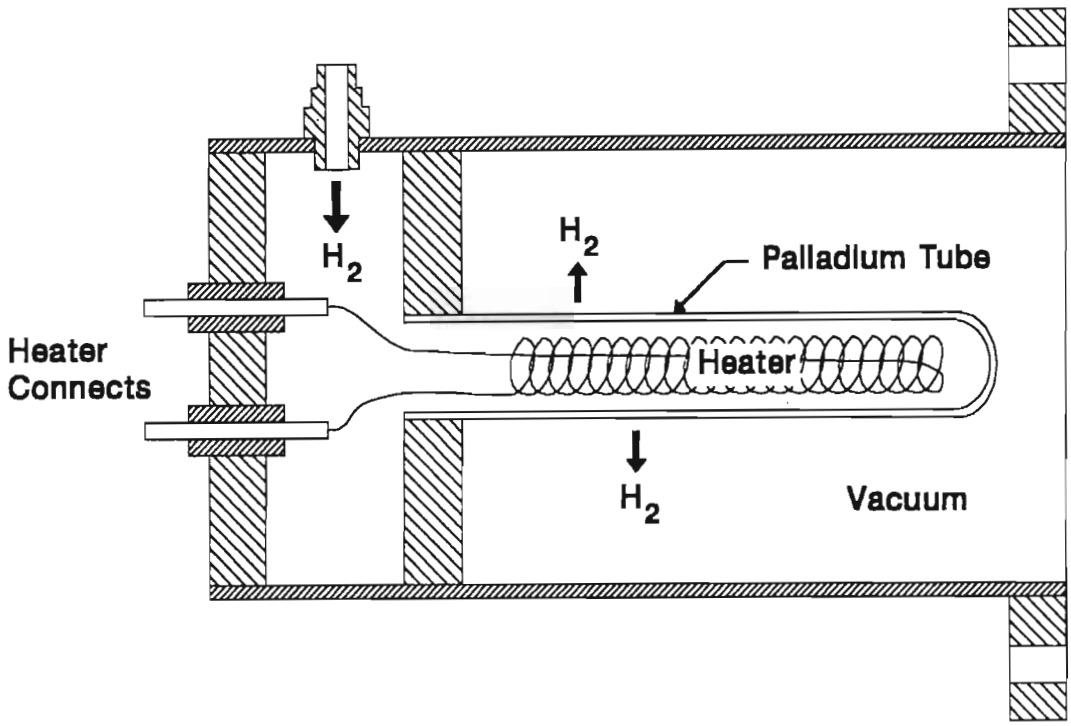

Figure 4.22 Hydrogen Leak Device Schematic

A hydrogen leak device was thus constructed which would allow the user to vary the input power to a heater wound around a palladium tube, and thus vary the permeability of the palladium (see figure 4.22). The tube formed part of the envelope of the vacuum system, and was exposed to hydrogen on the high pressure side. The partial pressure of the hydrogen reserve was kept below 10^{-1} torr to ensure that the palladium did not develop microscopic leaks, as is characteristic of the metal at high pressures and temperatures.

Using the hydrogen leak, the partial gas pressure within the tube could be altered and maintained for long periods of time. The focusing of the electron beam at different gas pressures was monitored by measuring the interception currents along the length of the helix SWS. Care was taken to optimise the magnet stack to ensure uniform interception by the helix longitudinally. Two scenarios were investigated; firstly the effects of pressure variation on the focusing of the electron beam in the drift tube for the gun under fixed focus conditions, and secondly the ability of the switching electrode to maintain constant focus conditions in the drift tube for different gas pressures. The results of the experiment are shown in figure 4.23.

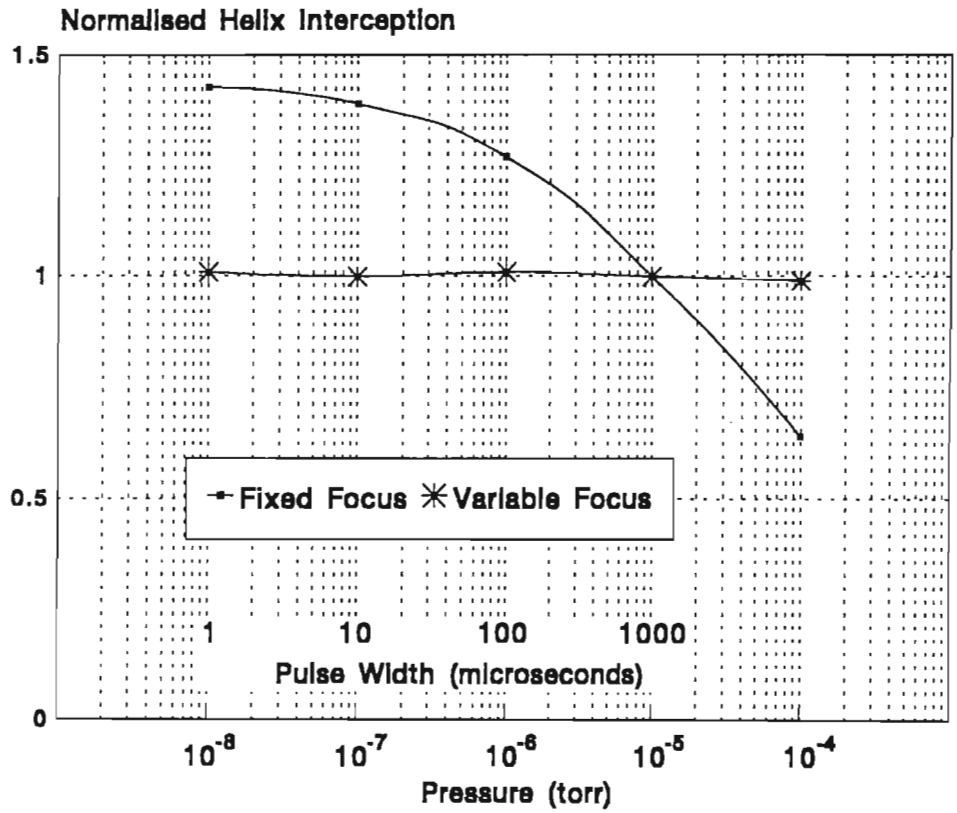

Figure 4.23 Effects of Ion Focusing on Helix Interception

The helix interception currents were normalised for discussion purposes to the mean value measured at 10^{-5} torr. This situation represented typical focusing conditions for CW operation. As the pressure was reduced below 10^{-4} torr for the fixed focus case, the decrease in the concentration of ions in the tube resulted in greater space charge forces within the electron beam itself, and the beam increased in diameter. This was evident from the increase in the helix interception currents by almost 50 per cent at pressures of the order of 10^{-8} torr. The adverse heating effect of this increased current was alarming.

For pulse widths of less than approximately 1 millisecond, the ion concentration is proportional to the width of the pulse. This is as a result of the build-up of ions with time throughout the length of the pulse. As the ion concentration is also proportional to the residual gas pressure under CW or long pulse conditions, varying the pressure will produce similar focusing effects as varying the pulse width. There just remains to find some datum point to relate these two phenomenon. From the measured results it is possible to assume that below 10^{-8} torr the effects of space charge

neutralisation are negligible due to the small concentration of ions produced at these pressures. Furthermore, Beck and Smith [12] found that for pulse widths less than 1 microsecond the total ion concentration was negligible, and hence these two limiting values were used as a datum in interpreting the results from TWT-LP10.

By varying the potential of the switching electrode slightly during the operation of the tube, the focusing of the electron beam could be kept constant for all gas pressures, as is shown by the uniform helix interception in the second trace of figure 4.23. From the above analogy it can be concluded that the modulated gun has the ability to compensate for the changing focus conditions experienced when an electron device is operated in a dual mode situation, as the beam diameter can be kept constant no matter what pulse width is used. Furthermore, the effects of ion build-up during a single pulse can be negated by suitably shaping the switching electrode voltage pulse.

SUMMARY

The incorporation of a switching electrode into the electron guns of the TWT demonstrators undoubtably resulted in an improvement in the performance of the tubes. The perveance of the guns could now be altered without changing the velocity of the beam, thus ensuring that the electron beam travelling down the tube and the RF signal propagating down the helix stayed in synchronism with one another, allowing mutual interaction and a resultant amplification of the signal. The excellent transmission results suggest an improvement in the quality of the electron flow within the beams, and further highlights the advantage of being able to redress the perturbing effects that may be present within the gun itself. The gun is effective as a dual mode device as the varying effects of ion formation on the beam's focusing for different pulse widths can be eliminated. The expensive "tweaking" of the magnetic focusing stack can be reduced to a slight alteration of the switching electrode potential, a process that can also be applied in a feedback loop to continually compensate for the different operating conditions of the tube. The gain of the TWTs could be optimised to produce a flatter gain curve with frequency, at the same time as raising the overall gain several decibels by bringing the electron beam into closer interaction with the RF signal.

REFERENCES

[1] J.R. Pierce, "Theory and Design of Electron Beams", New York: Van Nostrand, 1954.

[2] W.H. Kohl, "Materials and Techniques for Electron Tubes", New York: Reinhold, 1960, pp. 470-515.

[3] H-Y Yeh and H-G Yeh, "Failure Analysis of Ceramic Feed-throughs Used in Travelling Wave Tubes", *IEEE Transactions on Electron Devices*, vol. ED-34, no. 8, pp. 1862-1867, August 1987.

[4] W.B. Herrmannsfeldt, "EGUN - An Electron Optics and Gun Design Program", Stanford Linear Accelerator Centre, SLAC-331, October 1988.

[5] N. Vassilopoulos, B. Foulis, C. Reynolds and H.L. Nattrass, "Description of an Operational Travelling Wave Tube Amplifier Employing PPM Focusing", *IEEE Symposium on Antennas and Propagation and Microwave Theory and Techniques*, Johannesburg, pp. 25.1 - 25.8, August 1993.

[6] N. Vassilopoulos, "The Development of a Low Profile Broadband Connect Travelling Wave Tube", University of Natal Ph.D. thesis, 1994.

[7] A.W. Stokes, "Magnetic Focusing of Electron Beams for Linear Beam Tubes", University of Natal M.Sc.Eng. thesis, July 1990.

[8] reference [7], p. 180.

[9] reference [7], p. 181.

[10] C. G. Reynolds, "The Analysis, Simulation and Testing of an Experimental Travelling Wave Tube", University of Natal Ph.D. Thesis, unpublished.

[11] W. Espe, "Materials of High Vacuum Technology", Pergamon Oxford, 1966, pp.178-181.

[12] A.H.W. Beck and J.K. Smith, "Residual Gas Effects in a 25kW Ceramic Envelope Klystron", *4th International Conference on Residual Gases in Electron Tubes*, pp. 255-263, 1971.

CHAPTER 5.

IMPREGNATED TUNGSTEN CATHODES

"...cathode making continues to be an art practised, it seems, by artists with a good deal of witch doctor in their make-up. When something goes wrong, this or that demon is exorcised, and eventually things go right again. And, unlikely as it seems, cathodes continue to improve."

Such is the opinion of Pierce [1] on the difficulties of producing reliable cathodes, a matter not to be taken lightly considering the role played by cathodes in all microwave tubes. The principle of operation of a travelling wave tube, for instance, is the interaction of the RF signal with a thin pencil line beam of focused electrons. Naturally the source of these electrons is of great importance both from the point of view of a tube's life, and from the point of view of the energy required to emit the electrons. Thus a study of electron guns would not be complete without an investigation into the operation of cathodes as well.

The Travelling Wave Tube Demonstrator Project made use of the conventional oxide-coated cathode in the early guns that were manufactured [2]. Because of the advantages offered by dispenser cathodes, it was decided that tungsten impregnated cathodes be adopted in the latter stages of the project. This chapter outlines the development of such cathodes, up to the successful incorporation of them into the final demonstration travelling wave tubes.

5.1 THE EVOLUTION OF DISPENSER CATHODES

The list of literature on electron emission is extensive [3],[4],[6],[8],[14],[15], and relevant studies have been made on the subject by members of the Materials Science Research Group [2],[13]. However, it would be pertinent at this stage to outline briefly the mechanism of thermionic emission as a basis for understanding cathode operation.

5.1.1 Thermionic Emission

Although electrons can be produced by thermionic, secondary or field emission (or a combination of the three), only thermionic emission is used in travelling wave tube applications. Thermionic emission involves the heating of a metal surface until some electrons have sufficient energy to escape from the surface. The rate at which electrons escape is dependent on the temperature to which the metal is heated.

If one looks at the energy level diagram for electrons near a typical solid and vacuum interface as shown in figure 5.1, a difference in energy levels between the top of the conduction band in the solid and the vacuum energy level near the interface is observed. This difference in energy is known as the work function, and is the amount of energy that an electron needs to have directed at the surface of the solid in order to overcome the potential barrier and escape into the vacuum.

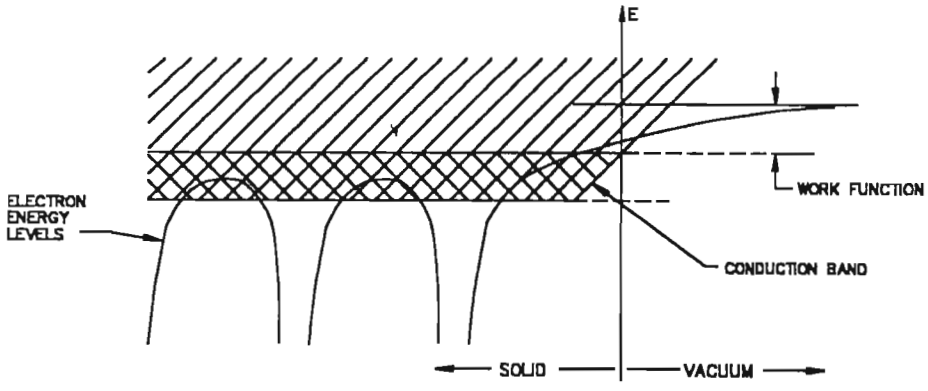

Figure 5.1 Energy Level Diagram for Electrons Near the Surface of a Metal [3]

An expression can be derived for the number of electrons per unit volume of the metal which, at temperature T, are excited to sufficiently high energy states to enable the electrons to overcome the surface forces. The emission current density is the emission current per unit area striking the metal surface, and is given by the Richardson-Dushman Equation:

$$J = \left(\frac{4\pi mek^2}{h^3}\right) T^2 e^{-\frac{e\phi}{kT}} \qquad A.m^{-2} \qquad (5.1)$$

where m = electron mass,

e = electron charge,

k = Boltzmann's constant,

h = Planck's constant,

and Φ = work function.

It is important to note the exponential variation of current density with work function and temperature, with the dependence on T^2 being negligible in comparison.

The Richardson-Dushman equation is very useful for analysing measured results if written in the form:

$$\ln\frac{J}{T^2} = \ln A_0 - \frac{e\phi}{kT} \qquad (5.2)$$

where:

$$A_0 = \frac{4\pi mek^2}{h^3}$$

This form suggests that a plot of J/T^2 versus $1/T$ should be a straight line with the work function, $e\Phi$, proportional to the slope of the line and $\ln A_0$ should be the intercept of the extrapolation of the line to infinite temperature ($1/T = 0$). Figure 5.2 shows a typical Richardson plot of this nature.

The Richardson-Dushman equation does not take into account the effect of an applied electric field at the cathode surface. It has been found that if a voltage is applied to an electrode adjacent to the cathode, electron emission increases. This is

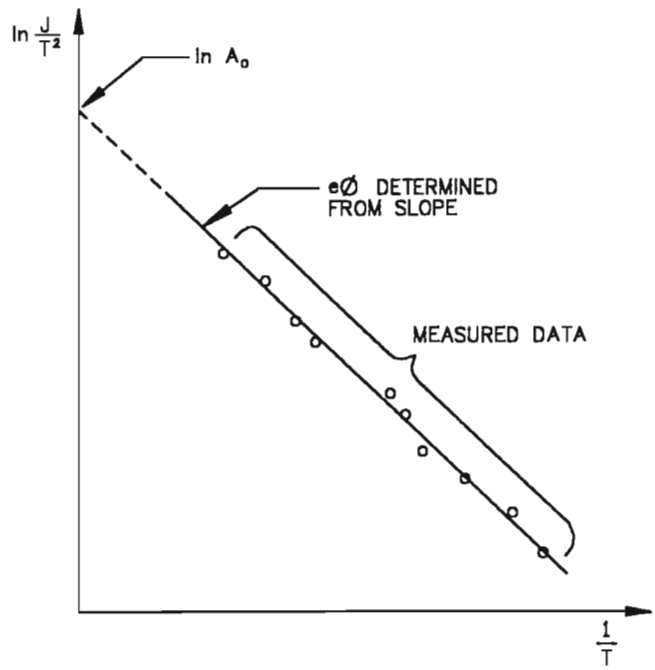

Figure 5.2 Richardson Plot for Determining Work Function & Emission Constant A_0 (after [3])

known as the Schottky Effect and is illustrated in figure 5.3. The applied field reduces the potential barrier which the electrons have to overcome, increasing the total number of electrons having sufficient energy to escape the emitting surface.

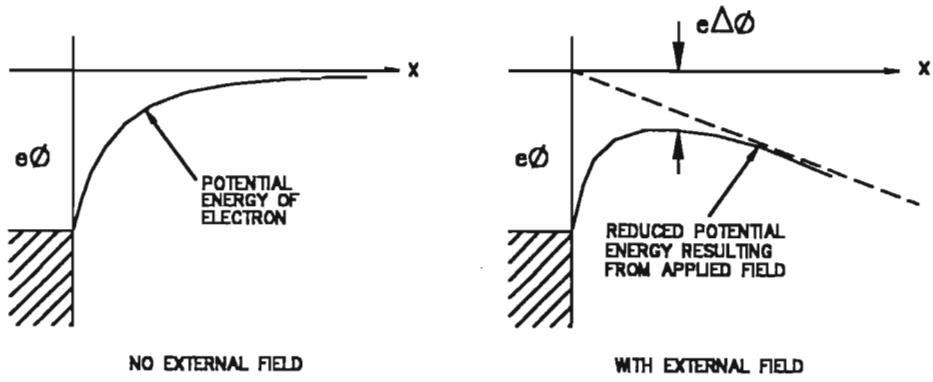

Figure 5.3 Illustration of the Schottky Effect (after [3])

The Schottky effect may be adjusted for by using the relationship:

$$J = J_0 e^{\left(\frac{eE}{4\pi\epsilon_0}\right)^{1/2}} \qquad (5.3)$$

where J_0 is the Richardson-Dushman current density given by (5.1), sometimes referred to as the *zero field* current density.

5.1.2 The Oxide Cathode

The oxide-coated cathode is used in most general-purpose tubes and consists of a thin coating of a metallic oxide mixture applied to a base of nickel or nickel alloy. The oxides are normally those of the alkaline earths, barium, strontium and calcium, and as such the oxides are extremely unstable under atmospheric conditions. To prevent the oxides from reacting with any moisture in the atmosphere during assembly, the coating is applied in the form of the corresponding carbonates, which are then broken down to oxide form during the processing of the tube. A by-product of this decomposition is vast quantities of CO_2, and care must be taken to ensure there is no contamination or oxidation of tube components during the activation process.

Tubes are usually "baked out" at around 400 °C for several hours to remove any absorbed gases on component surfaces. During this process, the nitrocellulose binder which holds the carbonate powder together decomposes into volatile gases and is pumped away. The carbonates themselves are broken down to oxide form by raising the cathode temperature to around 800 °C [4], with CO_2 gas as a by-product. The pure oxides are themselves an insulator, and as such are not capable of supporting sustained emission. By "activating" the cathode, the barium oxide is partially reduced to free barium, making the coating a semiconductor and increasing its emission capabilities. It has been found that the impurities within the nickel alloy diffuse to the metal and oxide interface and are instrumental in the reduction of the oxides, barium in particular. Drawing a current during activation causes electrolytic dissociation of the coating, aiding in the overall production of free barium atoms.

The oxide-coated cathodes used in the Materials Science Laboratory were of the "triple-carbonate" variety, containing barium, strontium and calcium oxides. Although they were employed with much success in the experimental tubes, there are several disadvantages of the oxide cathode which favoured the introduction of dispenser cathodes.

5.1.3 Shortfalls of the Oxide Cathode

If oxide coated cathodes are operated below 650 °C, their life is shortened by the fact that residual gas in the tube has a poisoning effect on the cathode. If operated above 850 °C their life is again shortened by gross evaporation of the oxide coating. Thus there is a narrow temperature band in which cathodes of this nature can be operated.

As the current density drawn from an oxide cathode is increased, the Joule heating due to the series resistance of the semiconductor coating causes overheating and vaporisation of the oxides. The situation can be improved by working with very thin layers of oxide coating to reduce the series resistance, however this is undesirable from a life point of view. The result is that oxide cathodes must be operated at current densities somewhat less than 1 $A.cm^{-2}$. For many applications, e.g. receiver valves requiring only 0.05 $A.cm^{-2}$, this figure is acceptable and will ensure long life for the valve. For transmitter valves requiring greater currents, the cathode dimensions may be increased to keep the current density down so long as the frequency is low enough to allow scaling in this manner. For frequencies approaching that of microwaves the situation is somewhat different as the dimensions of the tube are now determined to some extent by the frequency of operation, and use must be made of beam focusing to obtain the required current densities.

The effect of the series resistance of the oxide layer is substantial if one considers the heat balance of an oxide cathode. The two sources of heat for the emitting surface are the heater power input (P_{heater}) and the Joule losses in the oxide coating (I^2R_s). The two heat sinks are the radiated power from the cathode surface (cT^4) and the energy imparted to the electrons as they leave the emitting surface. The last term is made up of two parts, namely the energy required for the electrons to overcome the potential barrier at the metal surface, and the initial thermal velocities given to the electrons. At equilibrium:

$$P_{heater} + I^2R_s = cT^4 + I(\phi + \frac{2kT}{e}) \qquad (5.4)$$

When no current is drawn from the cathode, there is equilibrium between the heater power and the surface radiation:

$$P_{heater} = cT^4 \tag{5.5}$$

thus (5.4) reduces to:

$$I = \frac{1}{R_s}\left(\phi + \frac{2kT}{e}\right) \tag{5.6}$$

The cathode will violently overheat if this value of current is exceeded. For example, if an oxide cathode is operated at 1100 °K and 1 A.cm^{-2}, then $R_s \approx 1.6\ \Omega.cm^{-2}$. If the current density is increased to 2 A.cm^{-2}, then the increase in cathode temperature is greater than 20 per cent [5]!

Oxide cathodes exhibit tremendous emission decay during long pulses. Current densities of the order of 100 A.cm^{-2} may be drawn for periods of up to 10 microseconds, but for pulse widths of a few milliseconds or more, the pulse can decay by a factor of 10 or more. It is thought that the decay is due to poisoning of the cathode by gas released from the anode under electron bombardment, but the exact cause of the phenomenon is not well understood.

The life of an oxide cathode can be reduced somewhat by the build-up of a resistive interface between the base metal and the oxide coating. This layer reduces the effective conductance of the cathode, and emission degenerates. Impurities in the base metal alloy are usually introduced to aid with the activation process, and often increase the rate of growth of this interfacial layer. Gas, present due to incomplete pumping or desorption from electron bombardment of electrodes, can have a disastrous effect on oxide cathodes, causing poisoning and emission failure. Another limiting factor for cathode life is the rate of evaporation of barium from the oxide surface. With no reservoir to replenish barium reserves as in the case of dispenser cathodes, the overall work function of the emitting surface rises, causing an exponential decay in cathode emission.

5.1.4 Dispenser Cathodes

Dispenser cathodes are distinguished by having a porous metal matrix which acts as a reservoir from which the emitting material may diffuse to the matrix surface, thereby maintaining an active layer at the surface of the cathode. This active surface reduces the work function of the base metal and facilitates thermionic emission. The emitting material is located uniformly within the porous matrix of the cathode.

The "L" cathode was the first dispenser cathode, developed by Philips Research Laboratories in 1950, and consisted of an oxide mix located in a cavity behind a porous tungsten plug. Current density capabilities and emission life were greatly enhanced by the new cathode, but several difficulties were encountered. The joint between the porous plug and the molybdenum support body proved difficult to seal effectively so that barium vapour did not escape directly from the reservoir. Uniform cathode temperatures were also difficult as the thermal conduction through the bulk oxide mix to the porous plug was very low. Outgassing and activation had to be carried out over a narrow temperature range if good emission was to be obtained.

Coppola & Hughes [6] found that by mixing barium carbonate with aluminium oxide and firing the mixture at about 2000 °C, the carbonate would be converted to an oxide and barium aluminate would be formed. If this aluminate was then pressed with powdered tungsten, a cathode with superior activation properties and a reduced dependability on critical processing was obtained.

The first impregnated cathode, whereby a porous tungsten matrix was impregnated with barium aluminate, was developed by Levi and Hughes [7] in 1952 and became known as the Philips "A" cathode. The impregnated cathodes had the advantage of being machineable to intricate geometries, and the emitting surface could be made much smoother than pressed cathodes.

The addition of calcium oxide to the impregnant greatly improved the emission properties and reduced the sublimation rate of the barium considerably. The ratio most commonly used is a 5:3:2 mix of barium, calcium and aluminium oxide, and is known as the Philips "B" cathode. Other variations include the "S" cathode, having a ratio of 4:1:1 and even greater emission levels than the "B" cathode.

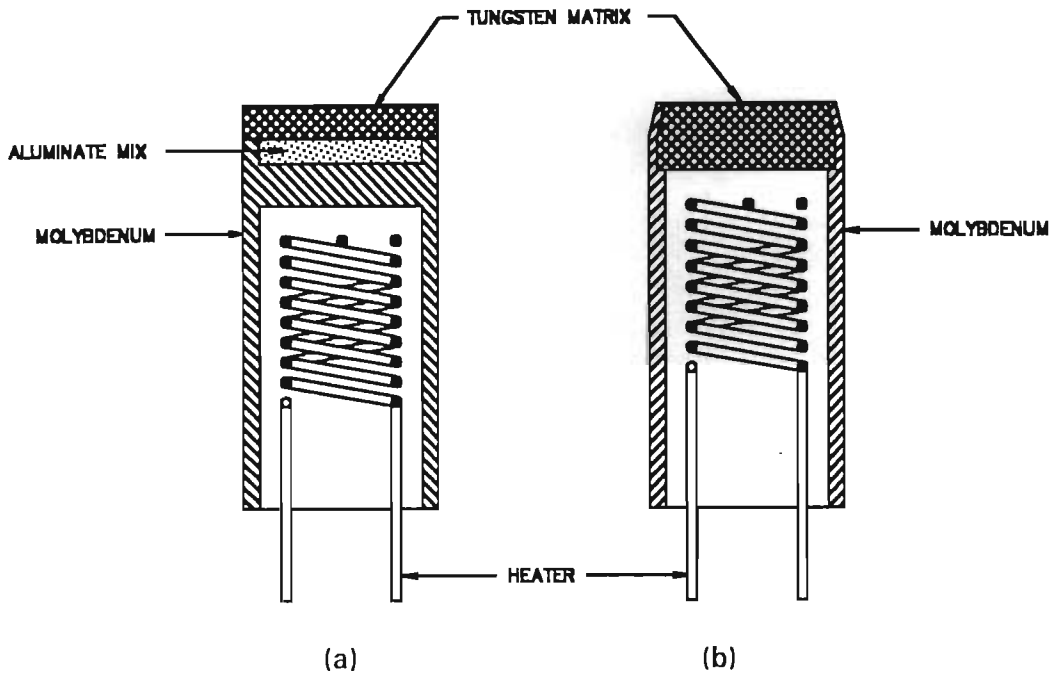

Figure 5.4 (a) A Typical "L" Cathode (b) The Philips "B" Cathode (after [4])

By adding a porous coating of certain refractory metals such as osmium or iridium to a base matrix of tungsten, the work function of the emitting surface can be further reduced. Although the work function of these metals is higher than that of tungsten, the overall work function is lower than that of tungsten alone. Cronin [8] reports a case whereby an increase in emission of well over 300 per cent was obtained at the same temperature for a cathode coated with a refractory metal. The inclusion of scandate (Sc_2O_3) in the aluminate mix is yet another exciting advance in modern cathode technology, but as with the refractory metal coatings, the method of application is somewhat difficult and in some instances dangerous. The standard "B" or "S" cathodes find excellent application in experimental tubes due to their simple and reliable operation.

5.2 MECHANISM OF OPERATION OF DISPENSER CATHODES

The reduction in work function of the tungsten emitter is brought about by the presence of free barium on the tungsten surface. During impregnation, the barium

carbonate is broken down to barium oxide by the following reaction:

$$BaCO_3 \rightarrow BaO + CO_2 \qquad (5.7)$$

Care must be taken during outgassing to prevent high cathode temperatures from causing the unwanted reaction:

$$BaCO_2 + \frac{1}{3}W \rightarrow \frac{1}{3}Ba_3WO_6 + CO \qquad (5.8)$$

as the Ba_3WO_6 is non-emissive. The next stage in the production of free barium is the reaction that occurs when the cathode is heated to operating temperature:

$$3BaO.Al_2O_3 \rightarrow 2BaO + BaO.Al_2O_3 \qquad (5.9)$$

$$6BaO + W \rightarrow 3Ba + Ba_3WO_6 \qquad (5.10)$$

The end of life of the cathode is denoted by the reaction (5.10) going to completion.

The free barium so liberated reaches the cathode surface by two means; migration over the pore surfaces, and more importantly via *Knudsen* flow through the impregnated pores themselves. The barium spreads over the cathode surface forming islands, the sizes of which are determined by the temperature of operation and the age of the cathode. Figure 5.5 shows the relative size of the islands for two different temperatures.

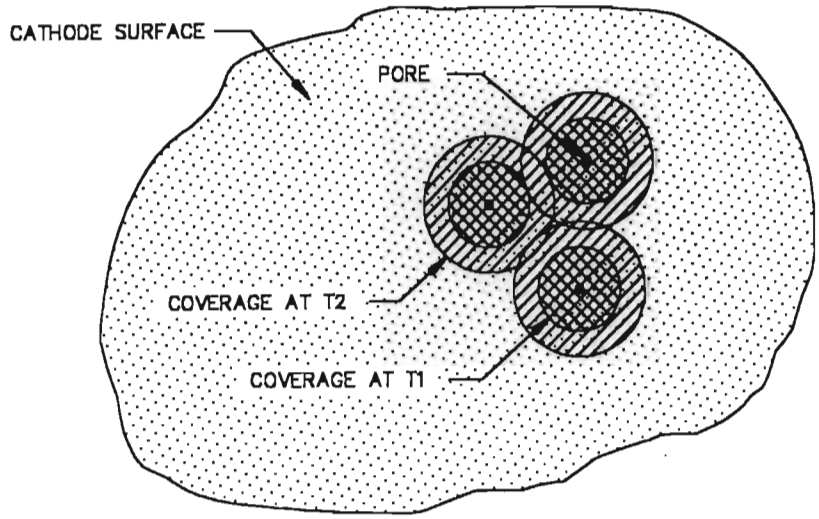

Figure 5.5 Barium Coverage of Cathode Surface for T2>T1 [9]

Where the barium is in contact with the tungsten, the work function of the tungsten is lowered forming a high emission site. The areas in between the barium islands retain their high work function and emit only a small proportion of the overall cathode current. Thus the current emitted from a cathode appears to originate from time variant patches on the emitter surface and not from the entire tungsten base.

5.3 PATCHY CATHODES

The emission from a cathode surface is not uniform in the case of most cathodes, but rather is made up by several high emission sites surrounded by a background area of low emission. These high emission sites exhibit low work functions and are randomly distributed over a relatively small proportion of the cathode surface. The number of emitting sites grows with time as the cathode ages, with an overall decrease in the cathode work function. Being able to monitor the patchiness of the cathode surface would provide the tube engineer with a figure of merit as to the quality of the cathode in use. It is for this reason that the author devoted some time to the theory of patchy cathodes, which proved to be a valuable exercise.

Figure 5.6 shows the I-V characteristic of a pure metal single crystal as well as that

for a typical dispenser cathode. For the single crystal cathode the current corresponds well with that obtained from Langmuir's theory and Schottky theory. The more rounded nature of the dispenser cathode curve is as a result of the cathode current being made up of a space charge limited component from the emission sites, and a temperature limited emission component from the high work function background. It is important to be able to characterise cathodes exhibiting this behaviour in order that a comparison of emission characteristics may be drawn.

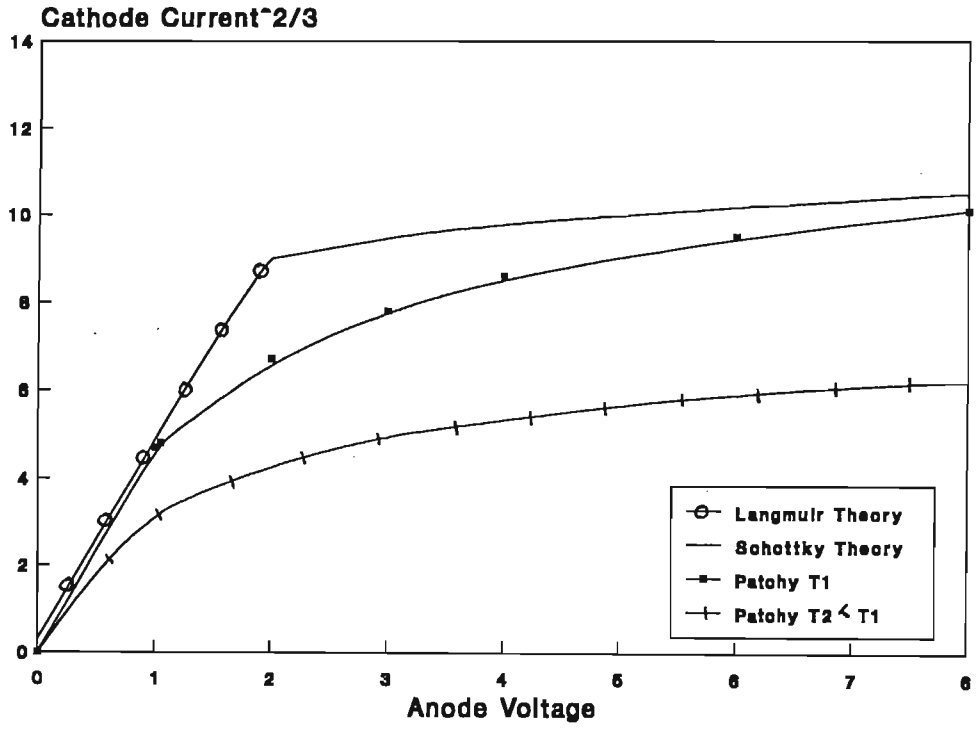

Figure 5.6 I-V Characteristics for Single Crystal Cathode and Typical Dispenser Cathode (T1 > T2)

Beck & Wang [10] proposed that the emission be modelled as a large number of highly emissive sites distributed in a random manner such that the emission from the *n*th site is described by the normal current density distribution function:

$$J_r = J_n \exp -\frac{(r-r_n)^2}{2\sigma_n^2} \qquad (5.11)$$

Using the central limit theorem, the emission from the whole cathode is given by:

$$J = J_m \exp\left(-\frac{r^2}{2\sigma^2}\right) \qquad (5.12)$$

where J_m and σ represent averages over J_n and σ_n.

Thus the cathode current behaves as though it originated from a single patch centred on $r = 0$, around which the current density varies according to (5.12).

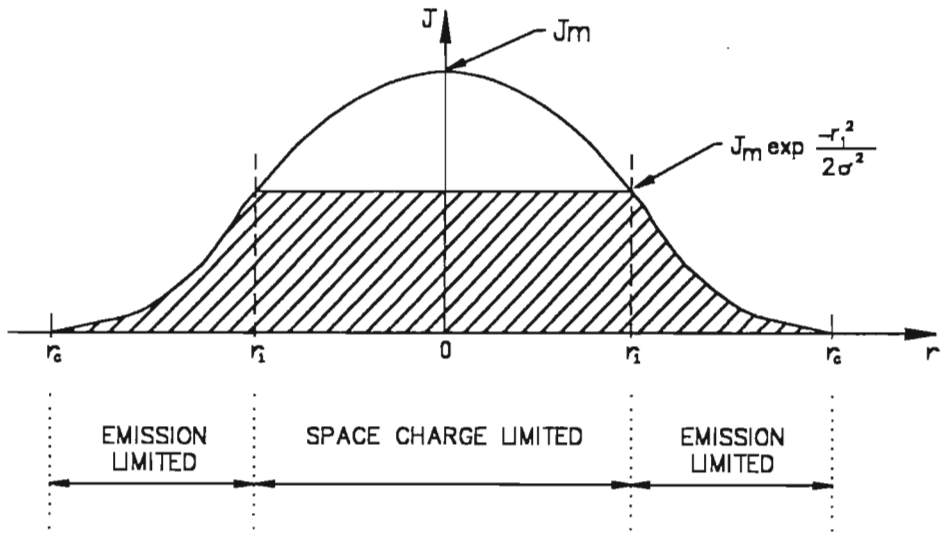

Figure 5.7 Current Density Distribution for Cathode of Radius r_c

If the applied voltage is V_1 and the diode perveance per unit area is p_0, then:

$$p_0 V_1^{3/2} = J_m \exp\left(-\frac{r_1^2}{2\sigma^2}\right) \qquad (5.13)$$

If V_1 is such that the zero field emission is drawn from an annulus of thickness δr_1 at r_1 then equation (5.13) gives the relationship between applied voltage and the radial coordinate at which space-charge limited current flow changes to temperature limited flow, as shown in figure 5.7.

If we now define a critical voltage V_c as being the highest voltage for which the

entire surface is in space-charge limited flow, then:

$$V_c^{3/2} = \frac{J_m}{p_0} \exp\left(-\frac{r_c^2}{2\sigma^2}\right) \tag{5.14}$$

For applied voltages less than V_c, ie. for space charge limited flow, the anode current is merely:

$$I_a = \pi r_c^2 p_0 V_a^{3/2} \tag{5.15}$$

For voltages greater than V_c the current comprises two components; a space-charge limited inner disk of radius r_1, and a temperature limited annulus of inner radius r_1 and outer radius r_c:

$$I_a = \pi r_c^2 p_0 V_a^{3/2} + J_m \int_{r_1}^{r_c} 2\pi r \exp\left(-\frac{r^2}{2\sigma^2}\right) dr \tag{5.16}$$

We can normalise (5.16) by defining V_m as the voltage which makes $r_1 = 0$, and I_m as the current which would be emitted if the cathode was uniform. Then, letting the normalised values be $i = I_a/I_m$, $v = V_1/V_m$, and defining $\alpha = r_c^2/2\sigma^2$ we obtain:

$$i = \frac{v^{3/2}}{\alpha}\left[1 - (3/2)\ln v - \frac{\exp(-\alpha)}{v^{3/2}}\right] \tag{5.17}$$

For $v > V_c/V_m$ equation (5.17) defines the characteristics of a patchy cathode where both i and v are the normalised cathode current and anode voltage respectively. If $i^{2/3}$ is plotted against v for different values of α, the curves shown in figure 5.8 are obtained, which resemble very closely the patchy characteristic of figure 5.6.

The above theory becomes useful when one can use it to determine a value of α from measured data as well as a value for J_m. This would provide information on the degree of patchiness of the cathode emitting surface (from α) and as to what the maximum current density obtainable from the cathode is (from J_m). In order to

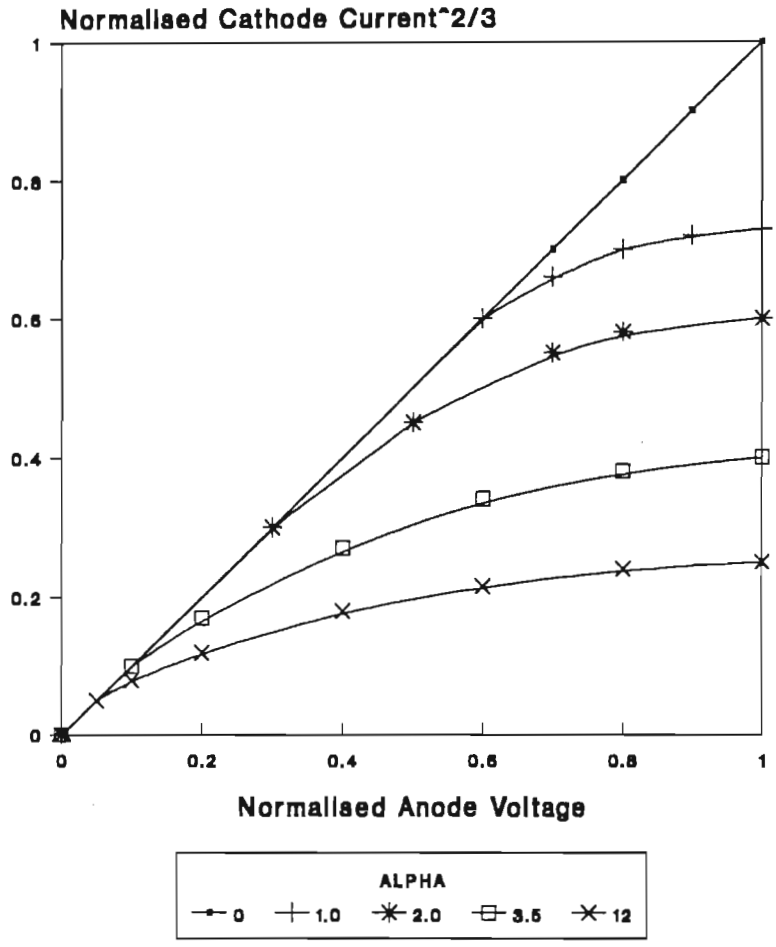

Figure 5.8 Plot of the Normalised I-V Characteristics for Different α

determine these parameters, Beck & Wang describe a method whereby the currents are recorded at three voltages, chosen such that one of them is the geometric mean of the other two, and the common ratio is N. If these three voltages are labelled V_1, V_2, V_3, and the corresponding measured currents I_1, I_2, I_3, then we can define:

$$\Delta = \frac{i_1 - i_2}{i_2 - i_3} \tag{5.18}$$

and

$$L(v) = v^{3/2} - \frac{3}{2} v^{3/2} \ln v \tag{5.19}$$

Making these substitutions into (5.17) gives us an expression for v_1 in terms of

measurable quantities:

$$\ln v_1 = \frac{\Delta \ln N}{\Delta - N^{3/2}} + \frac{2}{3}\left[1 - \frac{3 \ln N}{2(N^{3/2} - 1)}\right] \tag{5.20}$$

Knowing v_1, the three measured currents, N and a simple function $L(v)$, we can solve the following for α:

$$\exp(-\alpha) = \frac{\frac{I_1}{N^3}[L(v_1) + 3v_1^{3/2} \ln N] - I_3 L(v_1)}{I_1 - I_3} \tag{5.21}$$

In practice, the right hand side of (5.21) will be very small and as such I_1 and I_2 must be known to a high degree of accuracy. To make the solution complete we need to know the maximum current available from the patchy cathode, and this is given by:

$$\bar{I} = \frac{I_1(1 - \exp(-\alpha))}{L(v_1) - \exp(-\alpha)} \tag{5.22}$$

The above equations and measurement technique were incorporated into the automatic data logging program written in Hewlett Packard Instrument Basic by the author (see Appendix A). The program could measure an I-V curve for a particular cathode and then determine the degree of patchiness of the cathode, the overall work function of the emitting surface, the maximum real current obtainable from the cathode, and the maximum current that would be available if the cathode were a uniform emitter.

The information thus obtained from the cathodes manufactured was useful in monitoring the change in the cathode surface properties with time. As the cathodes aged, more and more emission sites were formed on the emission surface, and as a result the work function of the cathode was lowered. Furthermore, the value of α obtained was used as a figure of merit for the cathodes when comparing them with one another. Results obtained from this analysis are presented in Chapter 6.

5.4 FACTORS AFFECTING THE PERFORMANCE OF IMPREGNATED CATHODES

Although there are many external factors which have a large effect on the performance of a cathode inside an electron tube, such as residual gases, vacuum pressure, and ion bombardment to name a few, there are several internal factors which can be controlled to optimise the electron emission. Two of the more important factors are matrix porosity and impregnant composition.

5.4.1 Matrix Porosity

The reaction between the impregnant and the tungsten base produces free barium which migrates to the cathode surface. The equilibrium which is set up between the arrival rate of the barium and its evaporation rate is critical in determining the cathodes long-term emission characteristics. This equilibrium can only support a monolayer or less of barium at the cathode surface, and thus the arrival rate of the free barium must be just right to ensure that not too much arrives and is evaporated unnecessarily, or that too little arrives and a partial monolayer results. The rate of migration of the barium is controlled by the pore density, with an figure of 20 per cent generally being accepted as optimum [11] (see figure 5.9).

5.4.2 Impregnant Composition

Figure 5.10 shows the effect of varying the impregnant composition according to results obtained by Dudley [11]. The upper curve shows the influence of the calcium oxide molar composition for a fixed 4 moles of barium oxide and 1 mole of aluminium oxide. There is a large improvement in emission for an increase in CaO content from 0 moles to 1 mole but very little improvement for larger quantities. The lower curve shows how emission varies with BaO content for fixed values of CaO and Al_2O_3. The greatest deterioration of emission occurs for values of less than 2 moles of BaO.

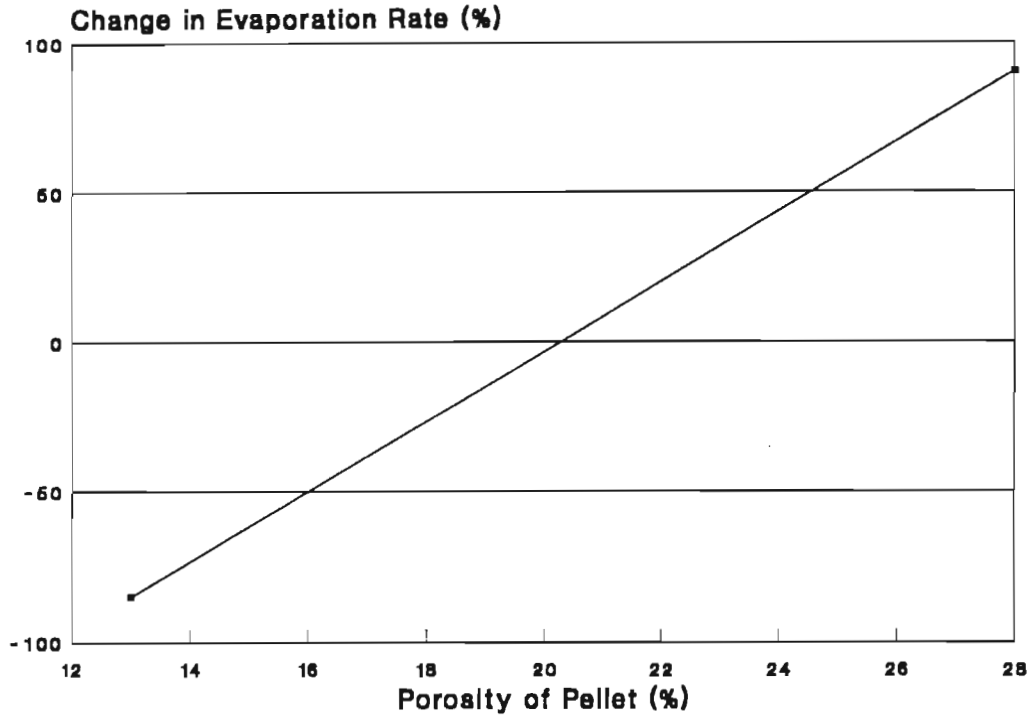

Figure 5.9 Evaporation Rate as a Function of Porosity [12]

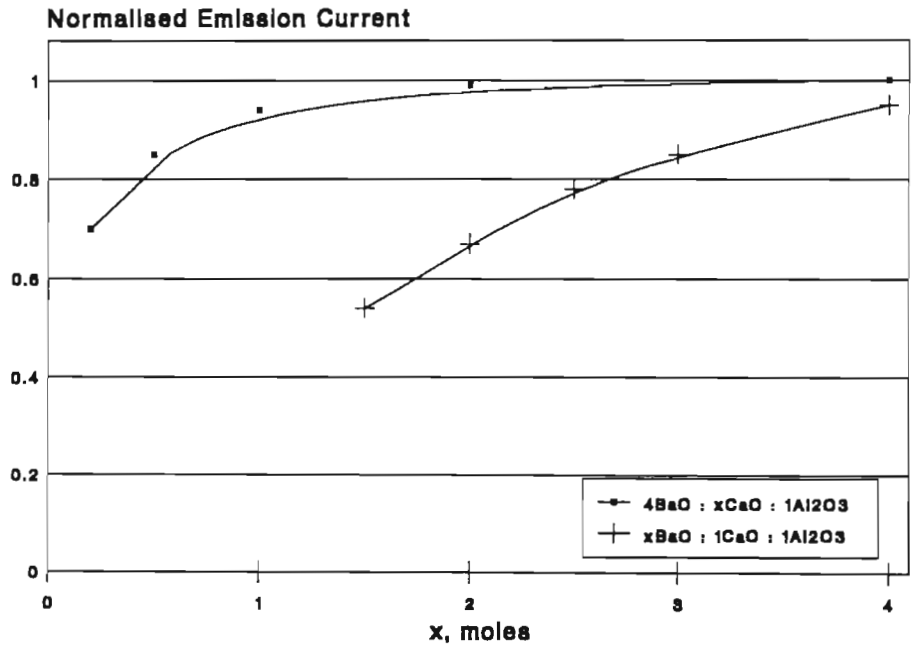

Figure 5.10 Emission Current vs Impregnant Composition [12]

5.5 CATHODE FABRICATION

5.5.1 Pellet Preparation

If tungsten powder of a known and constant grain size is compacted under a pressure of approximately 15 tons.cm^{-2} and then sintered at a temperature in the region of 1750 °C [6] a porous matrix of known porosity is obtained. By impregnating the matrix with a lower melting point metal such as copper, one is able to machine the tungsten to any desired shape while maintaining an open pore structure. The copper can then be removed and a clean porous pellet of intricate shape results.

All cathodes manufactured by the author were machined from 20.15 per cent* porosity sintered tungsten powder by Mr C. Johnson of the Electronic Engineering Department. The cathodes used for performance measurements in planar diodes all had cylindrical radii of 2.5 millimetres, whilst the cathodes used in the microwave tubes had spherical radii of 13.1 millimetres and cylindrical radii of 2.5 millimetres. All pellets were 2 millimetres in depth. The emitting surface of the cathodes was polished using 1000 grit grinding paste before being thoroughly cleaned in acetone and deionised water.

The copper within the tungsten matrix was removed by evaporating the copper off in an induction heater (see figure 5.11). The copper filled pellet was placed in a molybdenum crucible and heated to 1700 °C_B in a hydrogen atmosphere for approximately 60 minutes. The hydrogen was passed through a liquid nitrogen cold trap to ensure that no moisture was present which could oxidise the tungsten and thus destroy its emitting properties. X-ray scans of the pellets showed less than 0.001 per cent copper by weight present after this process [13].

Careful weighing of the matrix before and after copper removal gave an indication of the amount of copper liberated, and served as a check as to the porosity of the tungsten. The fired and extremely clean matrix was then ready for impregnation with

*Calculated value from weighing during impregnation.

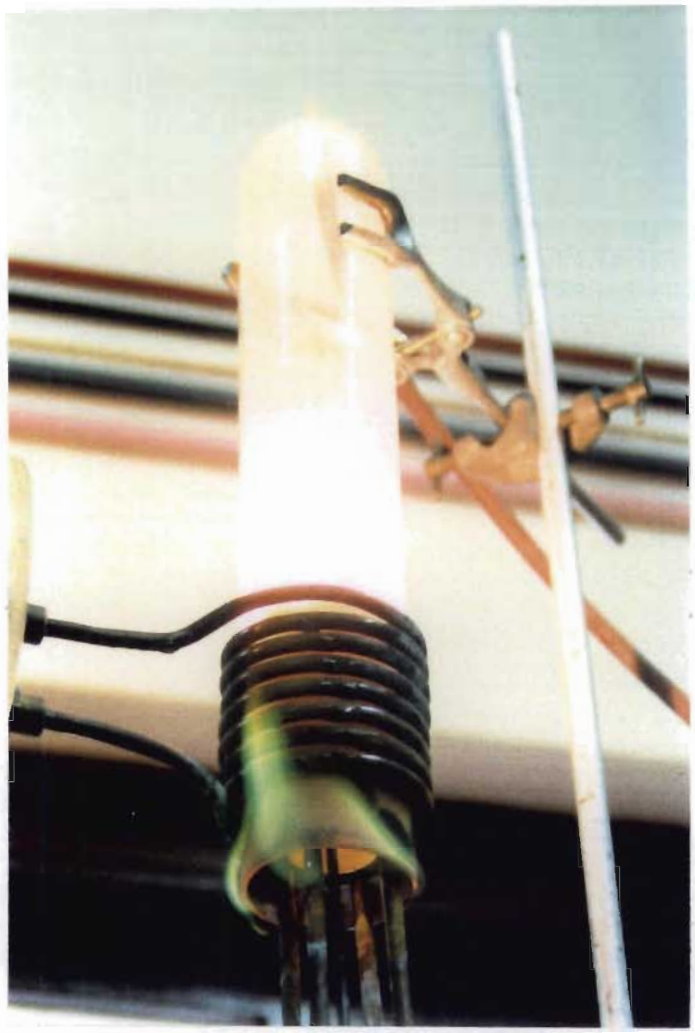

Figure 5.11 Copper Being Removed from Pellet in Induction Heater

the aluminate cathode mix of barium carbonate, calcium carbonate and aluminium oxide.

5.5.2 Impregnation of Porous Matrix

The cathodes manufactured were all S-type cathodes, having a 4:1:1 molar ratio of barium oxide, calcium oxide and aluminium oxide respectively. As the oxides of barium and calcium are extremely unstable when exposed to atmospheric conditions, their respective carbonates are first mixed and then broken down to oxide form in a reducing atmosphere of hydrogen.

The carbonates of barium and calcium are extremely hygroscopic, and as such care must be taken to ensure they are dry before mixing in order that the final ratio is

correct. The following table gives a summary of the amounts used for the mix:

	$BaCO_3$	$CaCO_3$	Al_2O_3
Required Ratio:	4	1	1
Molar Mass:	197.39 g	100.09 g	101.96 g
Final Mixture:	119.62 g	15.17 g	15.45 g

Table 5.1 Cathode Aluminate Mix

After careful weighing, the constituents were placed in a glass container along with an equal volume of glass beads and thoroughly mixed by rolling on a ball mill roller for 48 hours. Care was taken to ensure the seal on the container remained air-tight throughout this process.

A small portion of the mixture was weighed and placed on top of the tungsten pellet inside the molybdenum crucible, as shown in figure 5.12. A hole in the bottom of the crucible allowed the CO_2 liberated during impregnation to escape harmlessly without bubbling through the mixture. Again, dry hydrogen was used as a reducing atmosphere during impregnation.

The induction heater was used to bring the temperature of the cathode slowly up to 1000 $°C_B$. A marked change in colour of the mixture from white to light grey was noticed as the carbonates were broken down to oxide form. After 60 seconds at 1000 $°C_B$, the temperature of the pellet and crucible was raised rapidly to 1500 $°C_B$ where the mixture fused and soaked into the porous tungsten matrix. The induction heater was then immediately switched off and the finished cathode allowed to cool in a dry nitrogen atmosphere.

A small amount of excess impregnant remained on top of the cathodes in the form of a blue-grey glass, as shown in figure 5.13. This was removed by scraping with the

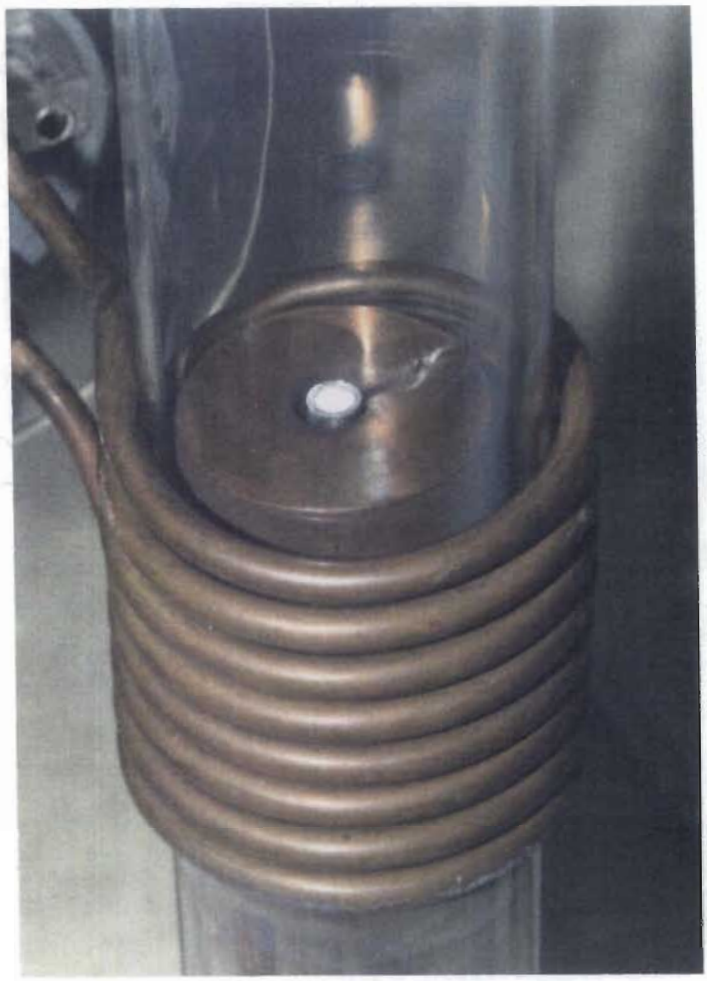

Figure 5.12 Aluminate Mix Inside Molybdenum Crucible in Induction Heater

end of a tungsten rod, and then blowing the pellet with high pressure dry nitrogen. The increase in mass of the pellet was noted as a check for adequate impregnation. The pellet was then crimped into a molybdenum cathode holder to avoid the use of brazing alloys which could have harmful effects on the cathode emission. The cathode holder was such that it could also be easily removed from the electron gun in the event of poisoning and a new one inserted.

5.5.3 Pumping and Activation

Because of the susceptibility of cathodes in general to poisoning, extreme care has to be taken during the exhaust and activation of a tube to ensure that invaluable time and effort is not wasted on a defective device. An error at this stage could result in

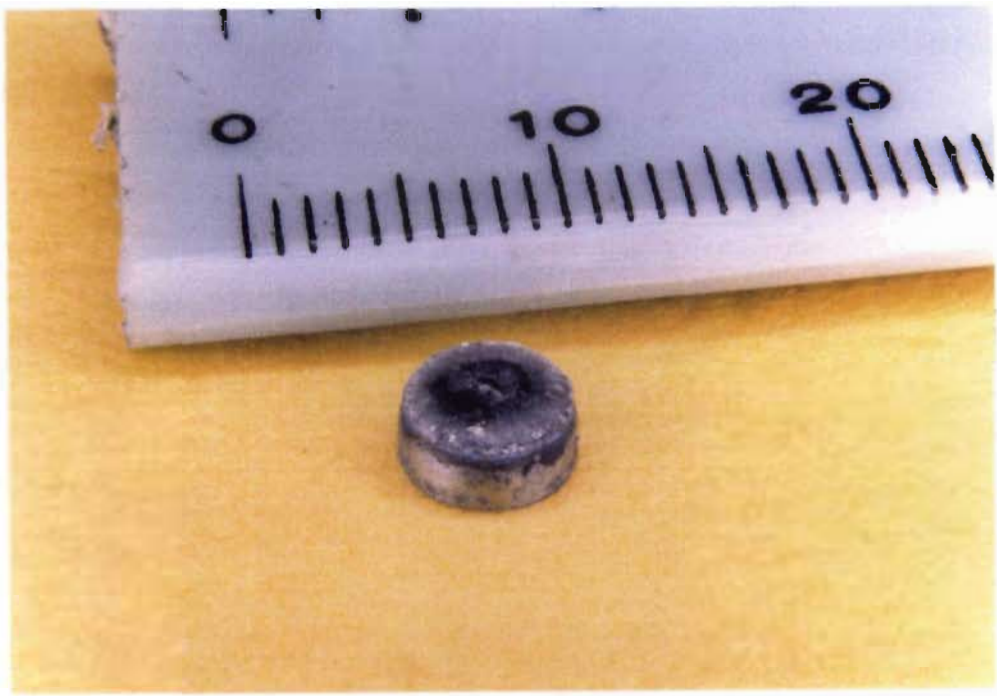

Figure 5.13 Cathode Pellet with Excess Impregnant on Top

reduced cathode emission which may or may not be reversible.

Once the cathode had been inserted into the tube, which was continually flushed with dry nitrogen before pumping to reduce moisture absorbtion, the pump port was sealed to the pump station. The pumping set consisted of a 30 litres per second ion pump backed by a separate rotary pump and absorbtion pump. An ion gauge for measuring pressure was located on the medium vacuum side (less than 10^{-3} Torr) while pressure readings for high vacuum were provided by the ion pump power supply.

A thermostatically controlled oven was lowered over the tubes which were then baked at 350 °C for several hours. This temperature was well above that at which most of the components would normally operate, and thus no further outgassing of these components should occur after the bake out process.

A distinct advantage of impregnated cathodes is that the conversion from carbonate to oxide, and the consequential evolution of vast quantities of CO_2, takes place outside the tube, thus reducing the risk of contamination or oxidation of tube

components. However, absorbed gases and water vapour on the cathode pellet and supporting structure surfaces require outgassing at temperatures above 350 °C before cathode activation proper can take place. For this reason the heater power was slowly increased over a period of approximately 45 minutes to ensure that the tube pressure never exceeded 10^{-5} Torr at any stage.

Once a cathode temperature of 1000 $^{\circ}C_B$ was attained the pressure inside the tube started to drop rapidly, enabling the heater power to be increased until the cathode was at 1150 $^{\circ}C_B$. At this point, voltage was applied to the anode and brought up to full potential over 60 seconds. After this period full cathode emission was obtained, and the cathode temperature could be reduced to the normal operating temperature of 1000 $^{\circ}C_B$.

Concluding Comments

The cathodes manufactured in the Materials Science Laboratory were simple, inexpensive and extremely reliable. While every precaution was taken to minimise the risk of contamination, no unnecessary or costly steps were followed during the impregnation and activation processes. By minimising the steps involved, the processes were repeatable and resulted in cathodes exhibiting very favourable emission characteristics.

REFERENCES

[1] J.R. Pierce, Extract from "Science Fiction", Street and Smith, 1946.

[2] D.M. Smith, "The Theoretical and Practical Analysis of Low Perveance Pierce Electron Guns", University of Natal M.Sc.Eng. thesis, 1990.

[3] A.S. Gilmour, "Microwave Tubes",Dedham: Artech House, 1986.

[4] J.W. Gewartowski and H.A. Watson, "Principles of Electron Tubes", New York: Van Nostrand, 1965.

[5] A.H. Beck, "High Current-Density Thermionic Emitters: A Survey", *IEE Proceedings*, vol. 106, part B, pp. 372-390, November 1958.

[6] P.P Coppola and R.C. Hughes, "A New Pressed Dispenser Cathode", *Proceedings of the IRE*, pp. 351-358, March 1956.

[7] R. Levi, "New Dispenser Type Thermionic Cathode", *Journal of Applied Physics*, vol 24, p. 233, 1953.

[8] reference [5], p. 373.

[9] reference [3], p. 128.

[10] A.H. Beck and D.A. Wang, "The I-V Characteristics for Planar Thermionic Diodes with Patchy Cathodes", *International Journal of Electronics*, vol. 51, pp. 717-733, 1981.

[11] K. Dudley, "Emission and Evaporation Properties of a Barium Calcium Aluminate Impregnated Cathode as a Function of its Composition", *Proceedings of the 5th National Conference*, pp. 6-9, September 1960.

[12] J.L. Cronin, "Modern Dispenser Cathodes", *IEE Proceedings*, vol. 128, part 1, no. 1, pp. 19-32, February 1981.

[13] H.W. Groothedde, "Electron Gun Cathode", final year thesis, University of Natal, unpublished, 1990.

[14] W.H. Kohl, "Materials and Techniques for Electron Tubes", New York: Reinhold, 1960, p.540.

[15] reference [12], p. 25.

CHAPTER 6.

CATHODE PERFORMANCE

So often in engineering applications, the success of a design is determined by the usefulness of the final device, and not by the exactness of the design itself. Many of the oxide cathodes used in the early stages of the project experienced premature failure due to poisoning, incorrect activation procedures or poor preparation, but in most cases emission was sustained for long enough to obtain useful information about the tube in question.

The move to impregnated cathodes marked the first step towards producing reliable cathodes exhibiting emission characteristics comparable with commercially obtainable cathodes. H.W. Groothedde [1] initiated the move by designing an impregnated cathode as part of a final year design project in the Materials Science Laboratory. Although Mr Groothedde investigated the relevant procedures and produced a carbonate mixture, no cathode was actually impregnated or tested.

It was at this stage that the author continued with the work on cathode development, and produced and tested several cathodes for use in the project's electron guns. Although useful emission was obtained from all such cathodes, the temperature needed to maintain space-charge-limited emission was somewhat higher than expected for cathodes of this nature. In order to investigate the work function of the cathodes, it was necessary to measure their saturation current densities, and to this end some sort of test diode was needed.

6.1 CONSTRUCTION OF THE TEST DIODES

6.1.1 The Glass Diode

In conjunction with a final year student [2], a close-spaced diode was constructed in a glass envelope to facilitate temperature measurement using optical pyrometry. The diode consisted of a tungsten impregnated cathode of similar geometry as those used in the electron guns, and an OFHC copper anode positioned 1.4 millimetres from the cathode surface. The electrode supports were of a similar construction to the gun modules, in which three ceramic rods were brazed to molybdenum support wires attached to each electrode. As in the case of Gun Number 1, a moveable glass shield was included in the diode to allow accurate temperature readings to be taken even after barium deposition had taken place on the envelope walls. Figure 6.1 shows the diode assembly attached to its valve base before being inserted into the glass envelope.

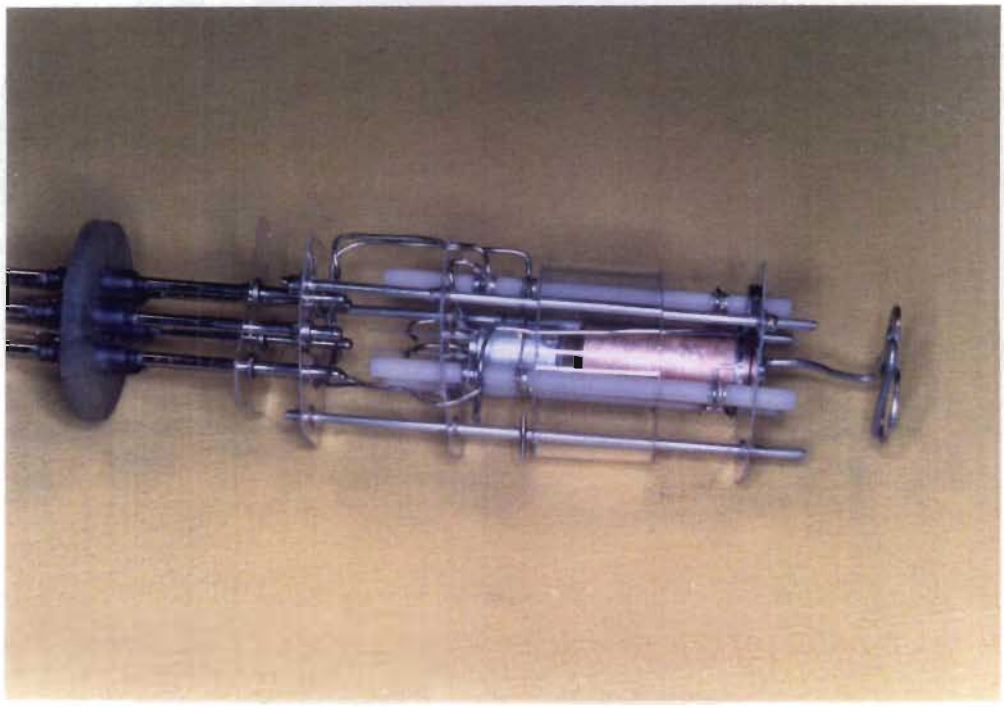

Figure 6.1 The Glass Diode Assembly

The same carbonate mixture of Mr Groothedde's was used for the impregnation of the cathode tested in this diode. As the cathode emission could now be saturated, the work function of the cathode was obtained from a Richardson plot, and was

found to have a somewhat high value of 2.43 ± 0.17 eV*. As the impregnation process had been carefully carried out, it was concluded that the less than ideal emission characteristics were as a result of the carbonate mix being contaminated due to poor preparation or storage conditions, and thus the author decided to start afresh with a new batch of aluminate mix.

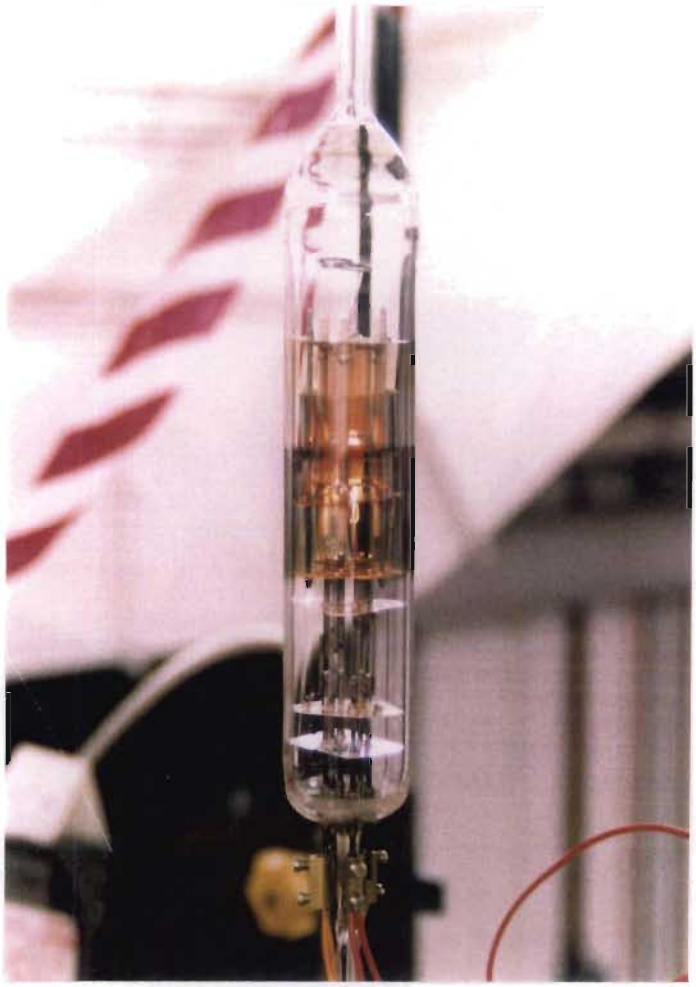

Figure 6.2 The Glass Diode Under Test

To make meaningful headway into the development of cathode technology, several cathodes needed to be tested in a short space of time. For this reason, a demountable test vehicle was required into which different cathodes could be inserted quickly and easily, reducing the assembly time per device.

---

*Gittens [3] gives values for aluminate cathodes as low as 2.1 eV.

6.1.2 A Water-Cooled Demountable System

The cathodes used for the tests were planar, and had a radius of 2.35 millimetres. In order to keep the anode-cathode spacing small in comparison to the cathode radius and thus reduce the influence of any fringing of electric fields, a spacing of 0.1 millimetre was chosen. This small distance also meant that the anode potential required to saturate the cathode was small, thus reducing the overall power into the anode.

If the anode was allowed to get too hot during the operation of the diode, impurities in the anode surface would be given off, affecting the results of the experiment. For this reason, the molybdenum anode was water cooled. To simplify the diode assembly, all the supporting ceramic tubes and kovar plates merely bolted together, making modifications to the structure quick and rudimentary. The assembled diode is shown in figure 6.3.

By first removing the heater, the cathode holder could be slid out of the first heat shield and replaced with a new holder, complete with cathode in position. The turn-around time from testing one cathode to the next, including letting the tube up to atmosphere, removing the heater and old cathode, replacing with a new cathode and heater, making electrical connections, pumping and baking, was reduced to approximately 2½ hours. This, combined with automated data logging of results, meant that the cathode development program could proceed at a far greater tempo than ever before.

The stainless steel water cooling jacket was brazed to a Varian conflat flange so that it could be sealed to a pump station using a copper pressure seal. Also included in the system was a glass window for temperature measurements and three insulated electrodes for making electrical connection to the diode. Figure 6.4 shows the diode bolted to the pump port together with the glass window on the left, and the electrical connects on the right (See Appendix D for assembly diagram).

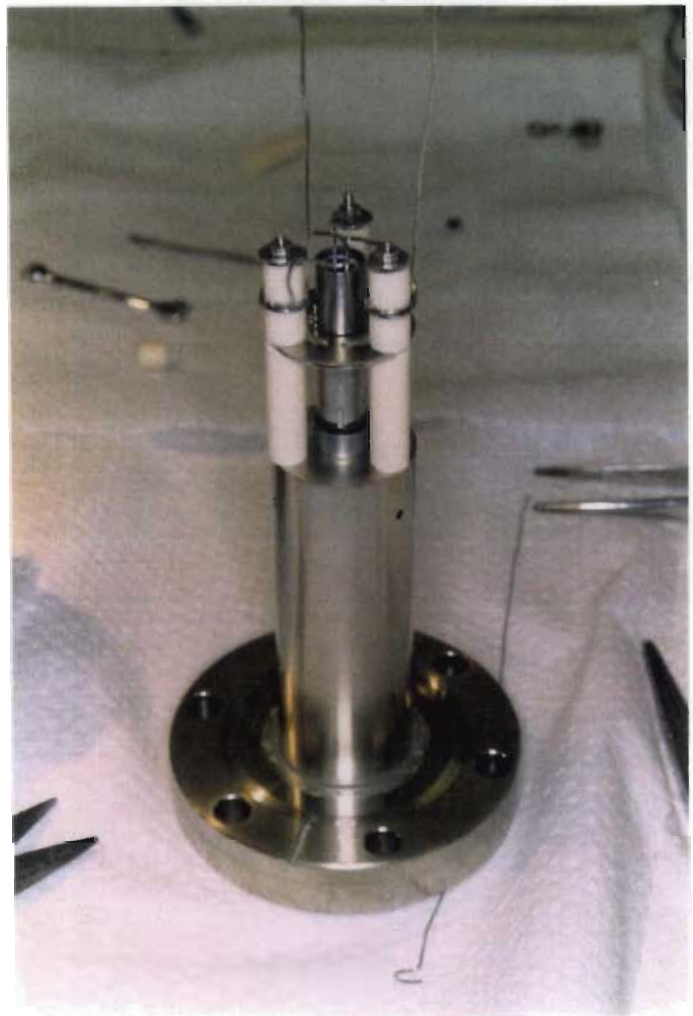

Figure 6.3 The Assembled Test Diode

Figure 6.5 shows a view of the diode under test through the glass viewing window. The cathode, glowing bright yellow, is situated just below the molybdenum anode shown at the top of the picture.

6.2 MEASUREMENT TECHNIQUES

6.2.1 Temperature Measurement

In order to make meaningful conclusions on the data collected on the cathodes, it was necessary to know accurately the temperature at which the readings were taken. Very often, the inclusion of thermocouples right at the emission surface is not practical, and thus another method must be used. By far the most popular is optical pyrometry, where the temperature of a body is determined from the amount of light

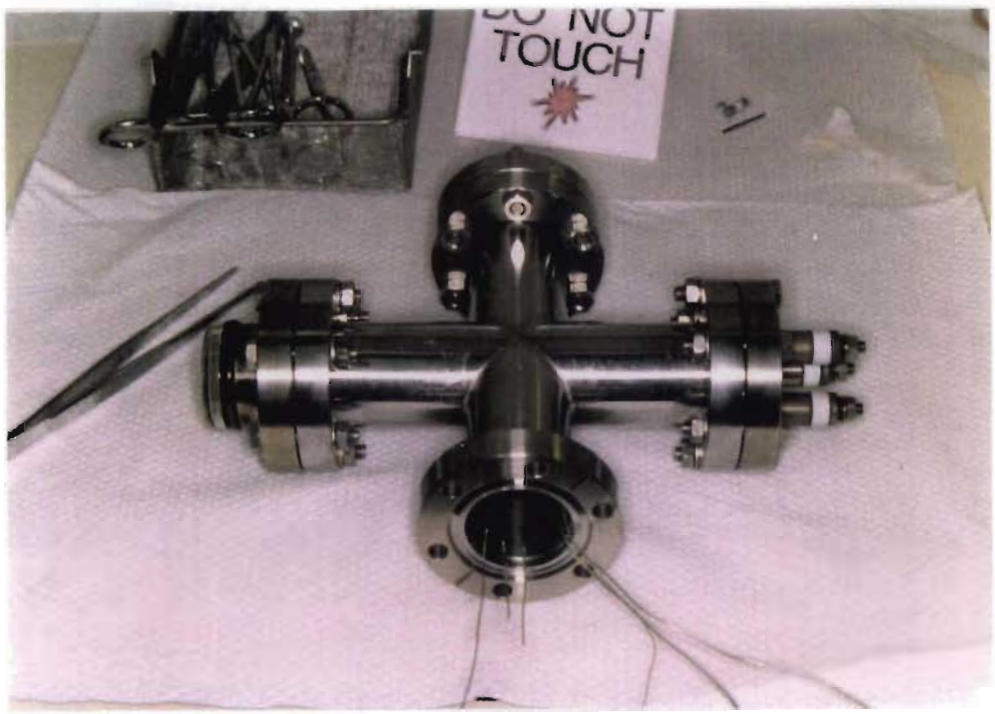

Figure 6.4 Diode Pump Port Assembly

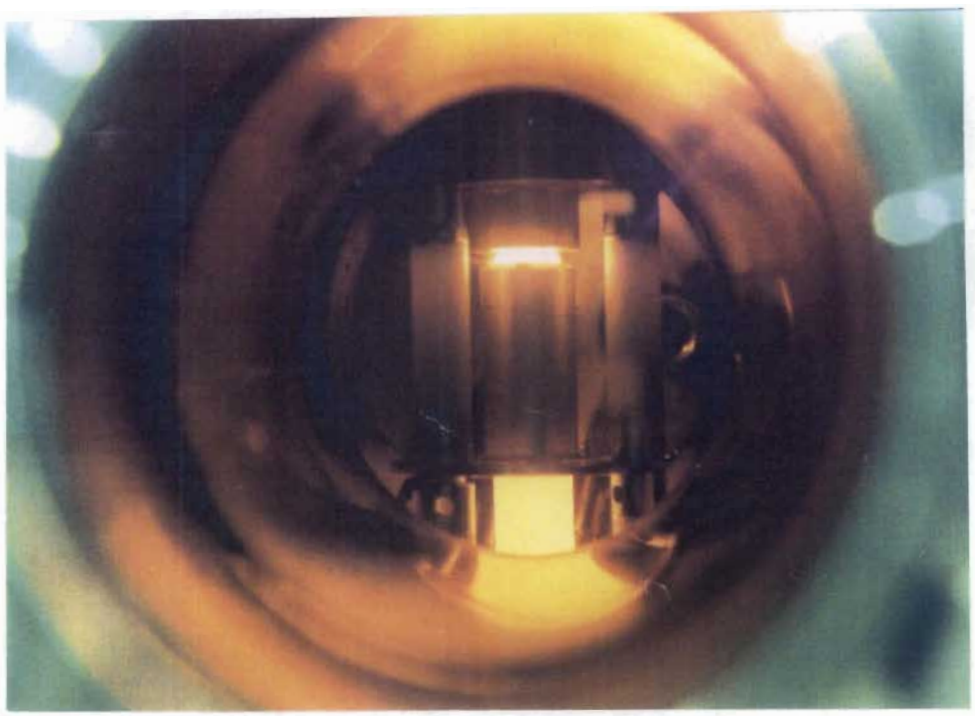

Figure 6.5 The Diode Under Test

being radiated from it. The only drawback to this method is that the object being measured must be in the line of vision of the pyrometer, and the object's temperature

must be such that it radiates in the visible spectrum (> 600 °C).

Optical pyrometers are calibrated to measure the temperature of *black bodies*, having a spectral emissivity of unity. Most practical materials have a spectral emissivity of less than unity, and corrections must be made to the measured brightness temperature to obtain the true temperature. Most literature sources on cathode evaluation give the brightness temperature of the emitting surface, and as such all temperatures quoted in this thesis having a subscript "B" are brightness temperatures as measured using an optical pyrometer. Many correction curves are available in the literature [4],[5], a table of which is included in Appendix C. As the emissivity of an object varies with the wavelength of the emitted light, most pyrometers contain filters which only allow through light of one particular frequency. In general, the wavelength of red light (650 μm) is used, as vacuum tubes emit sufficient red light to enable accurate readings to be taken. The accuracy of temperature readings using optical pyrometry is very high, as the increase in brightness of a hot body with temperature is four times as much as the percentage increase in temperature.

Most manual pyrometers are of the *disappearing filament* type, having a lamp filament located at the image plane of the objective lens. By varying the current through the filament, the brightness of the filament can be made to match that of the object, and subsequently the brightness temperature is obtained from the calibrated relationship between current and black body temperature. Figure 6.6 shows such a pyrometer in use during a cathode impregnation process.

Automatic optical pyrometers are available for instances where unattended temperature readings are needed. The pyrometer outputs an electrical signal depending on the temperature of the object, and by using suitable calibration curves, a brightness temperature may be calculated. The inherent subjectiveness of a manual pyrometer is thus eliminated, as the reading is no longer dependent on the operator's ability to compare brightness. An Ircon automatic optical pyrometer was used for temperature measurement of the cathode surfaces once automated data logging was introduced to the cathode development project. The estimated total measurement uncertainty of cathode temperature was ±5°C.

Figure 6.6 An Optical Pyrometer in Use

6.2.2 Automated Data Logging

Automatic logging of data is a tremendous advantage for the tube engineer. The delicate nature of vacuum tubes means that very often a tube might suffer premature failure before sufficient information is gleaned from it, if results have to be sought manually. Furthermore, if the turn-around time for experimental devices it to be kept to a minimum, automation of the processes involved is essential, especially if the tube is pulsed and several readings need to be taken during each pulse cycle.

An automated test station was developed by N. Vassilopoulos at the University of Natal's Materials Science Laboratory for just such a purpose. The station was primarily designed for the testing of the travelling wave tubes being developed in the laboratory, but has the capability of being utilised for many related applications. Some of the more important components of the station are:

(1) A 33 MHz 80486 personal computer.

(2) A PC-30 Data Acquisition card providing sixteen A/D channels with input buffer amplifiers, two 12 bit D/A channels, two 8 bit D/A channels and

twenty four digital I/O lines.

(3) An RF measurement panel, containing such components as a stepper motor controlled resonator, adjustable attenuators, bias "T"s, and RF loads.

(4) A computer interface for talking to the RF measurement panel and the sixteen A/D channels.

(5) Several Hewlett Packard instruments, including an HP-54601A Oscilloscope, an HP-437B Power Meter, an HP-3421A Data Acquisition Unit (DAU) and an HP-3478A Multimeter.

(6) An HP-37203A HP-IB extender for communicating to the DAU via a fibre optic link.

(7) A 20 kV transformer and rectifier, coupled with a 6.5 μF capacitor bank.

(8) A 6 kV regulated pulsed power supply.

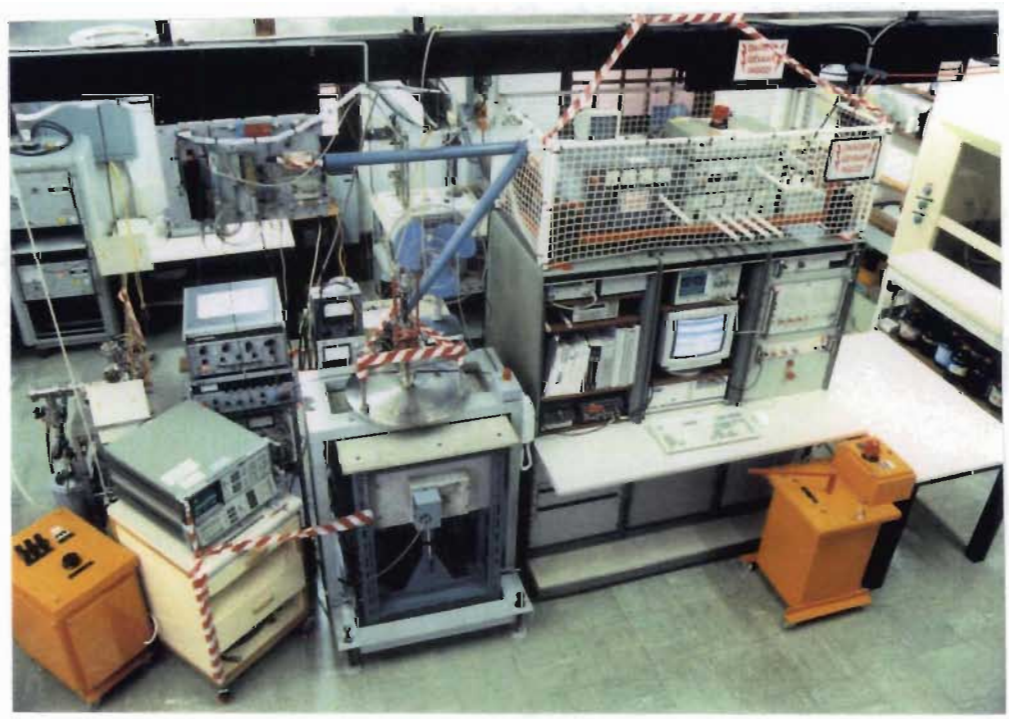

Figure 6.7 The Automated Test Station

The diodes and electron guns were wired positive earthed, with the heater supply and cathode measuring devices, such as the DAU, floated down to negative cathode potential. An insulated table was located on top of the test station to carry such

equipment, with control to the DAU being supplied via the HP-IB Extender. A schematic of the equipment configuration is shown in figure 6.8.

HP Instrument BASIC was used to write the software for the testing of the tubes. Software code for the operation of the various Hewlett Packard instruments was generated using a software development tool, "HP Interactive Test Generator II" (HP ITG II). The interactive tools included in HP ITG II allowed direct instrument control, the generation of software for instrument control, and facilities for analysing and graphing of data. Special software drivers had to be written for those instruments not supported by HP ITG II, such as the DAU.

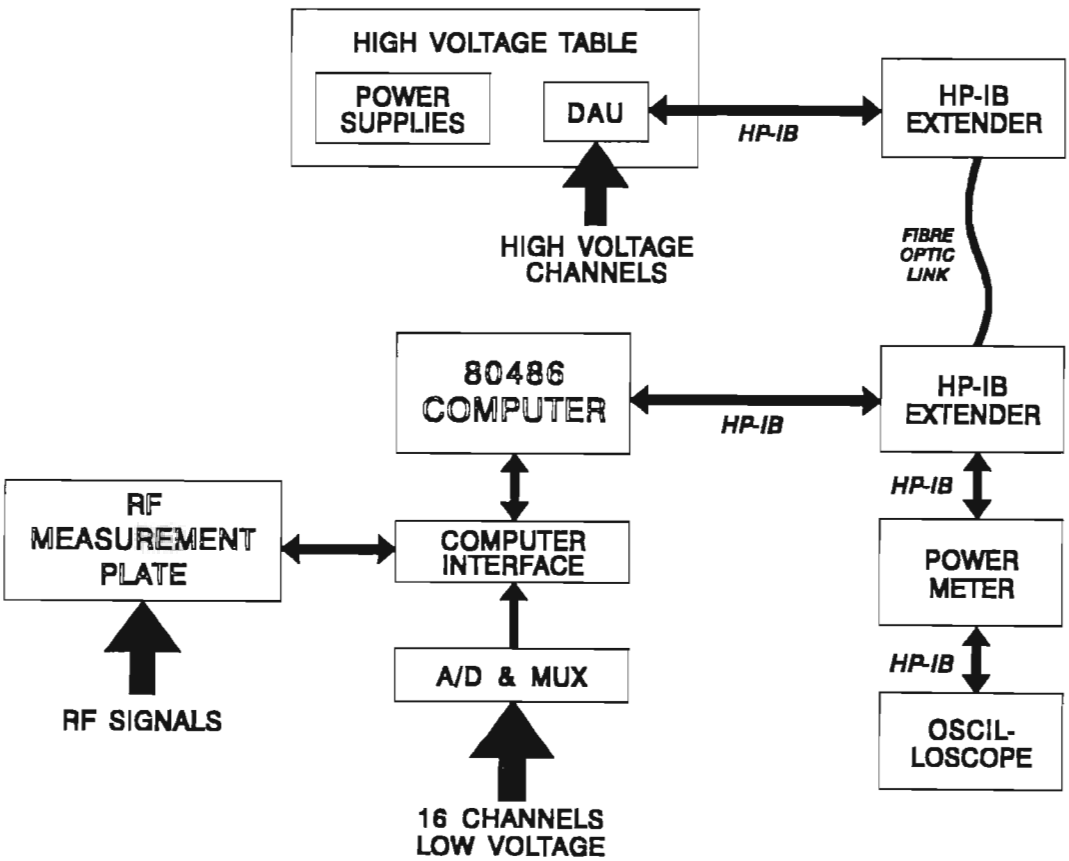

Figure 6.8 Schematic of Test Station Equipment

For the test and measurement of the cathode performances, two software programs were written by the author, print-outs of which are included in Appendix A. The first such program took measurements of the various cathode parameters, including anode voltage, cathode current, cathode temperature, and heater voltage and current, and

wrote the accumulated data to files. A sweep was made through different anode voltages and cathode temperatures to produce an I-V characteristic for each cathode, and the results then presented in graphical format.

The second program took the measured data and ran an analysis on it based on the cathode emission theory of Beck & Wang [6]. Without taking the cathode far into saturation, the program could predict from the I-V curves what the saturation current for that particular cathode would be, as well as the voltage at which saturation would occur. An indication of the degree of patchiness of the cathode was also given, allowing an extrapolation to be performed to calculate the maximum current that would be obtainable from the cathode if it were ideal, ie. of uniform emission across its surface. Finally, the work function of the cathode was calculated.

An analysis of this nature performed on each cathode was invaluable, as it allowed one to monitor the spread of emission sites across the cathode surface with time, and gave feedback as to the state of the cathode surface physics at any point in the cathode activation and ageing process. Often this process is so rapid that the recording of the change in emission characteristics with time would not be possible without the aid of automated logging.

6.3 CATHODE EMISSION RESULTS

The following results are typical of the cathodes produced in the Materials Science Laboratory, having a surface area of 0.175 cm^2 and positioned 0.1 millimetres from the planar anode surface. To reduce the overall power into the anode, a 10 millisecond voltage pulse was used with a 100:1 duty cycle. As is characteristic of impregnated cathodes, the output current pulse was good, with no signs of droop along its length. Again, keeping to cathode convention, temperatures quoted are brightness temperatures as measured using an optical pyrometer.

6.3.1 I-V Characteristics

The cathode current-voltage relationship for different temperatures of operation is shown in figure 6.9. The curves show distinctly the transition from the straight line relationship for space-charge-limited emission to the flatter relationship for when the emission became limited by the temperature of the cathode surface. As the temperature of the cathode was increased, so the value of cathode current at which saturation occurred increased.

To avoid the need for highly regulated heater power supplies and to minimise emission fluctuation associated with local poisoning, electron guns are operated in the straight line region of these curves. For example, in the travelling wave tube under development, the value of the 2/3 power of cathode current was only 0.18 $A^{2/3}$ meaning that cathode temperatures as low as 930 $^{o}C_{B}$ could be used.

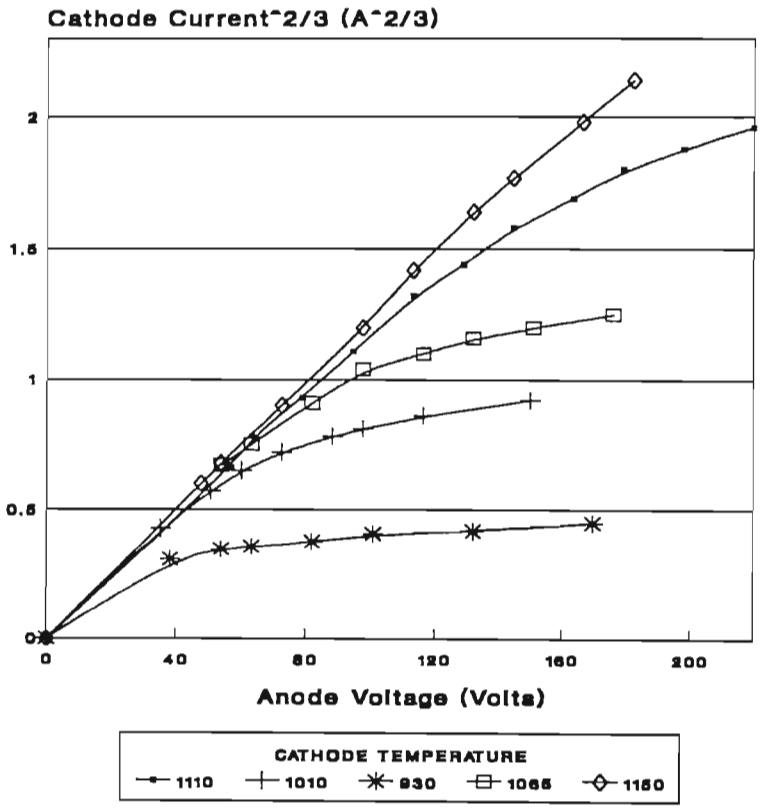

Figure 6.9 I-V Characteristics for Cathodes

The initial slope of the straight line of each curve is the perveance of the diode, which is dependent only on the diode geometry. The increasing slope of the lines suggests that the geometry was changing with temperature, an intimation which is substantiated if one considers the thermal expansion of the cathode holder, which would reduce the cathode-anode spacing as the temperature was increased, thus raising the perveance of the diode.

The Richardson-Dushman Equation can be written in the form:

$$\ln J = \ln J_0 + \left(\frac{eE}{4\pi\epsilon_0}\right)^{\frac{1}{2}} \qquad (6.1)$$

where J_0 is the *zero field* current density, or saturation current density. Equation (6.1) suggests that a plot of ln J versus E should be a straight line with an intercept, when extrapolated to $E=0$, of the value of ln J_0. This method was used to calculate the saturation current densities of the cathodes, and is illustrated in figure 6.10.

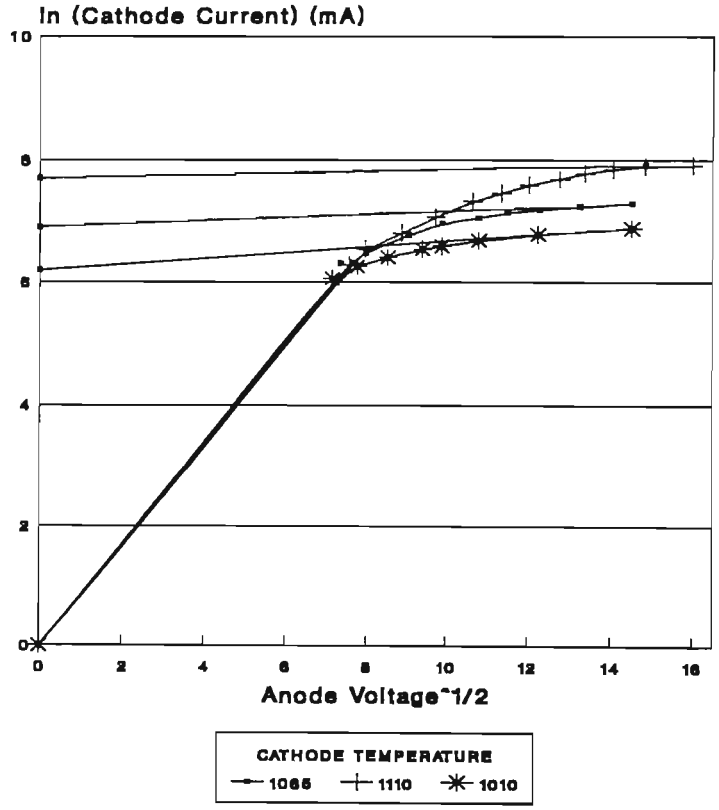

Figure 6.10 Determination of Zero Field Current Density

Typical saturation current densities thus obtained were 17.6 A.cm^{-2} at 1140 °C_B, 9.5 A.cm^{-2} at 1060 °C_B, and 6.7 A.cm^{-2} at 1025 °C_B. As the electron guns being developed operated at an emission density of only 0.41 A.cm^{-2}, cathode life was expected to be good.

6.3.2 Cathode Work Function

If equation (5.2) is plotted with $\ln(J_0/T^2)$ versus $1/T$, the slope of the straight line obtained will give the Richardson work function of the cathode. The work functions of the cathodes using the new aluminate mix were calculated from curves similar to that in figure 6.11 to be 2.03 eV, with an estimated total uncertainty of ±0.08 eV. This figure compares favourably with the findings of Cronin [7], who quotes figures for similar cathodes of 2.049 eV at 1343 K.

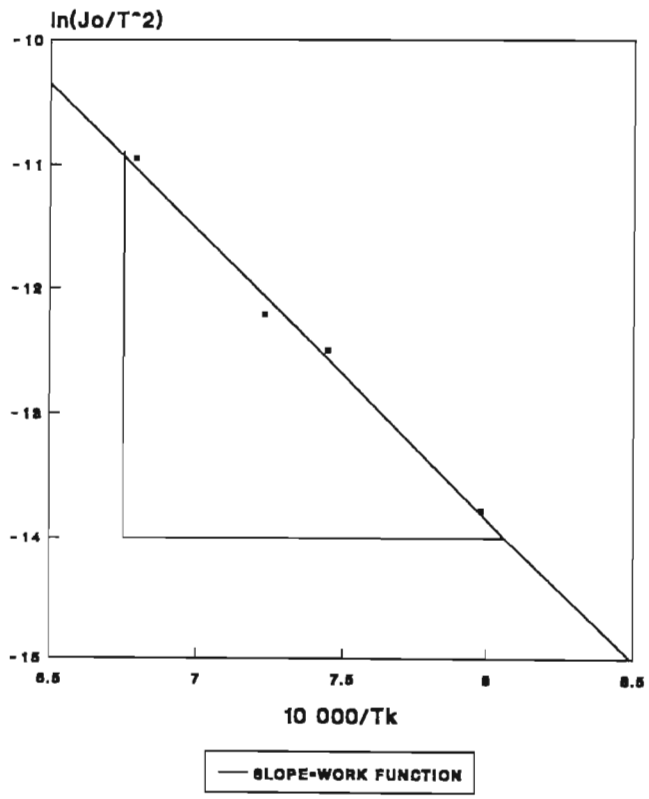

Figure 6.11 Richardson Plot to Determine Cathode Work Function

6.3.3 Cathode Patchiness

For the I-V characteristics obtained from the cathodes, a curve was fitted which satisfied equation (5.17) according to the Patch Theory of Beck & Wang. The curves predicted from this theory compared very closely to the measured data points, as shown in figure 6.12. From these results a value of α was obtained from the software program of 2.56, which implied that the emission from the cathode surface was not uniform, but concentrated in patches of low work function surrounded by areas of higher work function. Only in the case of controlled porosity cathodes does the emission density approach the ideal situation of being uniform across the entire cathode surface.

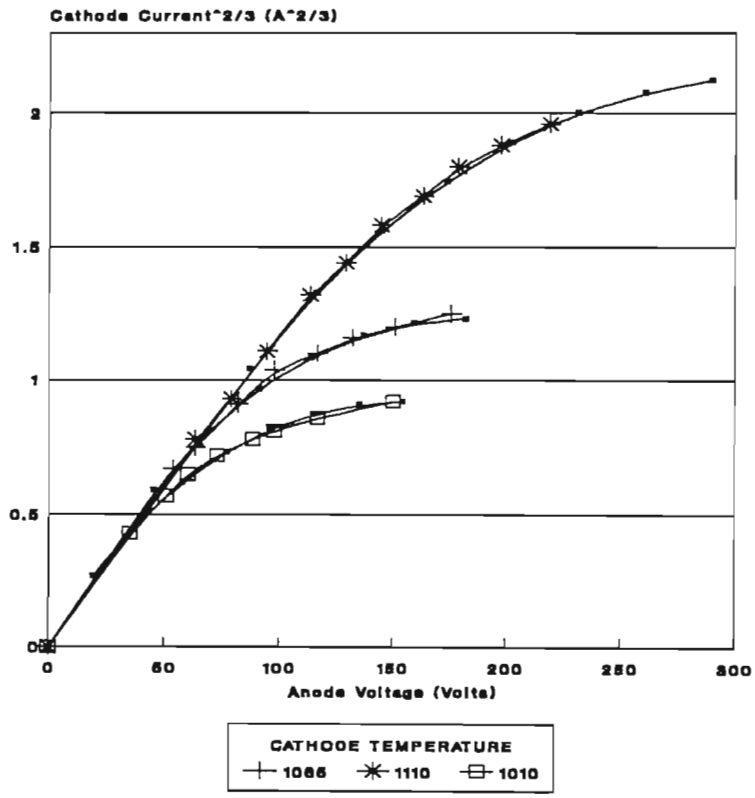

Figure 6.12 Comparison of Patch Theory (dashed lines) to Measured Data (solid lines)

To investigate the change in surface physics with time of a practical impregnated cathode, a cathode was analysed which had been stored in a glass capsule for some eighteen months. The cathode had shown signs of poisoning from this period of storage, and required an ageing process to restore its electron emission to an

acceptable level again. The curves shown in figure 6.13 were again calculated from the Patch Theory, and show a distinct decrease in α, and thus an increase in emission uniformity, with time. The bracketed figures in the figure legend indicate the value of α at that cathode age.

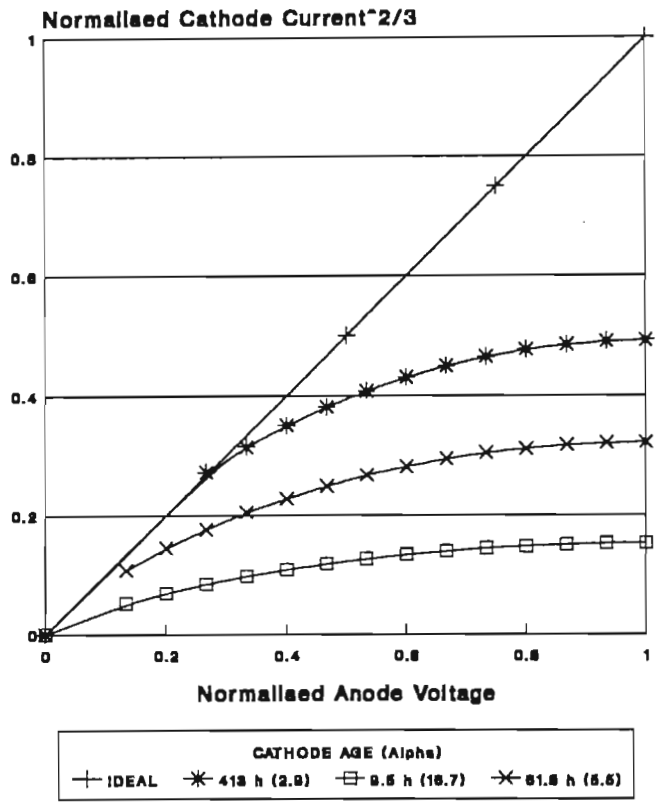

Figure 6.13 Reduction in α with Time

This increase in emission uniformity with time would be expected from a cathode which has had its surface impregnant contaminated, and which requires time to allow fresh barium to migrate to the surface from the reservoir below. Similar behaviour was observed to a lesser extent in "healthy" cathodes, with the final emission pattern stabilising after a few hours.

Again, the initial slope of the I-V curves increases with a decrease in α, implying an increase in diode perveance. As the emission spread further across the cathode surface, so the *effective* cathode surface area increased, thus raising the perveance of the diode.

REFERENCES

[1] H.W. Groothedde, "An Electron Gun Cathode", final year design project, University of Natal, November 1990.

[2] L.A. Pereira, "TWT Pulsed Cathode Development", final year design project, University of Natal, November 1991.

[3] J.F. Gittins, "Power Travelling Wave Tubes", London: English Universities Press, 1965, p. 242.

[4] M. Knoll, "Materials and Processes of Electron Tubes", Berlin: Springer-Verlag, 1959, p. 34.

[5] W.H. Kohl, "Materials and Techniques for Electron Tubes", New York: Reinhold, 1960, p.614.

[6] A.H. Beck and D.A. Wang, "The I-V Characteristics for Planar Thermionic Diodes with Patchy Cathodes", *International Journal of Electronics*, vol. 51, pp. 717-733, 1981.

[7] J.L. Cronin, "Modern Dispenser Cathodes", *IEE Proceedings*, vol. 128, no. 1, pp. 19-32, February 1981.

CHAPTER 7

CONCLUSION

This thesis does not document a revolution in electron gun design, but has shown how innovative technology was used to bring about an improvement in performance of the travelling wave tubes currently being manufactured at the University of Natal's Materials Science Laboratory.

Initial studies made on previous experimental guns showed that guns of this nature are prone to experiencing errors as a result of constructional tolerances. The effect of these tolerances was found to be significant, and care must be taken to ensure that assembly and jigging procedures do not compound these difficulties.

Simulations of the new switching electrode provided tremendous insight into the final geometry and positioning required, and the close correlation between actual measured data obtained from previous guns and similar simulations performed on them, gave credibility to the simulation results.

The new method of supporting the gun electrodes allowed greater accuracy to be achieved with the gun geometry, resulting in more consistent and predictable beam attributes, whilst still retaining the strength associated with ceramic technology. The simple electrical feed-through technique enabled considerable flexibility in gun design, with any number of electrodes being available in any one envelope. The problems associated with metal to ceramic joints of this nature were addressed, and a solution to leak free seals found using active brazing techniques.

Pulsing of the beam was possible with the new electrode, with no adverse effects on the laminar nature of the beam. No additional power supply was required, with a reduction in potential of the electrode to zero being sufficient to reduce the power into the tube to a safe level. By varying the "on" bias potential of the electrode, a

change in perveance was obtained with far less destructive effect on the electron trajectories as would be obtained with a conventional mesh grid. This was particularly useful for overcoming construction tolerances during the development stages of the guns.

The modulated gun resulted in an enhancement in the performance of the TWT demonstrators by reducing the transverse forces on the beam edge electrons and thus improving the laminarity of the electron flow. The position and diameter of the beam minimum could also be altered to coincide with the magnet stack entrant requirements, all factors which increased the effectiveness of the focusing field. Furthermore, the expensive process of "tweaking" the magnet stack to reduce helix interception could now be simplified by using feedback to control the beam focusing. The result was excellent transmission figures from the cathode to collector of the TWT. The RF gain of the tube could be optimised by using the switching electrode potential to alter the beam fill factor, raising the maximum attainable gain several decibels above that of the fixed focus case, and over the entire bandwidth of the tube.

Being able to adjust the focusing of the beam allowed one to use the tube as a dual mode device, with similar performance characteristics in either CW or pulsed mode. A non-flat current pulse shape, caused by the build-up of ions during the pulse, can be offset by shaping the voltage applied to the switching electrode.

An investigation into cathode operation found that dispenser cathodes had several advantages over their oxide-coated counterparts, including resistance to poisoning and increased life spans. It was also discovered that cathodes of this nature are not uniform emitters, but rather display a distinct patchy behaviour depending on the state of the surface physics of the cathode. Practical results obtained agreed very closely with this theory. Overall emission results from the impregnated cathodes were very promising indeed. Their work functions and saturation current densities were comparable to commercially available cathodes, while the technology of preparing the cathodes was kept as elementary as possible.

The overall objective of the project was to develop the technology to produce functional travelling wave tubes in South Africa. To meet this end, it was necessary

to concentrate one's efforts on finding practical solutions to the problems on hand, leaving little time for analysing every irregularity in tube performance. However, it can be stated with certainty that the objective was achieved, and even surpassed, by the innovative use of the resources available to the project. The success of the final TWT design must be gauged by the usefulness of the results to the general performance of vacuum tubes that will eventually use this technology, and not by how far back the frontiers of tube technology have been pushed. To quote Pierce:

> *"A person studying electron beams to understand them and improve the art should of course be very careful and thorough. The person who wants to use an electron beam for some particular purpose may lose precious time by trying to do better than well enough."*
>
> J.R. Pierce, "Theory & Design of Electron Beams"

APPENDIX A:

SOFTWARE PROGRAMS FOR CATHODE TESTING

```
10   OPTION BASE 1  ..... must be first line.
20
30
40                          "ALBERT.WF2"
50
60          Program to Measure the Performance Characteristics of
70               Cathodes Tested in a Close-Spaced Diode.
80
90                          by B.D. Foulis
100                         November 1992
110
120
130   GRAPHICS ON
140   ON ERROR CALL Hpt_error
150   CALL Hpt_ibasic_init("ALBERT")
160   CALL Hpt_init("ALBERT.WF2")
170   CLEAR SCREEN
180   CALL Test
190   CALL Hpt_close_all
200   END
210
220   SUB Hpt_error
230     DIM A$[255]
240     CALL Hpt_close_all
250     IF ERRN<1000 THEN
260       DIALOG "ERROR",ERRM$
270     ELSE
280       CALL Hpt_errmsg(A$)
290       DIALOG "ERROR",ERRM$&CHR$(13)&A$;
          SET("HEIGHT":400,"WIDTH":500)
300     END IF
310     STOP
320   SUBEND
330
340   SUB Test
350
360   *** HPITG Declarations Begin ***
370     INTEGER Hp3478a
380     INTEGER Hp54601a
390     REAL Vmax(100),Imax(100)
400     REAL H(10)
410     K=1
420   *** HPITG Declarations End ***
```

```
430
440 *** HPITG Initializations Begin ***
450    CALL Hpt_assign("HP3478A",0,Hp3478a)! 0 is CONVENTIONAL
460    CALL Hpt_assign("HP54601A",0,Hp54601a)! 0 is CONVENTIONAL
470 *** HPITG Initializations End ***
480
490 *** HPITG Actions Begin ***
500    CALL Hpt_push(Hp54601a,"RESET")
510    CALL Hpt_set_str(Hp54601a,"VIEW_CH2","ON")
520    CALL Hpt_set(Hp54601a,"TIME_SENS",.005)
530    CALL Hpt_set(Hp54601a,"SENS_CH2",.2)
540    CALL Hpt_set(Hp54601a,"SENS_CH1",.1)
550    CALL Hpt_set_str(Hp54601a,"TRIG_MODE","NORMAL")
560    CALL Hpt_set_str(Hp54601a,"TRIG_SOURCE","C1")
570    CALL Hpt_set(Hp54601a,"TRIG_LEVEL",-.04)
580    CALL Hpt_set_str(Hp54601a,"TRIG_SLOPE","NEG")
590    CALL Hpt_set(Hp54601a,"OFFSET_CH1",-.304)
600    CALL Hpt_set(Hp54601a,"OFFSET_CH2",.592)
610
620 Measure_data:!
630
640    FOR L=1 TO 100000
650    NEXT L   ! wait before first reading
660    CALL Hpt_set_str(Hp54601a,"MEAS_SOURCE","C1")
670    CALL Hpt_take_readin(Hp54601a,"MEAS_V_BASE")
680    CALL Hpt_peek(Hp54601a,"MEAS_V_BASE",Vmax(K))
690    CALL Hpt_set_str(Hp54601a,"MEAS_SOURCE","C2")
700    CALL Hpt_take_readin(Hp54601a,"MEAS_V_TOP")
710    CALL Hpt_peek(Hp54601a,"MEAS_V_TOP",Imax(K))
720    IF Imax(K)>7 THEN GOTO 670
730    GOTO Temp    ! TAKE TEMPERATURE READING
740
750 Prt_data_screen:!
760
770    IF Vmax(K)>10 THEN Vmax(K)=0
780    IF Imax(K)>4 THEN Imax(K)=0
790    H(1)=Vmax(K)*1000
800    H(2)=Imax(K)*1000
810    PRINT TAB(7);"Va= ";H(1);TAB(18);"V";
820    PRINT TAB(24);"Ik=";H(2);TAB(34);"mA";
830    PRINT TAB(42);"Temp=";Temp;"B"
840    BEEP
850
860    DISP "ADJUST ANODE VOLTAGE"
870    FOR L=1 TO 200000
880    NEXT L! WAIT A WHILE
```

```
890
900     INPUT "HIT <RETURN> TO TAKE ANOTHER READING (Q TO PRINT
        GRAPH)",A$
910     IF A$="Q" OR A$="q" THEN GOTO Sort
920     IF A$="D" OR A$="d" THEN GOTO Measure_data  !DELETE LAST DATA
        POINT
930     K=K+1
940     GOTO Measure_data
950
960 Sort:!
970
980     Flag=0
990     Numpt=K
1000
1010 Sort_loop:!
1020
1030    FOR K=1 TO Numpt-1
1040      IF Vmax(K)>Vmax(K+1) OR Vmax(K)=Vmax(K+1) THEN GOTO 1120
1050      Itemp=Imax(K)
1060      Vtemp=Vmax(K)
1070      Imax(K)=Imax(K+1)
1080      Vmax(K)=Vmax(K+1)
1090      Imax(K+1)=Itemp
1100      Vmax(K+1)=Vtemp
1110      Flag=1
1120    NEXT K
1130    IF Flag=0 THEN GOTO Write_to_file
1140    Flag=0
1150    GOTO Sort_loop
1160
1170 Write_to_file:!
1180
1190    PURGE "C:\DIODE\DATA"
1200    CREATE "C:\DIODE\DATA",1
1210    ASSIGN @File TO "C:\DIODE\DATA";FORMAT ON
1220    OUTPUT @File USING "SDDDD.DD";0,0
1230
1240    FOR K=1 TO Numpt
1250      OUTPUT @File USING "SDDDD.DD";-Vmax(K)*1000,(Imax(K))^(2/3)
1260    NEXT K
1270
1280    Slope=(Imax(1)^(2/3))/Vmax(1)
1290    I_ideal(1)=Vmax(Numpt)*Slope!    IDEAL NON-SATURATED CURRENT
1300    I_ideal(0)=0
1310    V_ideal(0)=0
1320    V_ideal(1)=-1000*Vmax(Numpt)
1330
```

```
1340    OUTPUT @File USING "SDDDD.DD";V_ideal(0),I_ideal(0)
1350    OUTPUT @File USING "SDDDD.DD";V_ideal(1),I_ideal(1)
1360    ASSIGN @File TO *! CLOSE FILE
1370
1380 Graph:!
1390
1400    ASSIGN @File TO "C:\DIODE\DATA";FORMAT ON
1410    FOR K=0 TO Numpt
1420      ENTER @File;Vmax(K),Imax(K)!  Vmax IS IN mV & Imax IN Amps
1430    NEXT K
1440    ENTER @File;V_ideal(0),I_ideal(0)
1450    ENTER @File;V_ideal(1),I_ideal(1)
1460
1470 CREATE x-y GRAPH
1480
1490    ASSIGN @Plot TO WIDGET "XY GRAPH";SET("VISIBLE":0)
1500    GESCAPE CRT,35!  WINDOW TO TOP
1510    GESCAPE CRT,30!  MAXIMISE WINDOW
1520
1530    CONTROL @Plot;SET("POINT CAPACITY":Numpt+1)
1540    CONTROL @Plot;SET("HEIGHT":580,"WIDTH":800)
1550    CONTROL @Plot;SET("CURRENT TRACE":1)
1560    CONTROL @Plot;SET("TRACE LABEL":"MEASURED VALUES OF I & V")
1570    CONTROL @Plot;SET("Y DATA":Imax(*))
1580    CONTROL @Plot;SET("X DATA":Vmax(*))
1590    CONTROL @Plot;SET("CURRENT TRACE":2)
1600    CONTROL @Plot;SET("TRACE LABEL":"INITIAL SLOPE OF CURVE")
1610    CONTROL @Plot;SET("Y DATA":I_ideal(*))
1620    CONTROL @Plot;SET("X DATA":V_ideal(*))
1630    CONTROL @Plot;SET("BACKGROUND":1)
1640    CONTROL @Plot;SET("TITLE":"I-V CHARACTERISTICS FOR
        CATHODE#6")
1650    CONTROL @Plot;SET("CURRENT AXIS":"X")
1660    CONTROL @Plot;SET("AXIS LABEL":"ANODE VOLTAGE (Volts)")
1670    CONTROL @Plot;SET("AUTOSCALE":1)
1680    CONTROL @Plot;SET("CURRENT AXIS":"Y")
1690    CONTROL @Plot;SET("AXIS LABEL":"CATHODE CURRENT^2/3")
1700    CONTROL @Plot;SET("AUTOSCALE":1)
1710    CONTROL @Plot;SET("VISIBLE":1)
1720
1730 To_clipboard:!
1740
1750    LOADSUB ALL FROM "C:\IBASIC\CLIP.CSB"
1760    CALL Graphtoclipbrd
1770    LOOP
1780    END LOOP   ! leave graph on screen
1790
```

```
1800 Temp:!
1810
1820    CALL Hpt_push(Hp3478a,"RESET")
1830    CALL Hpt_take_readin(Hp3478a,"READING")
1840    CALL Hpt_peek(Hp3478a,"READING",Tk)
1850
1860    Tk=100*Tk/(.05*.45)!    50mV AND ADJUST FOR EMITTANCE OF
        TUNGSTEN
1870    Temp=.00355898*Tk^3-.3862748*Tk^2+16.76991*Tk+865.7824
1880    Temp=INT(Temp)
1890    GOTO Prt_data_screen
1900
1910  SUBEND
1920
1930  *** HPITG Actions End ***
```

```
8                          "BENJAMIN.BAS"
10
12                    Program to Evaluate the Performance
14                          of a Patchy Cathode
15
16                             by B.D. Foulis
17                            October 1992
18
20        Reference: A.H.Beck & De-An Wang  "The I-V Characteristics
22             for Planar Thermionic Diodes with Patchy Cathodes"
24          Int. Journal of Electronics, 1981, vol 51, no 6, pp717-733
26
28           The data for this program to analyse was generated by
30           "Albert", a cathode measurement program written in HP
32                    Instrument BASIC, also by B.D.Foulis
34
36
100   CLS
110   E=3 : PI=3.14159265#
120   DIM X(100),Y(100),W(100),C(100),I(100)
130   EE=1.6E-19 : A0=120.4 :  e AND RICHARDSON-DUSHMAN CONSTANT
      (A/cm^2)/K
140   KK=1.381E-23 :'          BOLTZMANN'S CONSTANT
150
200   ************************ INPUT DATA ************************
210
220   GOSUB 1120 :' DISPLAY TITLE ON SCREEN
230   PRINT:PRINT:PRINT TAB(16);"ENTER CATHODE CYLINDRICAL RADIUS
      (2.5mm):";:INPUT CR$
240   IF CR$="" THEN CR=.0025 ELSE CR=VAL(CR$)/1000
250   GOSUB 3000 : ENTER DATA FROM FILE & FIT POLYNOMIAL TO POINTS
260   PRINT TAB(16);"ENTER RANGE OF TEST POINT VOLTAGES
      (min,max):";:INPUT VLO,VHI
270   PRINT:PRINT
280   PRINT TAB(20);"*** SEARCHING FOR TEST POINTS ***"
290   GOSUB 4000 :'     FIND THREE TEST POINTS
300   IF NOGOOD=1 THEN PRINT TAB(16);"RANGE DOES NOT CAUSE
      CONVERGENCE!":PRINT:PRINT TAB(16);"SHOW TABLE (Y/N):";:INPUT
      A$:IF A$<>"Y" THEN 260 ELSE VM=VHI:GOSUB 6000
310   GOSUB 700 :  CALCULATE REST OF DATA
320   GOSUB 4500:  GENERATE i-v FUNCTION ACCORDING TO BECK & WANG
330   SOUND 3000,2
340   GOSUB 2000 :      PRINT OUT DATA
350   IF A$="Y" THEN GOSUB 5000 :'    PRINT DATA TO FILE
360   PRINT:PRINT:PRINT TAB(23);"OUTPUT TO PRINTER (Y/N):";:INPUT A$
370   IF A$="Y" THEN GOSUB 5500 :'    PRINT TO PRINTER
380   PRINT:PRINT:PRINT TAB(23);"ANOTHER ANALYSIS (Y/N):";:INPUT A$
```

```
390   IF A$="Y" THEN RUN
400   END
410
500 ******** SUBROUTINE TO CALCULATE ALPHA & EXALPHA ***********
510
520   DELTA=(I(1)-I(2))/(I(2)-I(3))
530   N=(V(1)/V(2)+V(2)/V(3))/2 :'   AVERAGE OF TWO COMMON RATIOS
540   V1=EXP(DELTA*LOG(N)/(DELTA-N^(3/2))+(2/3)*
      (1-3*LOG(N)/(2*N^(3/2)-2)))
550   IF V1=0 THEN ALPHA=100: RETURN
560   VM=V(1)/V1
570   L=V1^(3/2)-(3/2)*V1^(3/2)*LOG(V1)
580   EXALPHA=((I(1)/N^3)*(L+3*V1^(3/2)*LOG(N))-I(3)*L)/(I(1)-I(3))
590   IF EXALPHA=0 THEN RETURN
600   ALPHA=-1*LOG(ABS(EXALPHA))
610   RETURN
620
700   ******* SUBROUTINE TO CALCULATE Jmax,Imax,SIGMA,etc **********
710
720   IMAX=(I(1)*(1-EXALPHA))/(L-EXALPHA):   IMAX=REAL PEAK CURRENT
730   SIGMA=SQR(CR^2/(2*ALPHA))
740   JMAX=(I(1)/(2*PI*SIGMA^2))/(L-ABS(EXALPHA)): MAX J FROM IDEAL
      CATHODE
750   JMAX=JMAX*.0001: '  CONVERT TO A/CM^2
760   JMAX=JMAX*.001 : '  CONVERT TO AMPS FROM mA
770   I=JMAX*(PI*CR^2):I=I*10000:'   CONVERT TO cm^2
780   I=I*1000:REM CONVERT TO mA FROM AMPS
790   J=IMAX/(PI*CR^2):J=J*.0001:'   CONVERT TO cm^2
800   J=J*.001:'                     CONVERT TO AMPS FROM mA
810
820   **** I ASSUME THAT CR/SIGMA=12 IS 0% EMISSION, AND CR/SIGMA=0
830   IS 100% EMISSION....FROM CURVES pg721 OF BECK & WANG.    ****
840
850   ACTIVE=100*(1-(CR/SIGMA)/12)
860
870   ***************** WORK FUNCTION **************************
880
890   TEMP=LOG(JMAX/(A0*TK^2))
900   WORK=TEMP*(-1*KK*TK/EE)
910   RETURN
920
1000 ********************* PRINT RESULTS ***********************
1010
1020 GOSUB 1120 :'   PRINT TITLE ON SCREEN
1030 GOSUB 2000 :'   OUTPUT ANSWERS
1040 END
1050
```

```
1070
1100 ************** SUBROUTINE TO PRINT TITLE ******************
1110
1120 CLS:PRINT:PRINT"-------------------------------------------------------------------------------"
1130 PRINT TAB(2);LEFT$(TIME$,5);TAB(30);"CATHODE EVALUATION:";
     TAB(69);DATE$
1140 PRINT  "-------------------------------------------------------------------------------"
1150 RETURN
1160
2000 ****************** SUBROUTINE TO PRINT RESULTS **************
2010
2020 CLS:PRINT:GOSUB 1120:'    PRINT TITLE
2030 PRINT:PRINT:PRINT TAB(8);"Maximum real current obtainable:";
     TAB(55);INT(IMAX*100)/100;TAB(63);"mA"
2040 PRINT TAB(8);"Corresponding average current density:";
     TAB(55);INT(J*1000)/1000;TAB(64);"A/cm^2"
2050 PRINT
2060 PRINT TAB(8);"Maximum current from ideal cathode:";
     TAB(55);INT(I*100)/100;TAB(64);"mA"
2070 PRINT TAB(8);"Maximum current density if cathode ideal:";
     TAB(55);INT(JMAX*1000)/1000;TAB(64);"A/cm^2"
2080 PRINT
2090 PRINT TAB(8);"Percentage of cathode surface active:";
     TAB(55);INT(ACTIVE*10)/10;TAB(64);"%"
2100 PRINT TAB(8);"Work function of cathode:";
     TAB(55);INT(WORK*1000)/1000;TAB(64);"eV"
2110 PRINT
2120 PRINT TAB(8);"Value of Alpha:";TAB(55);INT(ALPHA*1000)/1000
2130 PRINT TAB(8);"Saturation voltage:";TAB(55);INT(VM*10)/10;TAB(64);"Volts"
2140 PRINT
2150 PRINT:PRINT TAB(23);"HIT <RETURN> TO SEE DATA TABLE";:INPUT A$
2160 CLS:GOSUB 1120:REM  PRINT HEADING
2170 PRINT:PRINT:PRINT TAB(23);"V (Volts)";TAB(35);"POLYFIT (mA)";
     TAB(50);"CALCULATED (mA)":PRINT
2180 FOR X=1 TO NUM:P=C(1)
2190 V=X*VM/NUM
2200 FOR K=1 TO M:P=P*V+C(K+1):NEXT K
2210 PRINT TAB(22);INT(V*1000)/1000;TAB(32);":";TAB(36);
     INT(P*1000)/1000;TAB(46);":";TAB(52);INT(I(X)*I*1000)/1000
2220 NEXT X
2230 PRINT:PRINT:PRINT TAB(23);"PRINT DATA TO FILE (Y/N):";:INPUT A$
2240 RETURN
2250
2500 * SUBROUTINE TO CONVERT BRIGHTNESS TEMP TO REAL KELVIN **
2510
2520 TK=TB+273+65 :'       ASSUME 65 DEGREES DIFFERENCE FOR NOW
2530 RETURN
```

```
2540
3000 ************************* POLYFIT *************************
3010
3020 LN=1000: LD=11
3030 DEF FNMI(X,Y)=(X<Y)*(-X)+(Y<=X)*(-Y)
3040 N=0: M=0: S2=0: S4=0: P1=0: P2=0: P3=0: I=0:
     J=0: J1=0:K=0:VR=0
3050 R2=0: MF=0: S1=0: S3=0: MM=0: WT=0: P=0
3060 DIM D1(LD),D2(LD),D3(LD),D4(LD),D5(LD),D6(LD)
3070
3080 GOSUB 3500 :' READ DATA FROM FILE MADE BY "ALBERT"
3090 GOSUB 2500 :' CONVERT TEMP TO TRUE VALUE
3100
3110 N=NUM:PM=FNMI(LD-1,N-1):REM  N=# OF POINTS
3120 M=4:'  ---- DEGREE OF POLYNOMIAL ----
3130 IF MF>0 AND M>MM THEN J1=MM+1: MM=M: GOTO 3190
3140 J1=1:MM=M: S1=0: S2=0: S3=0: S4=0
3150 FOR I=1 TO N: WT=W(I)
3160 S1=S1+WT*X(I):S2=S2+WT:S3=S3+WT*Y(I):S4=S4+WT*Y(I)*Y(I)
3170 NEXT I
3180 D4(1)=S1/S2: D5(1)=0: D6(1)=S3/S2: D1(1)=0: D2(1)=1:
     VR=S4-S3*D6(1)
3190 FOR J=J1 TO MM: S1=0: S2=0: S3=0: S4=0
3200 FOR I=1 TO N: P1=0: P2=1
3210 FOR K=1 TO J: P=P2: P2=(X(I)-D4(K))*P2-D5(K)*P1: P1=P:NEXT K
3220 WT=W(I): P=WT*P2*P2
3230 S1=S1+P*X(I): S2=S2+P: S3=S3+WT*P1*P1: S4=S4+WT*Y(I)*P2:
     NEXT I
3240 D4(J+1)=S1/S2: D5(J+1)=S2/S3: D6(J+1)=S4/S2:
3250 D3(1)=(-D4(J))*D2(1)-D5(J)*D1(1)
3260 IF J<4 THEN 3280
3270 FOR K=2 TO J-2: D3(K)=D2(K-1)-D4(J)*D2(K)-D5(J)*D1(K): NEXT K
3280 IF J>2 THEN D3(J-1)=D2(J-2)-D4(J)*D2(J-1)-D5(J)
3290 IF J>1 THEN D3(J)=D2(J-1)-D4(J)
3300 FOR K=1 TO J: D1(K)=D2(K): D2(K)=D3(K):
     D6(K)=D6(K)+D3(K)*D6(J+1):
     NEXT K
3310 NEXT J
3320 FOR J=1 TO M+1: C(J)=D6(M+2-J):NEXT J
3330 P2=0: FOR I=1 TO N:P=C(1)
3340 FOR J=1 TO M: P=P*X(I)+C(J+1): NEXT J
3350 P=P-Y(I): P2=P2+W(I)*P*P: NEXT I
3360 S2=0:IF N>M+1 THEN S2=P2/(N-M-1)
3370 R2=1: IF VR<>0 THEN R2=1-P2/VR: IF R2<0 THEN R2=0
3380 RETURN
3390
```

```
3500 ********* SUBROUTINE TO READ IN I-V CHARACTERISTICS **********
3510
3520 OPEN "C:\DIODE\DATA" FOR INPUT AS #1
3530 INPUT#1, TB,NUM :' BRIGHTNESS TEMP & NUMBER OF POINTS
3540 FOR X=1 TO NUM
3550 INPUT#1,X(X),Y(X)
3560 NEXT X
3570 CLOSE#1
3580 RETURN
3590
4000 ********** SUBROUTINE TO FIND TEST POINTS ************
4010
4020 NOGOOD=0
4030 FOR N=1.85 TO 1.05 STEP -.05
4040 FOR V=VHI TO VLO STEP (VLO-VHI)/100
4050 V(1)=V:V(2)=V(1)/N:V(3)=V(2)/N
4060 FOR X=1 TO 3:I(X)=C(1)
4070 FOR K=1 TO M:I(X)=I(X)*V(X)+C(K+1):NEXT K
4080 NEXT X
4090 GOSUB 500:REM CALCULATE ALPHA
4100 IF (L-EXALPHA)<0 THEN 4120
4110 IF EXALPHA>0 AND EXALPHA<1 THEN RETURN
4120 NEXT V:NEXT N
4130 BEEP:NOGOOD=1:RETURN
4140
4500 ********* SUBROUTINE TO GENERATE i-v ACCORDING TO BECK *******
4510
4520 FOR X=1 TO NUM
4530 V=X/NUM
4540 I(X)=(V^1.5/ALPHA)*(1-1.5*LOG(V)-EXALPHA/(V^1.5))
4550 NEXT X
4560 RETURN
4570
5000 ********** SUBROUTINE TO PRINT DATA TO FILE ************
5010
5020 CLS:PRINT
5030 GOSUB 1100:'     PRINT TITLE
5040 PRINT:PRINT:PRINT TAB(23);"*** PRINTING DATA TO FILE ***"
5050 FOR K=1 TO 10000:NEXT K
5060 OPEN "C:\HG\CATHDATA.DAT" FOR OUTPUT AS#1
5070 FOR X=1 TO NUM:P=C(1)
5080 V=X*VM/NUM
5090 FOR K=1 TO M:P=P*V+C(K+1):NEXT K
5100 IF I(X)<0 THEN I(X)=0
5110 IF P<0 THEN P=0
5120 PRINT #1,INT(V*1000)/1000,INT(P^(2/3)*1000)/100000!,
     INT((I(X)*I)^(2/3)*1000)/100000!
```

```
5130 NEXT X
5140 FOR K=1 TO 10:PRINT#1,"          ":NEXT K
5150 CLOSE #1
5160 RETURN
5170
5500 ***************SUBROUTINE TO PRINT TO PRINTER**************
5510
5520 CLS:PRINT:PRINT:GOSUB 1100
5530 PRINT:PRINT:PRINT TAB(23);"*** OUTPUTING DATA TO PRINTER ***"
5540 OPEN "LPT1:" FOR OUTPUT AS #2
5550 PRINT #2,;TAB(10);"OUTPUT DATA FOR CATHODE EVALUATION ON ";
     DATE$;" @ ";LEFT$(TIME$,5)
5560 PRINT#2,"":PRINT #2,""
5570 PRINT #2,TAB(18);"V (Volts)";TAB(30);"POLYFIT (mA)";
     TAB(45);"CALCULATED (mA)":PRINT #2,""
5580 FOR X=1 TO NUM:P=C(1)
5590 V=X*VM/NUM
5600 FOR K=1 TO M:P=P*V+C(K+1):NEXT K
5610 PRINT #2,TAB(17);INT(V*1000)/1000;TAB(28);":";
     TAB(31);INT(P*1000)/1000;TAB(41);":";TAB(47);INT(I(X)*I*1000)/1000
5620 NEXT X
5630 PRINT#2,""
5640 PRINT#2,TAB(20);"SATURATION VOLTAGE: ";VM;" Volts"
5650 PRINT#2,TAB(20);"MAXIMUM IDEAL CURRENT: ";I;" mA"
5660 PRINT#2,TAB(20);"MAXIMUM REAL CURRENT: ";IMAX;" mA"
5670 PRINT#2,TAB(20);"VALUE OF ALPHA: ";ALPHA
5680 PRINT#2,CHR$(12):'     FORM FEED
5690 RETURN
5700
6000 ******** SUBROUTINE TO PRINT DATA FOR NO CONVERGENCE ******
6010
6020 GOSUB 2160:'   PRINT TABLE ON SCREEN
6030 IF A$="N" THEN RUN
6040 GOSUB 5000:'   PRINT DATA TO FILE
6050 RUN
6060
6070 ************************************************************
```

APPENDIX B:

CH4 ACTIVE BRAZE MATERIAL

PRODUCT DESCRIPTION:

To avoid the need for pre-metallising the ceramic surface before brazing to a metal, brazing alloys were developed that reacted directly with the ceramic surface in contact with the alloy. A range of products have been developed by Degussa A.G. in Germany in which the active element is titanium. The composition of the different alloys available are given in table B1.

	%Cu	%Ag	%Ti	%In
CH1	19.5	72.5	3.0	5.0
CH2	-	96.0	4.0	-
CH3	6.0	91.0	3.0	-
CH4	26.5	70.5	3.0	-

Table B1 Composition of Various Active Braze Alloys

From extensive tests performed by N.P. Hensley*, CH4 was chosen as the most suitable alloy for the TWT development. The alloy was available in 0.1 millimetre and 0.2 millimetre thick foil from which different preforms could be punched.

BRAZING TECHNIQUES:

The ceramic components were cut to size using a diamond cutter and the end faces polished using 600 grit grinding paste. Any holes in the tube walls that required drilling were done so with an ultrasonic drill and diamond paste. It was generally found that the finer grits, although taking longer to drill through the ceramic, left a smooth ceramic face which led to more reliable joints. All components were thoroughly cleaned in deionised water, acetone and freon. A brief summary of the

*Hensley, N.P., "The Construction and Testing of an Experimental TWT Amplifier" University of Natal, M.Sc Thesis, January 1990

preparation of the three joints developed by the author follows:

Vacuum Envelope: 0.2 millimetre washers of CH4 were sandwiched between the ceramic envelope and the kovar end plates of the gun envelope. The plates were lapped using 1000 grit water paper. A pressure of 500 $g.cm^{-2}$ was applied to the plates throughout the brazing cycle.

Electrode Supports: The molybdenum support wires were wrapped loosely around the ceramic rods to allow for expansion differences during heating. CH4 washers, having an inside diameter of 3 millimetres and a total thickness of 0.3 millimetre, were placed over the ceramic rods and rested on the molybdenum wires. The surface tension of the CH4 ensured that the alloy flowed throughout the joint.

Electrical Feed-Throughs: Each molybdenum pin was machined in such a manner that a flat face was in contact with the outer wall of the ceramic envelope. A 0.2 millimetre washer was sandwiched between this face and the ceramic, and pressure applied using molybdenum wire wrapped around the pin and ceramic tube. The lower expansion coefficient of molybdenum over ceramic ensured that the pressure would be maintained during the braze cycle.

Many different braze profiles were experimented with, and adjusted to meet the requirements of the design. Figure B1 shows the final profile used for the above mentioned joints. Note the 15 minute *soaking* period at 750 °C to allow for thermal equilibrium to be reached between the large jigs and the gun components. Also of importance is the slow cooling cycle at the end of the braze to reduce the thermal shock to the ceramic.

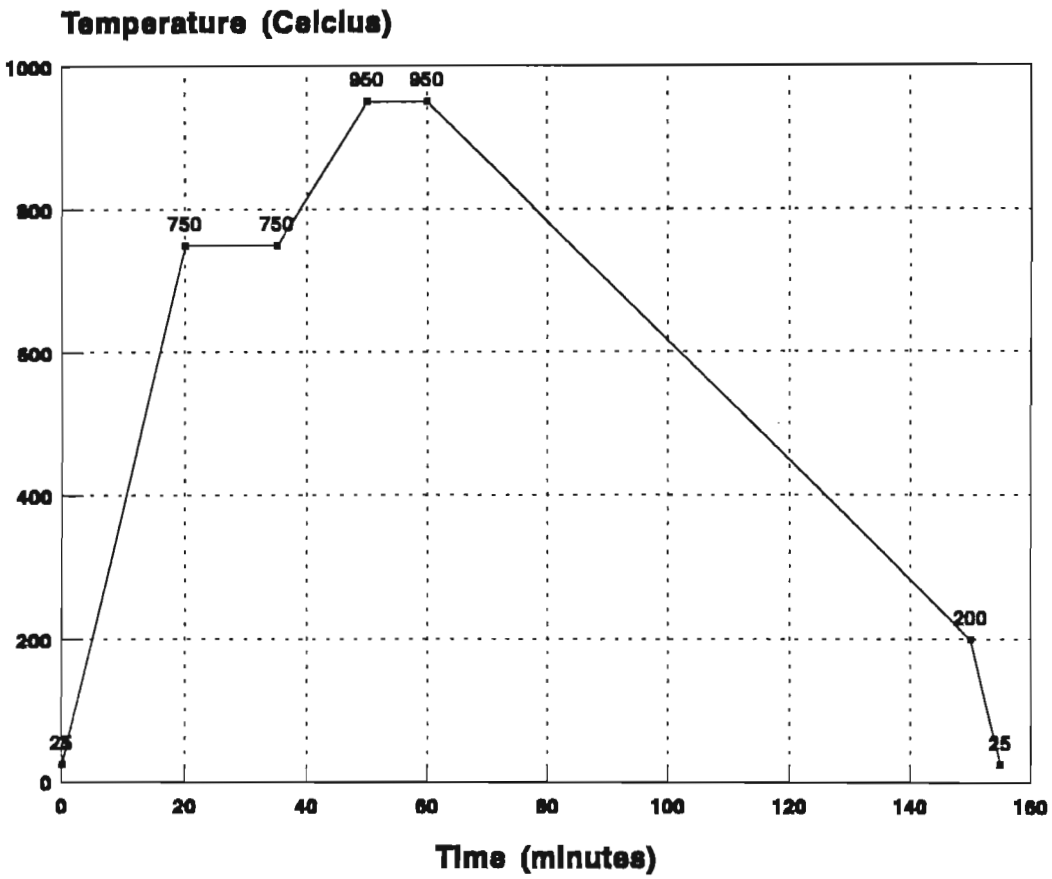

Figure B1 Braze Profile for CH4 Active Brazing

APPENDIX C:

TEMPERATURE CORRECTION TABLE

The following tabled values are the temperatures in degrees Kelvin that must be added to the brightness temperature of the object, as measured using an optical pyrometer, to obtain the true object temperature. The correction is tabled for various spectral emissivities of the object:

Emis-sivity: e	Brightness Temperature (Degrees Kelvin)						
	1000	1100	1200	1300	1400	1500	1600
0.1	119	146	176	209	246	286	329
0.2	80	98	118	140	163	189	217
0.3	59	72	86	102	119	137	157
0.4	44	54	64	76	89	102	117
0.5	33	40	48	57	66	76	87
0.6	24	29	35	41	48	55	63
0.7	17	20	24	29	33	38	43
0.8	10	13	15	18	21	24	27
0.85	7	9	11	13	15	17	19
0.9	5	6	7	8	10	11	13
1.0	0	0	0	0	0	0	0

Table C1 Correction Factors for Brightness to True Temperature Conversion (from M. Knoll, "Materials and Processes of Electron Devices")

The spectral emissivity of the tungsten pellet as used in the cathode manufacture was taken to be 0.45 at the temperature of interest.

APPENDIX D:

TUBE ASSEMBLY DIAGRAMS

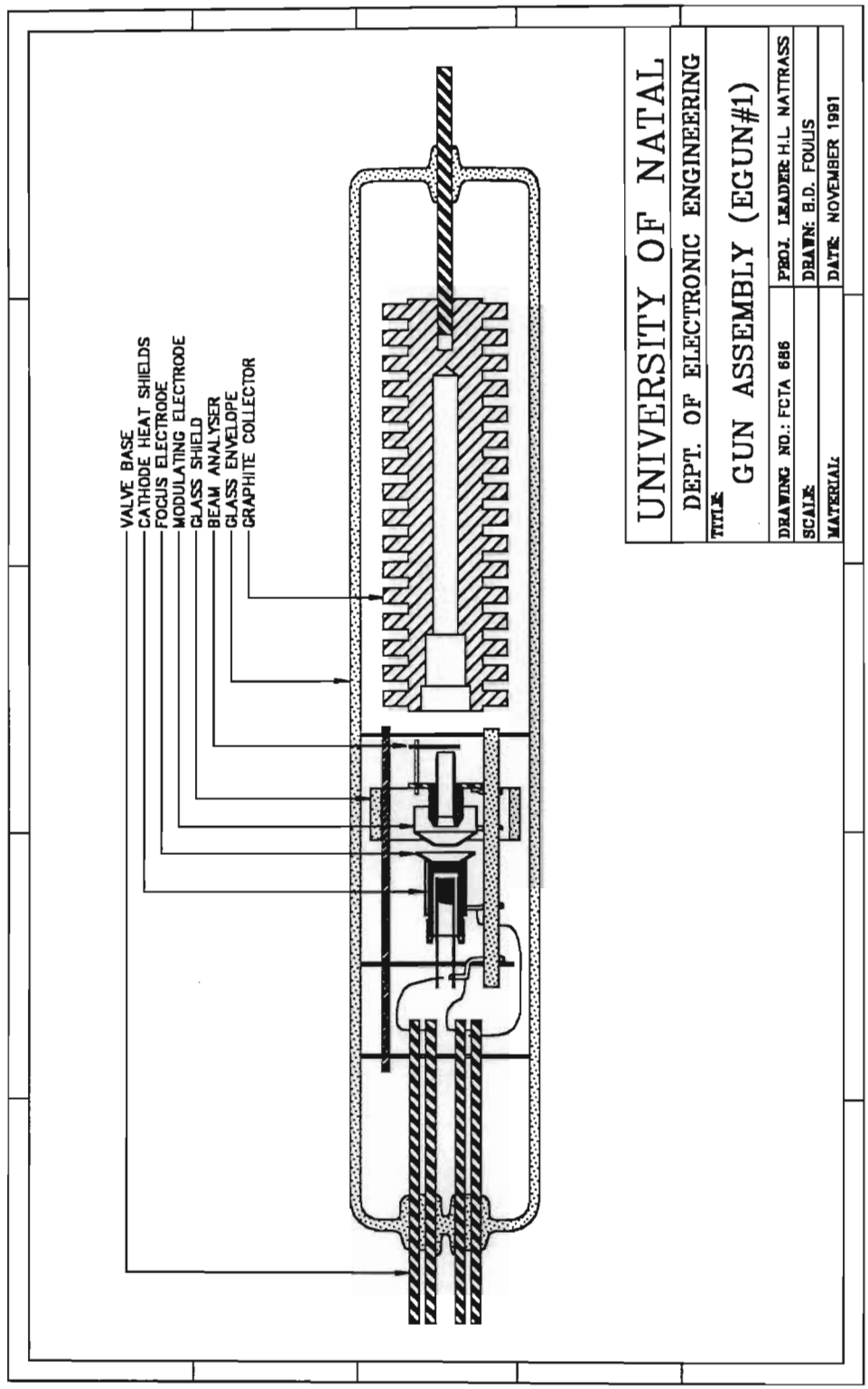

Figure D1 Glass Test Gun Assembly

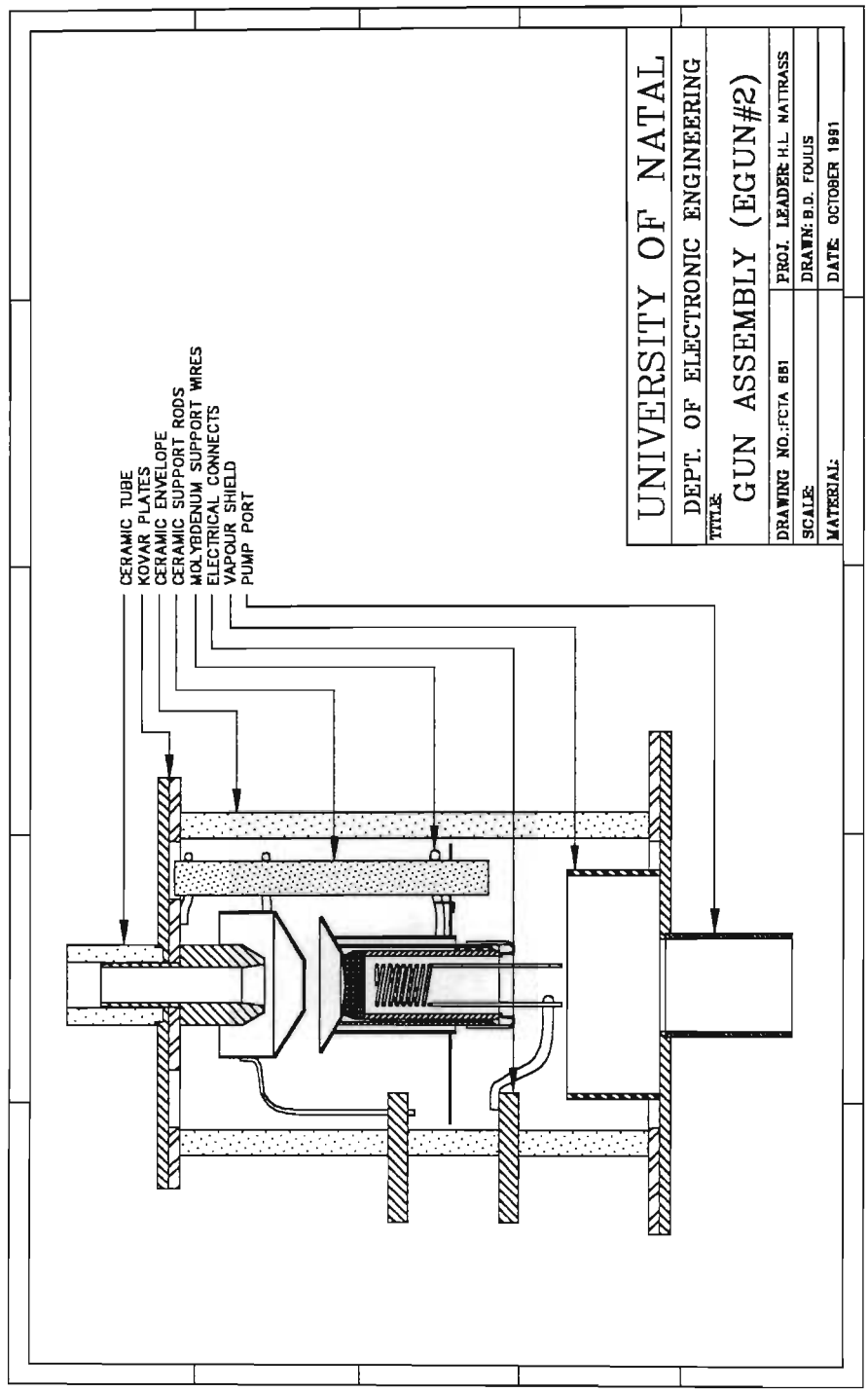

Figure D2 Ceramic Gun Assembly

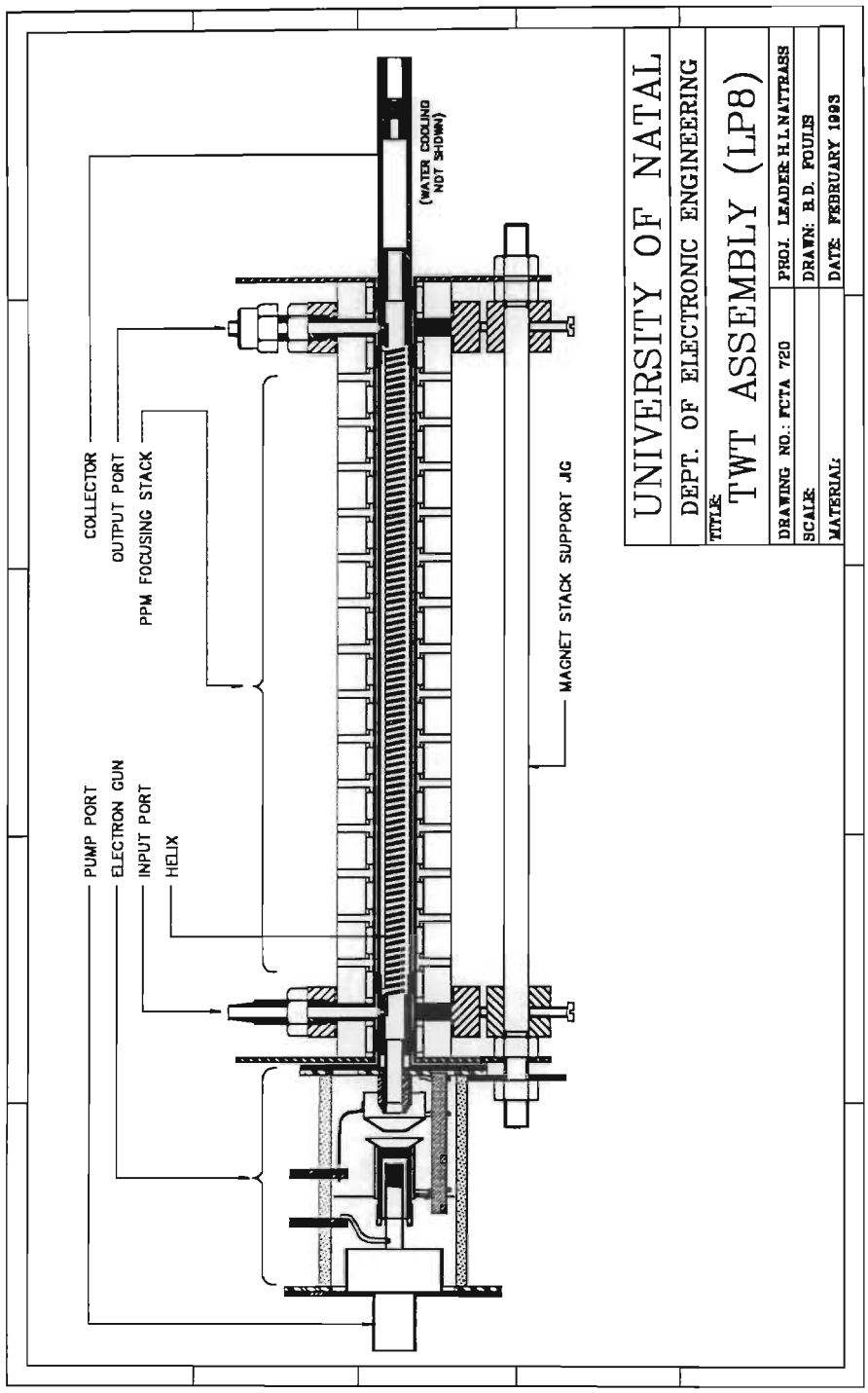

Figure D3 TWT Assembly

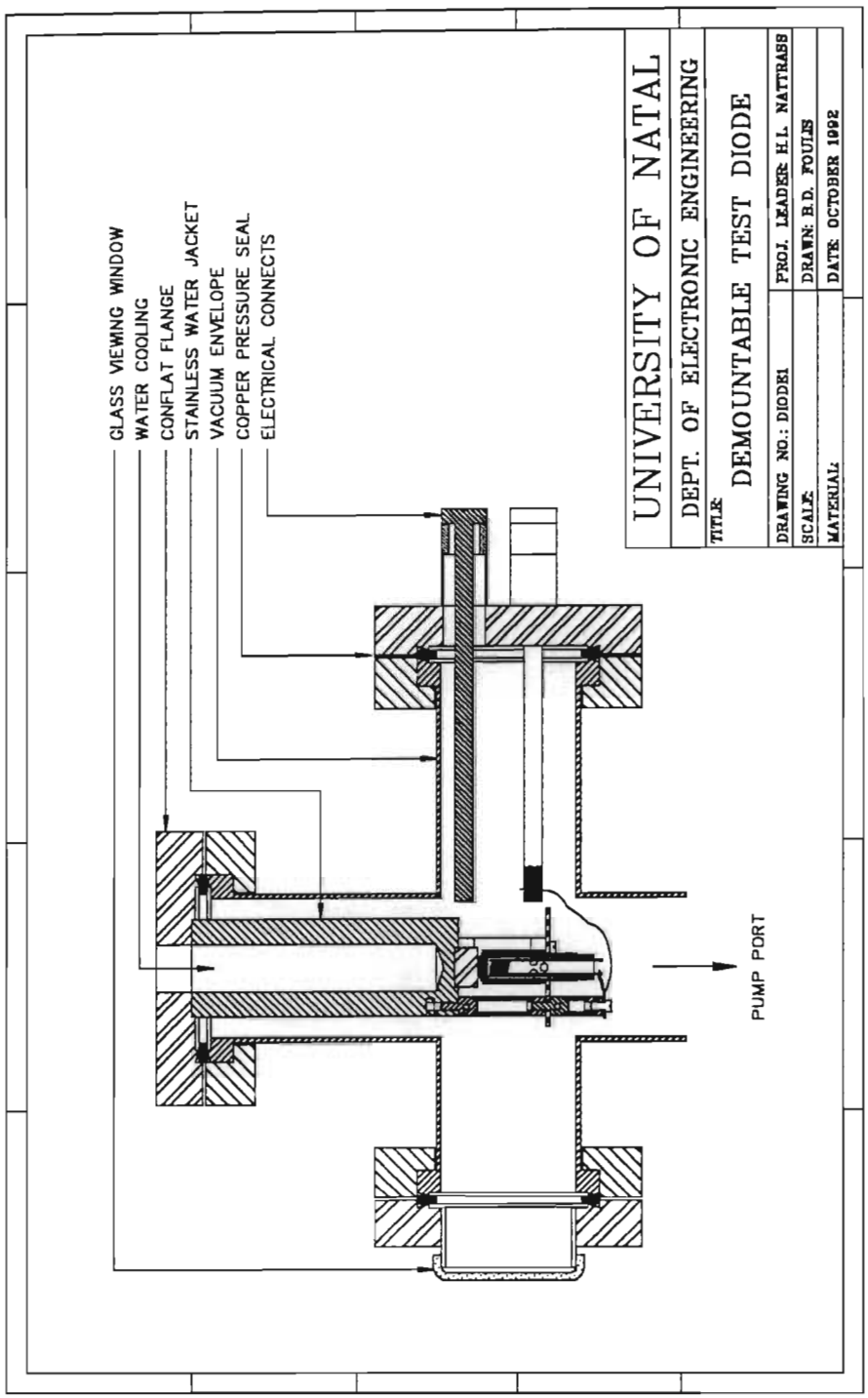

Figure D4 Demountable Diode for Cathode Tests